Doctoral Thesis

Impact of TonEBP in myeloid cells on neuroinflammation and obesity-induced insulin resistance

Gyu Won Jeong

Department of Biological Sciences

Ulsan National Institute of Science and Technology

2023

Impact of TonEBP in myeloid cells on neuroinflammation and obesity-induced insulin resistance

Gyu Won Jeong

Department of Biological Sciences

Ulsan National Institute of Science and Technology

Impact of TonEBP in myeloid cells on neuroinflammation and obesity-induced insulin resistance

A thesis/dissertation submitted to
Ulsan National Institute of Science and Technology
in partial fulfillment of the
requirements for the degree of
Doctor of Philosophy

Gyu Won Jeong

11.29.2022 of submission

Approved by

Hyug Moo Kwon

Advisor

Hyug Moo Kwon

Impact of TonEBP in myeloid cells on neuroinflammation and obesity-induced insulin resistance

Gyu Won Jeong

This certifies that the thesis/dissertation of Gyu Won Jeong is approved.

11.29.2022 of submission

Signature

Hyug Moo Kwon

Advisor: Hyug Moo Kwon

Signature

Chan Young Park

Chan Young Park

Signature

Myung Gon Ko

Signature

Sung Ho Park

Signature

Sung Hoon Back

Abstract

Tonicity-responsive enhancer-binding protein (TonEBP, also called NFAT5) is stress protein that mediates cellular responses via pleiotropic actions. In stress conditions, TonEBP regulates transcription of many genes using different mechanisms: transcription factor, transcriptional suppressor or cofactor. During my degree, I investigated impact of TonEBP in myeloid cells on neuroinflammation and obesity-induced insulin resistance.

Inflammation is biological response to harmful stimuli but also largely considered as contributor to disease development. Neuroinflammation is related with neurodegenerative disease showing memory loss and cognitive deficits. In the brain, Inflammatory stimulus prime microglia cell. This results in a constant production of inflammatory cytokines and chemokines (NO, TNF-α, and IL-1β) by these cells; in turn, the cytokines and chemokines maintain activation of the primed cells. This process results in a vicious circle, and finally causing neuron loss and neurodegeneration. Transcription factors NF-κB and AP-1 are key mediators of inflammation associated with many inflammatory diseases including AD. Here we report that TonEBP promotes neuroinflammation and neuronal cell death through microglial activation. In the microglia cell line BV2, TonEBP deficiency reduced LPS-induced expression and secretion of pro-inflammatory cytokines TNF-α and IL-1β in association with decreased activity of both NF-κB and AP-1. This was due to a reduced assembly of pro-inflammatory transcriptional complex which consisted of TonEBP, NF-κB, AP-1, and p300. As expected, myeloid-specific TonEBP deletion blunted the LPS-induced microglia activation and neuroinflammation. Cerulenin, a small molecule which disrupted the assembly of the pro-inflammatory transcriptional complex, suppressed the LPS-induced activation of microglia and memory loss in association with alleviation of neuronal cell death.

The incidence of obesity worldwide has increased drastically during recent decades. Obesity is associated with increased risk of insulin resistance, type 2 diabetes. Visceral adipose tissue expansion is associated with chronic low-grade inflammation and metabolic dysfunction characterized by progressive accumulation of immune cells. Here, we show that myeloid cell-specific TonEBP depletion reduced inflammation and insulin resistance in mice with high-fat diet-induced obesity, but did not affect adiposity. This phenotype was associated with a reduced accumulation and a reduced M1-like/M2-like ratio of macrophages; decreased expression of inflammatory factors related to insulin resistance; and enhanced insulin sensitivity in epididymal white adipose tissue and the liver. TonEBP expression in macrophages was elevated by concentrations of palmitate and gut-derived endotoxin found in obese individuals, and Sp1 was identified as a central regulator of TonEBP induction. TonEBP

in macrophages promotes obesity-associated systemic insulin resistance and inflammation, and downregulation of TonEBP may induce a healthy metabolic state during obesity.

In conclusion, TonEBP in myeloid cells is a major factor in the immune response that accelerates disease development. Thus, TonEBP is a promising therapeutic target for neuroinflammation and obesity-induced insulin resistance.

Contents

Abstract ---------- 1

Contents ---------- 3

List of figures and tables ---------- 5

Abbreviations ---------- 7

Chapter 1. Background

1.1 Tonicity-responsive Enhancer Binding Protein (TonEBP) ---------- 10

1.2 Alzheimer's disease (AD) ---------- 12

1.3 Adipose tissue macrophage (ATM) ---------- 14

1.4 References ---------- 16

Chapter 2 Microglial TonEBP mediates LPS-induced inflammation and memory loss as transcriptional cofactor for NF-κB and AP-1

2.1 Abstract ---------- 18

2.2 Introduction ---------- 19

2.3 Methods ---------- 20

2.4 Results ---------- 24

2.5 Discussion ---------- 35

2.6 Conclusions ---------- 36

2.7 Supplementary Figures ---------- 37

2.8 References ---------- 38

Chapter 3. TonEBP in myeloid cells promotes obesity-induced insulin resistance and inflammation through adipose tissue remodeling

3.1 Abstract ---------- 42

3.2 Introduction ---------- 43

3.3 Research design and Methods ---------- 45

3.4 Results ---------- 48

3.5 Discussion ---------- 65

3.6 Supplementary Tables & Figures ---------- 68

3.7 References ---------- 80

Conclusion ---------- 84

Acknowledgement ---------- 86

List of figures and tables

Chapter 1. Background

Figure 1-1. Physiology of TonEBP in hypertonicity

Figure 1-2. Pleiotropic actions of TonEBP

Figure 1-3. Neuroinflammation in Alzhemier's Disease

Figure 1-4. Heath problems associated with Obesity

Figure 1-5. M1/M2 macrophage

Figure 1-6. Inflammatory response during obesity

Chapter 2. Microglial TonEBP mediates LPS-induced inflammation and memory loss as transcriptional cofactor for NF-κB and AP-1

Figure 2.1. TonEBP in LPS-induced inflammation in BV2 cells.

Figure 2.2. Cerulenin inhibits LPS-induced inflammation in BV2 cells.

Figure 2.3. Cerulenin blocks LPS-induced secretion of neurotoxins by BV2 cells.

Figure 2.4. Cerulenin inhibits AP-1 transcriptional activity by disrupting its interaction with TonEBP.

Figure 2.5. Myeloid TonEBP is required for LPS-induced microglia activation.

Figure 2.6. Cerulenin inhibits LPS-induced microglia activation.

Figure 2.7. Myeloid TonEBP is required for blocking LPS-induced loss of short-term memory.

Figure 2.S1. Model of TonEBP in microglia-mediated memory loss induced by LPS.

Figure 2.S2. Effects of cerulenin in phosphorylation and nuclear translocation of c-jun.

Chapter 3. TonEBP in myeloid cells promotes obesity-induced insulin resistance and inflammation through adipose tissue remodeling

Figure 3.1. Myeloid TonEBP deficiency prevents HFD-induced glucose intolerance and insulin resistance.

Figure 3.2. Myeloid TonEBP deficiency reduces HFD-induced macrophage accumulation and inflammation in adipose tissue and the liver.

Figure 3.3. TonEBP deficiency promotes macrophage polarization toward improvement of insulin sensitivity.

Figure 3.4. TonEBP deficiency in macrophages improves insulin sensitivity of adipocytes under obesity-mimicking conditions in vitro.

Figure 3.5. Sp1 is a central mediator of TonEBP induction in response to TLR4 stimulation in macrophages.

Figure 3.6. The TonEBP mRNA expression level in PBMCs is positively correlated with blood glucose levels in mice and humans.

Table 3.S1. Primary antibodies used for flow cytometry analysis and immunoblotting

Table 3.S2. Primers used in qPCR for gene expression analysis and ChIP assay

Table 3.S3. Clinical characteristics of diabetic and non-diabetic subjects studied

Figure 3.S1. Supplementary figure related to Fig. 1

Figure 3.S2. Supplementary figure related to Fig. 3

Figure 3.S3. Supplementary figure related to Fig. 3

Figure 3.S4. Supplementary figure related to Fig. 4

Figure 3.S5. Supplementary figure related to Fig. 5

Figure 3.S6. Supplementary figure related to Fig. 6

Abbreviations

AD: Alzheimer's disease

ALT: alanine aminotransferase

AP-1: active protein-1

AR: androgen receptor

AST: aspartate aminotransferase

ATM: adipose tissue macrophage

BBB: blood brain barrier

BCA: bicinchoninic acid

BGT1: betaine-GABA transporter 1

BM: bone marrow

BMDM: bone marrow-derived macrophages

BSA: bovine serum albumin

C/EBP: CCAAT/enhancer binding protein

CD: control diet

ChIP: Chromatin immunoprecipitation

CLS: crown-like structures

CM: conditioned medium

CNS: central nervous system

COX-2: cyclooxygenase-2

CTL: control

CTX: cortex

DMEM: dulbecco's modified eagle's medium

DMSO: dimethyl sulfoxide

DN: diabetic nephropathy

DNMT1: DNA (cytosine-5)-methyltransferase 1

EDTA: ethylene-diamine-tetraacetic acid

EGTA: ethylene-glycol-tetraacetic acid

ELISA: enzyme-linked immunosorbent assay

FBS: fetal bovine serum

FFA: free fatty acid

GTT: Glucose tolerance test

H&E: hematoxylin–eosin

HFD: high-fat diet

HIP: hippocampus

HOMA-IR: homeostasis model assessment of insulin resistance

HRP: horseradish peroxidase

IFN: interferon

IL: interleukin

ITT: insulin tolerance test

KO: knockout

LPS: lipopolysaccharide

M-CSF: macrophage colony-stimulating factor

M-MLV: moloney murine leukemia virus

MACS: magnetic associated cell separation

MEF: embryonic fibroblasts

MKO: myeloid-specific TonEBP knockout mice

MMe: metabolically activated

MTT: 3-(4,5-dimethylthiazol-2-yl)-2,5-diphenyltetrazolium bromide

NF-κB: nuclear factor kappa B

NFAT: nuclear factor of activated T cell 5

NO: nitric oxide

PA: palmitate

PAGE: polyacrylamide gel electrophoresis

PBMC: peripheral blood mononuclear cell

PBS: phosphatebuffered saline

PPAR: peroxisome proliferator-activated receptor

qPCR: quantitative real-time polymerase chain reaction

ROS: reactive oxygen species

SDS: sodium dodecyl sulfate

SMIT: sodium-myoinositol cotransporter

STAT: signal transducer and activator of transcription

SVF: stromal vascular fraction

T2D: type 2 diabetes

TLR: Toll-like receptor

TNF: tumor necrosis factor

TUNEL: terminal deoxynucleotidyl transferase dUTP nick end labeling

WAT: white adipose tissue

WT: wild-type

Chapter 1. Background

1.1. Tonicity-responsive enhancer binding protein (TonEBP)

TonEBP, also known as nuclear factor of activated T cell 5 (NFAT5), binds DNA via Rel-homology domain like NF-κB. TonEBP was identified as a transcriptional factor in response to hypertonic stress by regulating genes such as like *BGT1, SMIT, AR* and *HSP70* (1) (Fig. 1-1). Recent studies show that TonEBP regulates transcription of many genes using different mechanisms such as a transcriptional cofactor (2-3) and a transcriptional suppressor (4-7). TonEBP also regulates intracellular signaling via protein-protein interaction (8-9).

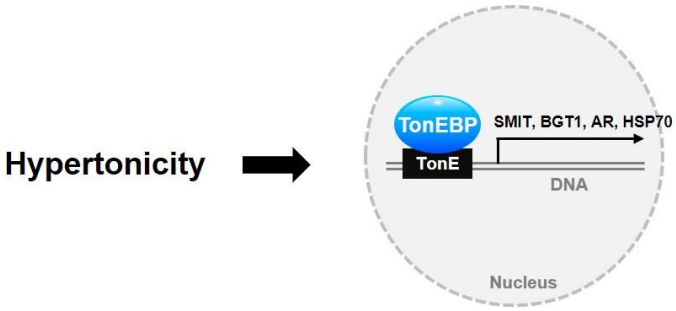

Figure 1-1. Physiology of TonEBP in hypertonicity

Recent studies show that TonEBP is a critical regulator in various inflammatory diseases such as diabetic nephropathy, rheumatoid arthritis, atherosclerosis, obesity, hepatocellular carcinoma and brain inflammation (Fig. 1-2). In rheumatoid arthritis model, TonEBP is required for dendritic cells maturation. TonEBP promotes p38 pathway followed by differentiation of pro-inflammatory Th1 and Th17 cells (10). In obesity, TonEBP recruits DNMT1 which leads to DNA methylation and suppression of Adrb3 promoter (7). Thus, TonEBP deficiency enables to express thermogenic and beige genes, which promotes energy expenditure of WAT. In hepatocellular carcinoma, TonEBP expression in tumour regions and non-tumour regions is associated with recurrence and metastasis (3). Therefore, TonEBP deficiency prevents disease progression by reducing inflammatory response. these findings raise novel therapeutic strategy to prevent other inflammatory disease.

1. Diabetic Nephropathy

Diabetes 55:1450-1455 (2006)
JASN 29: 492-504 (2018)

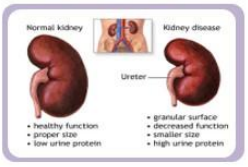

4. Brain inflammation

Nature 496(7446): 518-22 (2013)
Cell death differ. 21: 1095-1106 (2014)

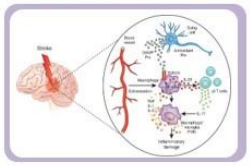

7. Obesity

Nature communications 10(1):3536 (2019)

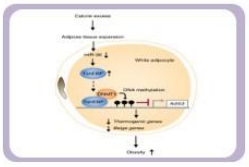

2. Rheumatoid Arthritis

Arthritis Rheum 63: 1843-1852 (2011)
J Clin Invest. 2017;127(3):954-969

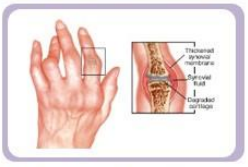

5. Diabetic Retinopathy

Experimental Eye Research 122: 13-19 (2014)

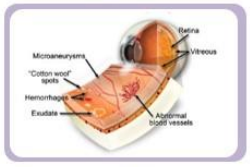

8. Genomic integrity

iScience Vol. 19: 177-190 (2019)
NAR (2020)

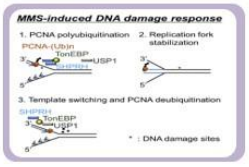

3. Atherosclerosis

Frontiers Physiol 3: 1-7 (2013)

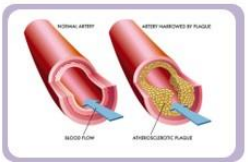

6. Hepatocellular carcinoma

Gut 68(2):347-358. (2019)

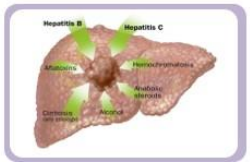

Figure 1-2. Pleiotropic actions of TonEBP

1.2. Alzheimer's disease (AD)

Alzheimer's disease (AD) is an aging-related neurodegenerative disease showing memory loss and cognitive deficits. AD is the 5th leading cause of death in people age 65 and older. 1 in 9 people over the age of 65 years have AD. The number of AD patients almost doubles every 20 years. These increase and the consequential economic impact become a huge burden on society. However, there are still no effective treatment to halt, prevent, or reverse AD even with diagnostic tools. The exact cause of Alzheimer's disease is not known, but recent neuroinflammation has emerged as an important component in Alzheimer's disease pathology (11-13). Because systemic increase in pro-inflammatory mediators enhances activation of microglia. Immune system-mediated actions contribute to and drive Alzheimer's disease (AD) pathogenesis (Fig. 1-3).

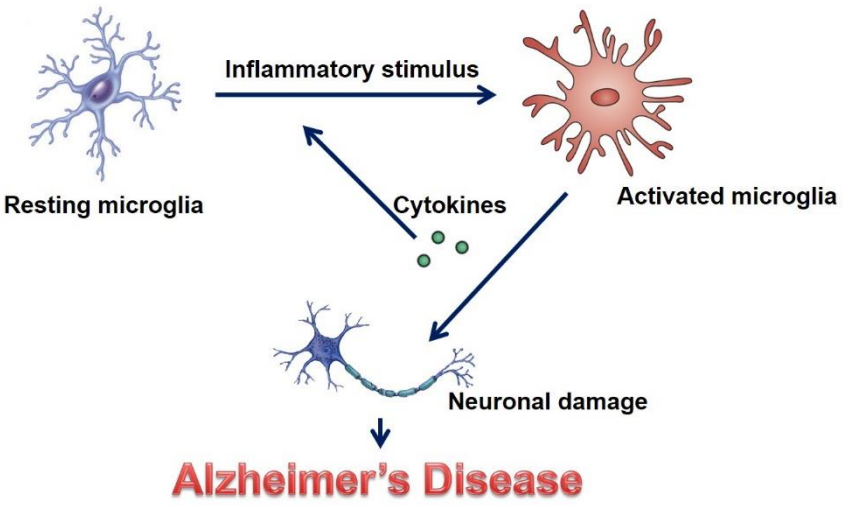

Figure 1-3. Neuroinflammation in Alzhemier's Disease

Neuroinflammation is an inflammation in brain or spinal cord in response to injection, brain injury or aging. In brain, there are glial cells such as microglia, astrocytes, and oligodendrocytes. Microglia are resident macrophages in the CNS and contribute to innate immune response in CNS. In the inflammatory stimulus, microglia and astrocyte are activated and release neurotoxic factors for eliminate the inflammatory stimulus. Peripheral monocytes which are infiltrated through leaky blood brain barrier (BBB) also participate in phagocytosis and debris clearance (14). If these inflammatory responses are not well regulated, they become disease-promoting factors. In AD, excessive neurotoxic factors such as NO, TNF-α, and IL-1β cause neuronal damage and eventually neuronal death (11-13).

There are several ways in which microglia induce neuronal death. Primed microglia induce neuronal

death via inflammatory pathway (15). Cytokines and chemokines (TNF- α, IL-1 β, C1q) induces A1 astrocyte which function like M1. A1 astrocyte has toxicity to neurons and oligodendrocytes (16). Another pathway is microglia mediated synapse loss (16). Thus, regulating activation of microglia is important to prevent neuronal loss and impairment of cognitive function, which drives AD.

1.3. Adipose tissue macrophage (ATM)

Obesity has become a global health problem. It is caused by excessive fat accumulation and is associated with various other diseases such as insulin resistance, type 2 diabetes, fatty liver disease, atherosclerosis, hypertension and stroke (17) (Fig. 1-4). 1 billion adults worldwide are overweight and 658 million of whom are clinically obese in 2022. As the obese population continues to rise, it is necessary to interest in obesity treatment.

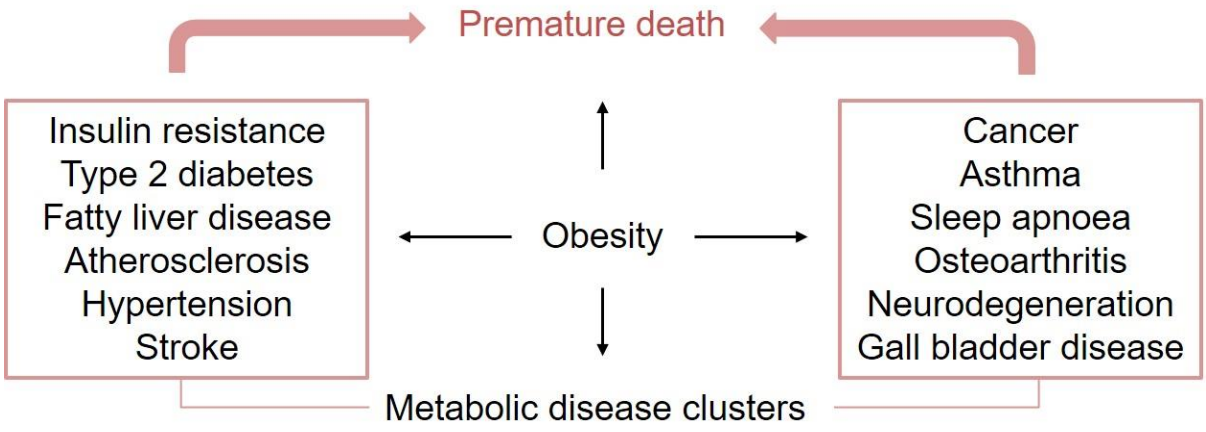

Figure 1-4. Heath problems associated with Obesity

Visceral adipose tissue expansion is associated with chronic low-grade inflammation and metabolic dysfunction characterized by progressive accumulation of immune cells (18). The phenotypic and functional plasticity of adipose tissue macrophages during obesity play a crucial role in orchestration of adipose and systemic inflammation. Adipose tissue is comprised of adipocyte and stromal vascular fraction (SVF) including pre-adipocyte, fibroblasts, endothelial cells, macrophage and monocytes (19). During obesity, immune cells accumulate in metabolic tissues, which is proportional to adiposity. Among them, macrophage is a major cell type that contributes to the inflammatory response and adipose tissue macrophage (ATM) are key mediator in adipose tissue inflammation (20).

Macrophages exist in various type involved in adipose tissue inflammation. It was generally classified as M1 or ‘classically activated’ macrophage with pro-inflammatory function and M2 or ‘alternatively activated’ macrophage with anti-inflammatory function (21) (Fig 1-5). Obese mice mainly show the M1 macrophage phenotype and lean mice have the M2 macrophage phenotype (22) (Fig 1-6). M1 macrophages are typically activated by IFN-γ or lipopolysaccharide (LPS) and produce nitric oxide (NO) and proinflammatory cytokines. M2 macrophages are typically activated by IL-4, IL-10, or IL-13 and secrete arginase-1, IL-10 and anti-inflammatory cytokines (21).

During obesity, ATMs is exposed to metabolic cues like excess free fatty acids (FFAs), glucose, and low doses of endotoxins, rather than cytokines, and undergo a phenotypic switch from the M2 polarization state to a more M1-like polarization state, which is thought to promote insulin resistance and T2D (23). Selective depletion of M1 ATMs reverses insulin resistance even in subjects fed a high-fat diet (HFD) and with obesity (24). Thus, differential accumulation of these two ATM populations could result in distinct metabolic states.

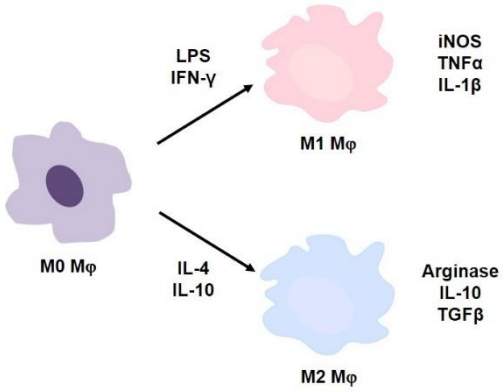

Figure 1-5. M1/M2 macrophage

Figure 1-6. Inflammatory response during obesity

1.4. References

1. Miyakawa, H.; Woo, S. K.; Dahl, S. C.; Handler, J. S.; Kwon, H. M., Tonicity-responsive enhancer binding protein, a rel-like protein that stimulates transcription in response to hypertonicity. *Proc Natl Acad Sci U S A* **1999,** *96* (5), 2538-2542.
2. Lee, H. H.; Sanada, S.; An, S. M.; Ye, B. J.; Lee, J. H.; Seo, Y. K.; Lee, C.; Lee-Kwon, W.; Kuper, C.; Neuhofer, W.; Choi, S. Y.; Kwon, H. M., LPS-induced NFkappaB enhanceosome requires TonEBP/NFAT5 without DNA binding. *Sci Rep* **2016,** *6*, 24921.
3. Lee, J. H.; Suh, J. H.; Choi, S. Y.; Kang, H. J.; Lee, H. H.; Ye, B. J.; Lee, G. R.; Jung, S. W.; Kim, C. J.; Lee-Kwon, W.; Park, J.; Myung, K.; Park, N. H.; Kwon, H. M., Tonicity-responsive enhancer-binding protein promotes hepatocellular carcinogenesis, recurrence and metastasis. *Gut* **2019,** *68* (2), 347-358.
4. Lee, J. H.; Lee, H. H.; Ye, B. J.; Lee-Kwon, W.; Choi, S. Y.; Kwon, H. M., TonEBP suppresses adipogenesis and insulin sensitivity by blocking epigenetic transition of PPARgamma2. *Sci Rep* **2015,** *5*, 10937.
5. Choi, S. Y.; Lee, H. H.; Lee, J. H.; Ye, B. J.; Yoo, E. J.; Kang, H. J.; Jung, G. W.; An, S. M.; Lee-Kwon, W.; Chiong, M.; Lavandero, S.; Kwon, H. M., TonEBP suppresses IL-10-mediated immunomodulation. *Sci Rep* **2016,** *6*, 25726.
6. Yoo, E. J.; Lee, H. H.; Ye, B. J.; Lee, J. H.; Lee, C. Y.; Kang, H. J.; Jeong, G. W.; Park, H.; Lim, S. W.; Lee-Kwon, W.; Kwon, H. M.; Choi, S. Y., TonEBP Suppresses the HO-1 Gene by Blocking Recruitment of Nrf2 to Its Promoter. *Front Immunol* **2019,** *10*, 850.
7. Lee, H. H.; An, S. M.; Ye, B. J.; Lee, J. H.; Yoo, E. J.; Jeong, G. W.; Kang, H. J.; Alfadda, A. A.; Lim, S. W.; Park, J.; Lee-Kwon, W.; Kim, J. B.; Choi, S. Y.; Kwon, H. M., TonEBP/NFAT5 promotes obesity and insulin resistance by epigenetic suppression of white adipose tissue beiging. *Nat Commun* **2019,** *10* (1), 3536.
8. Kang, H. J.; Park, H.; Yoo, E. J.; Lee, J. H.; Choi, S. Y.; Lee-Kwon, W.; Lee, K. Y.; Hur, J. H.; Seo, J. K.; Ra, J. S.; Lee, E. A.; Myung, K. J.; Kwon, H. M., TonEBP Regulates PCNA Polyubiquitination in Response to DNA Damage through Interaction with SHPRH and USP1. *iScience* **2019,** 19, 177-190.
9. Kang, H. J.; Cheon, N. Y.; Park, H.; Jeong, G. W.; Ye, B. J.; Yoo, E. J.; Lee, J. H.; Hur, J. H.; Lee, E. A.; Kim, H. T.; Lee, K. Y.; Choi, S. Y.; Lee-Kwon, W.; Myung, K. J.; Lee, J. Y.; Kwon, H. M., TonEBP recognizes R-loops and initiates m6A RNA methylation for R-loop resolution. *Nucleic Acids Res.* **2021,** 29(1), 269-284.

10. Ye, B. J.; Lee, H. H.; Yoo, E. J.; Lee, J. H.; Kang, H. J.; Jeong, G. W.; Park, H.; Lee-Kwon, W.; Choi, S. Y.; Kwon, H. M., TonEBP in dendritic cells mediates pro-inflammatory maturation and Th1/Th17 responses. *Cell Death Dis*. **2020,** 11(6), 421.
11. Heneka, M. T.; Kummer, M. P.; Latz, E. Innate immune activation in neurodegenerative disease. *Nat Rev Immunol.* **2014,** 14(7), 463-77.
12. Heppner, F. L.; Ransohoff, R. M.; Becher, B. Immune attack: the role of inflammation in Alzheimer disease. *Nat Rev Neurosci.* **2015,** 16(6), 358-72.
13. Heneka, M. T.; Golenbock, D. T.; Latz, E. Innate immunity in Alzheimer's disease. *Nat Immunol.* **2015,** 16(3), 229-36.
14. Varvel, N. H.; Neher, J. J.; Bosch, A.; Wang, W.; Ransohoff, R. M.; Miller R. J.; Dingledine, R. Infiltrating monocytes promote brain inflammation and exacerbate neuronal damage after status epilepticus. *Proc Natl Acad Sci U S A.* **2016,** 113(38), e5665-74.
15. Frakes, A. E.; Ferraiuolo, L.; Haidet-Phillips, A. M.; Schmelzer, L.; Braun, L.; Miranda, C. J.; Ladner, K. J.; Bevan, A. K.; Foust, K. D.; Godbout, J. P.; Popovich, P. G.; Guttridge, D. C.; Kaspar, B. K. Microglia induce motor neuron death via the classical NF-κB pathway in amyotrophic lateral sclerosis. *Neuron.* **2014,** 81(5), 1009-1023.
16. Li, Q.; Barres, B. A. Microglia and macrophages in brain homeostasis and disease. *Nat Rev Immunol.* **2018,** 18(4), 225-242.
17. Hotamisligil, G. S. Inflammation and metabolic disorders. *Nature.* **2006,** 444(7121), 860-7
18. Zatterale, F.; Longo, M.; Naderi, J.; Raciti, G. A.; Desiderio, A.; Miele, C.; Beguinot, F. Chronic Adipose Tissue Inflammation Linking Obesity to Insulin Resistance and Type 2 Diabetes. *Front Physiol.* **2020,** 10, 1607.
19. Lenz, M.; Arts, I. C. W.; Peeters, R. L. M.; Kok, T. M. D.; Ertaylan, G. Adipose tissue in health and disease through the lens of its building blocks. *Sci Rep.* **2020,** 10(1), 10433.
20. Russo, L.; Lumeng, C. N. Properties and functions of adipose tissue macrophages in obesity. *Immunology*. **2018,** 155(4), 407-417.
21. Lee, C. H.; Choi, E. Y. Macrophages and Inflammation. *J Rheum Dis.* **2018,** 25(1), 11-18.
22. Kraakman, M. J.; Murphy, A. J.; Jandeleit-Dahm, K.; Kammoun, H. L. *Fornt Immunol.* **2014,** 5, 470.
23. Lumeng, C.N.; Bodzin, J. L.; Saltiel, A. R. Obesity induces a phenotypic switch in adipose tissue macrophage polarization. *J Clin Invest.* **2007,** 117(1), 175-84.
24. Patsouris, D.; Li, P. P.; Thapar, D.; Chapman, J.; Olefsky, J. M.; Neels, J. G. Ablation of CD11c-positive cells normalizes insulin sensitivity in obese insulin resistant animals. *Cell Metab.* **2008,** 8(4), 301-9.

Chapter 2. Microglial TonEBP mediates LPS-induced inflammation and memory loss as transcriptional cofactor for NF-κB and AP-1

2.1. Abstract

Background: Microglia are brain-resident myeloid cells involved in the innate immune response and a variety of neurodegenerative diseases. In macrophages, TonEBP is a transcriptional cofactor of NF-κB which stimulates the transcription of pro-inflammatory genes in response to LPS. Here, we examined the role of microglial TonEBP.

Methods: We used microglial cell line, BV2 cells. TonEBP was knocked down using lentiviral transduction of shRNA. In animals, TonEBP was deleted from myeloid cells using a line of mouse with floxed TonEBP. Cerulenin was used to block the NF-κB cofactor function of TonEBP.

Results: TonEBP deficiency blocked the LPS-induced expression of pro-inflammatory cytokines and enzymes in association with decreased activity of NF-κB in BV2 cells. We found that there was also a decreased activity of AP-1 and that TonEBP was a transcriptional cofactor of AP-1 as well as NF-κB. Interestingly, we found that myeloid-specific TonEBP deletion blocked the LPS-induced microglia activation and subsequent neuronal cell death and memory loss. Cerulenin disrupted the assembly of the TonEBP/NF-κB/AP-1/p300 complex and suppressed the LPS-induced microglial activation and the neuronal damages in animals.

Conclusions: TonEBP is a key mediator of microglial activation and neuroinflammation relevant to neuronal damage. Cerulenin is an effective blocker of the TonEBP actions.

Keywords: Microglial activation, Neuronal cell death, TonEBP

2.2. Introduction

Neuroinflammation is inflammation in the brain or spinal cord in response to a variety of insults or cues including infection, brain injury, or aging. Like other forms of inflammation, neuroinflammation is mediated by the production of cytokines, chemokines, reactive oxygen species (ROS), and secondary messengers [1]. These inflammatory factors are produced by various cell types in the central nervous system (CNS) such as microglia, astrocytes, endothelial cells, other glial cells, and peripherally derived immune cells. Neuroinflammation can be protective or pathogenic depending on the context and type of molecules involved [1].

Microglia are resident macrophages of the CNS. During embryonic development, primitive macrophages generated in the yolk sac give rise to embryonic microglia [2]. After birth, bone marrow-derived macrophages cross blood brain barrier and supplement the microglial population. Microglia serve two major functions [3]. Microglia contribute to maintenance of CNS homeostasis by controlling neuronal proliferation and differentiation. Microglia also play a critical role in innate immunity in CNS and brain disease. In settings of pathogenesis, inflammatory stimuli can prime microglial cell leading to a constant production of inflammatory cytokines and chemokines which, in turn, maintain activation of the primed cells [4]. These cycles finally lead to neuronal loss and neurodegeneration via inflammatory pathways or activation of A1 astrocytes [5, 6]. Tonicity-responsive enhancer binding protein (TonEBP), also known as nuclear factor of activated T cells 5 (NFAT5), belongs to the Rel family of transcription factors, which includes nuclear factor-κB (NF-κB) and NFAT 1–4 [7, 8]. TonEBP is involved in a variety of physiological and pathological processes by controlling transcription of different sets of genes through distinct mechanisms [9]. For example, in the renal medulla, TonEBP stimulates transcription of aquaporin 2 as a cis-acting transcriptional enhancer [10]. In macrophages, TonEBP regulates transcription of proinflammatory genes such as tumor necrosis factor-α (TNF-α) and cyclooxygenase-2 (COX-2) as a transcription cofactor of NF-κB independent of DNA binding [11]. As such, TonEBP is a key regulator of systemic inflammation. In the brain, TonEBP expression is limited to neurons without detectable expression in glial cells or other nonneuronal cells [12]. We recently reported that TonEBP expression is specifically elicited in microglia in response to direct injection of lipopolysaccharide (LPS) [13]. Here, we investigated the role of TonEBP in microglia. Our data show that TonEBP is a key mediator of microglial activation and neuroinflammation relevant to neuronal damage.

2.3. Method

2.3.1. Cells in culture

BV2 cells, a mouse microglial cell line (cat. no. CRL-2467, ATCC) [14], was cultured in Dulbecco's Modified Eagle's Medium (DMEM) containing 5% fetal bovine serum (FBS, Thermo Fisher Scientific, Inc., MA, USA) and penicillin/streptomycin (100 U/ml and 100 μg/ml; GE Healthcare Life Sciences, UT, USA). For HT22 cells, a mouse hippocampus neuronal cell line (SCC129) [15] and mouse embryonic fibroblasts (MEFs) cells [11] DMEM containing 10% FBS was used. Cells were maintained at 37 °C in an incubator with 5% CO_2. BV2 cells were transfected with TonEBP shRNA-harboring lentiviral particles (Santa Cruz Biotechnology) in the presence of polybrene (5 μg/ml). Stable cells were selected in the presence of puromycin (10 μg/ml). Cells were pretreated with cerulenin and BAY 11-7082 (Sigma Aldrich, USA) for 1 h and exposed to lipopolysaccharide (LPS; Sigma Aldrich). Neuroinflammation is inflammation in the brain or spinal cord in response to a variety of insults or cues including infection, brain injury

2.3.2. Immunoblot assay

Cells were washed twice with 1x cold phosphatebuffered saline (PBS) and lysed in RIPA buffer: 0.01M Tris, pH 7.4, 0.15M NaCl, 0.001M EDTA, 0.001M EGTA, 1% Triton X-100, phosphatase inhibitor cocktail (Sigma Aldrich), and protease inhibitor (Roche, Rotkreuz, Switzerland). The lysates were cleared by centrifugation for 15 min at 17,000 g. Protein concentration was measured by BCA assay (Pierce Biotechnology, IL, USA). Equal amounts of protein (30 μg) were separated by SDS-PAGE and immunoblotted with specific primary antibodies overnight at 4 °C. 1:1000 Anti-c-jun (cat. no. 60A8, Cell Signaling Technologies, Berkeley, CA, USA), 1:1000 p65 (cat. no. D14E12, Cell Signaling Technologies), 1:1000 COX-2 (cat. no. 4842S, Cell Signaling Technologies), 1:10000 anti-actin (A5441, Sigma Aldrich, USA), and 1:3000 anti-TonEBP antibody [7] were used. 1:10000 HRP-conjugated mouse or rabbit secondary antibodies were used for detection. Antigen-antibody binding was detected by chemiluminescent detection reagent (GE Healthcare, NJ, USA).

2.3.3. RNA isolation and quantitative PCR

Total RNA from BV2 cells and mouse hippocampus and cortex was isolated using TRIzol reagent

(Invitrogen, CA, USA) according to the manufacturer's instructions. cDNA was synthesized by M-MLV reverse transcriptase (Promega). After cDNA synthesis, quantitative PCR was performed with SYBR Green I Master Mix and a Light-Cycler 480 II instrument (Roche) using primers shown in Supplementary Table S1. RNA quantity was normalized to the cyclophilin A mRNA.

2.3.4. ELISA

TNF-α in cell culture media was analyzed by ELISA using a commercial kit (cat. no. MTA00B, R&D Systems, MN, USA).

2.3.5. MTT assay

1.5×10^6 BV2 cells were seeded in 10 ml of culture medium and grown overnight. The medium was replaced by 5 ml of medium containing 100 ng/ml of LPS, and then, cultured 24 h to obtain conditioned medium. Each conditioned medium was filtered with a 0.45 μ membrane. HT22 cells were seeded on 96-well plates at a density of 1×10^4 cells per well with 0.2 ml culture medium. After overnight culture, the medium was replaced by the microglia conditioned medium. Twenty-four hours later, 20 μl of 50 mg/ml 3-(4,5-dimethylthiazol-2-yl)-2,5-diphenyltetrazolium bromide (MTT) was added. Reduced MTT was measured by absorbance at 490 nm.).

2.3.6. TUNEL assay

HT22 cells were plated on coverslips and grown overnight. The cells were then switched to the microgliaconditioned medium. After 24 h, TUNEL assay was performed using the DeadEnd™ Fluorometric TUNEL System (cat. no. G3250, Promega, WI, USA) following manufacturer's instructions.

2.3.7. Luciferase assay

Cells were transfected with either an AP-1 luciferase reporter (3xAP1pGL3, www.addgene.org) or a κB-driven luciferase plasmid [11]. Luciferase activity was measured using the Dual-Luciferase Assay System (cat. no. E1910, Promega) as described [11].

2.3.8. Immunoprecipitation assay

MEF cells were treated without or with 10 μM cerulenin (Sigma Aldrich) for 1 h followed by a 1 h treatment with 100 ng/ml LPS. Cell lysates were immunoprecipitated overnight at 4 °C using an anti-c-jun antibody (1:50 dilution) (Cat. No. 60A8, Cell Signaling Technologies) as described previously [11].

2.3.9. Mice

All methods involving live mice were carried out in accordance with approved guidelines. All experimental protocols were approved by the Institutional Animal Care and Use Committee of the Ulsan National Institute of Science and Technology (UNISTACUC-12-15-A). TonEBP$^{fl/fl}$ LysM-Cre and TonEBP$^{fl/fl}$ mice described previously [11] and C57BL/6 J mice were used. The littermates were kept together in the same cage. LysM-Cre mice were purchased from the Jackson Laboratory (cat. No. 004781, Bar Harbor, ME, USA). For experiments, 8-week-old male mice were used.

2.3.10. Stereotaxic surgery

Eight-week-old male mice were anesthetized by intraperitoneal injection of zoletil (20 mg/kg) and rompun (5mg/kg). Animals were positioned on a stereotaxic apparatus and received 3 μl LPS (1 μg/μl 1x PBS) or 1x PBS at a 1 μl/min rate into the left ventricle (0.6mm posterior; 1.2mm lateral; 1.8mm ventral from bregma) following the previously reported stereotaxic coordinates [16]. Some animals received administration of 2mM cerulenin in 3 μl water (6 nmol) or water alone at a rate of 1 μl/min.

2.3.11. Immunohistochemistry

For immunohistochemistry, mice were anesthetized by injecting a mixture of zoletil and rompun as described above. After perfusion with 1x PBS containing 150mM NaCl, 60mM nitrate, and heparin (200u/ml), whole brain was excised and fixed in 8% paraformaldehyde in PBS (pH 7.4) at 4 °C. After 1 day, the fixative solution was replaced with 30% sucrose for an additional 1 day at 4 °C. The fixed brains were cryosectioned at 30 μm and stored in stock solution containing glycerol, ethylene glycol, and 0.2M phosphate buffer. For immunofluorescence detection, sections were washed twice with 1x PBS for 15 min and permeabilized with 0.2% Triton X-100 in BSA/PBS for 1 h. For immunostaining, sections were incubated with 1:500 anti-Iba-1 antibody (cat. no. 019-19741, Wako, Richmond) or 1:500

anti-NeuN antibody (cat. no. MAB377, Millipore) in 0.5% BSA/PBS overnight at 4 °C. Antibody binding was detected with goat anti-rabbit Alexa Fluor 594 or goat anti-mouse Alexa Fluor 594-conjugated secondary antibodies respectively.

2.3.12. Behavior tests

Passive avoidance test Passive avoidance test was used to access short-term memory [17]. Passive avoidance apparatus (cat. no. LE872, Panlab) consists of a light and a dark compartment with an automated sliding door, across which mice can pass. All the tests were performed at 1:00 PM which is in resting phase (light period 06:00–18:00). On day 1 of the experiment, mice were positioned in the light compartment and allowed 30 s of exploration. The sliding door was then opened to induce movement to the dark compartment. This process is repeated 3 times for habituation. On day 2 of the experiment, the same protocol was conducted, but entry into the dark compartment was punished with a mild inescapable electrical shock (0.15 mV). On day 3 of the experiment, the procedure was repeated, and the latency time of each mouse was measured, with a maximum latency time of 5 min. Before each trial, to erase any scent cues, the interior of the maze was sprayed with 70% ethanol. All behavioral experiments were conducted over the same time frame.

Y-maze tests Y-maze test was used to measure spatial working memory by spontaneous alteration [18–20]. Each mouse was placed in the same arm of the maze and allowed to move freely for 10 min. The number of different arm choices and the sequence of choices were recorded to assess percent alteration. Prior to each trial, to erase any scent cues, the interior of the maze was sprayed with 70% ethanol.

2.3.13. Nuclear fractionation

Cell lysates were centrifuged at 500 g. The cell pellet was washed by suspension with 1x PBS. Nuclear and Cytoplasmic extraction kit (cat. no. 78833, Pierce) according to manufacturer's instruction was used for separating the cell nucleus and cytoplasm. Nuclear fraction was confirmed by Lamin B.

2.3.14. Statistical analysis

Data are expressed as the mean + SD or SEM. Statistical significance was estimated using one-way ANOVA or two-way ANOVA with Tukey's post hoc test for multiple comparisons where applicable. All statistical analyses were performed using the GraphPad Prism 5.0 software (GraphPad, CA, USA).

2.4. Results

2.4.1. TonEBP is required for inflammation in BV2 cells

In macrophages [11] and hepatocytes [21], TonEBP is a key component of transcriptional machinery for proinflammatory gene expression in response to LPS and other signals. TonEBP expression increases dramatically in response to LPS in microglia in association with increased iNOS mRNA expression [13] as in macrophages and hepatocytes. We asked what was the role of TonEBP in LPS stimulated expression of pro-inflammatory genes in microglia. To answer this question, we first examined a glial cell line BV2 cells. TonEBP expression increased in response to LPS treatment (Fig. 1a) as in microglia discussed above. iNOS expression also increased in association with elevated levels of nitrite which is a degradation product of nitric oxide (Fig. 1b). The increased iNOS expression was associated with elevation of iNOS mRNA levels along with mRNA levels for other pro-inflammatory enzyme and cytokines COX-2, TNF-α, IL-1β, and IL-6 (Fig. 1c). As expected from the elevated mRNA levels, expression of COX-2 and production of TNF-α also increased (Fig. 1 a and d). When TonEBP was knocked down using lentivirus, mRNA and protein product of the pro-inflammatory enzymes and cytokines all decreased (Fig. 1a–d) indicating a critical role of TonEBP in BV2 cells as in macrophages and hepatocytes. Activated microglia are known to secrete toxic molecules such as reactive oxygen species including nitric oxide, prostaglandin E_2, and cytokines that kill neuronal cells [22]. We found that LPS stimulation of microglia produced neurotoxins as measured by reduced survival of a neuronal cell line HT22 cells (Fig. 1e) that might be due to the secretion of neurotoxins by microglia. The production of neurotoxins was reduced in TonEBP deficient BV2 cells consistent with the reduced production of inflammatory cytokines.

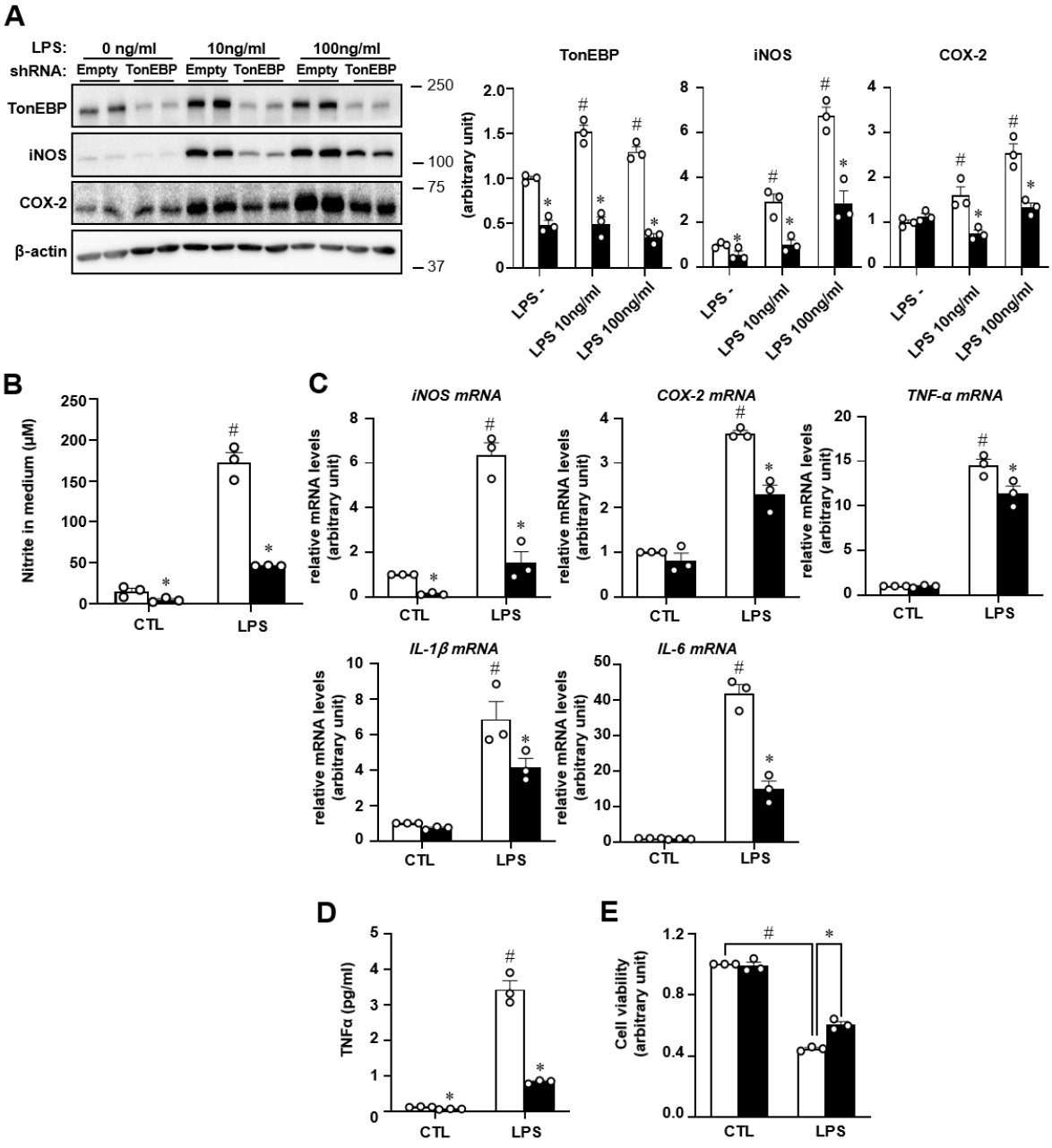

Figure 2.1. TonEBP in LPS-induced inflammation in BV2 cells. BV2 cells were stably transfected using lentivirus containing empty shRNA (open bars in b–e) or TonEBP targeting shRNA (solid bars in b–e) as indicated. **a** The cells were then treated for 24 h with 0 to 100 ng/ml of LPS as indicated and immunoblotted for TonEBP, iNOS, COX-2, and β-actin as shown in left. Right panels show band intensity for TonEBP, iNOS, and COX-2 corrected by intensity of corresponding β-actin band. **b** Nitrite was measured in the media of cells treated for 24 h with 0 (CTL:1x PBS) or 10 ng/ml LPS using Griess reagent. **c** RT-qPCR was performed on cells treated for 1 h (for TNF-α and IL-1β) or 6 h (for iNOS, COX-2, and IL-6) with LPS as in **b**. **d** TNF-α was measured in the medium after the cells were treated

for 6 h with LPS. **e** The stably transfected cells were treated for 24 h with 0 (CTL:1x PBS) or 100 ng/ml LPS to obtain conditioned media. HT22 cells grown in regular medium were switched to the conditioned media. After 24 h, cell viability was measured using MTT assay. Mean + SD, n = 3. *P < 0.05 compared to empty shRNA. #P < 0.05 compared to CTL

2.4.2. Cerulenin blocks LPS-induced inflammation by disrupting TonEBP interaction with NF-κB and AP-1

In macrophages and hepatocytes, TonEBP is central scaffold in the assembly of NF-κB enhanceosome in which TonEBP connects DNA-bound NF-κB to the histone acetyl transferase p300 [11]. Cerulenin inhibits NF-κB actions by breaking up the assembly of the NF-κB enhanceosome. We used cerulenin to ask whether the NF-κB enhanceosome was responsible for the proinflammatory gene expression in BV2 cells. As shown in Fig. 2, cerulenin inhibited mRNA expression and protein expression of the pro-inflammatory enzymes and cytokines demonstrating that the NF-κB enhanceosome was responsible for the transcriptional stimulation. In addition, cerulenin showed clear inhibition on mRNA expression and nitrite production under basal conditions (without LPS treatment). Cell death by the conditioned media was reduced by cerulenin (Fig. 3a) as might be expected from the reduced production of cytokines. In order to exclude the possibility that the presence of cerulenin in the conditioned media was responsible for the reduced neurotoxic activity, cerulenin was directly added to the LPS conditioned medium (Fig. 3b). The presence of cerulenin did not affect neurotoxic activity indicting that cerulenin in the medium was not responsible for the reduced neurotoxic activity. Since the neurotoxic activity was due to cell death by apoptosis [23], we examined apoptosis in the HT22 cells treated with the conditioned medium. The LPS-conditioned media stimulated apoptosis dramatically (Fig. 3c). On the other hand, conditioned media obtained from BV2 cells treated with LPS in the presence of cerulenin caused much less apoptosis indicating that products of the pro-inflammatory genes were responsible for the neuronal death. We noticed that the production of potential neurotoxins was also inhibited by an NF-κB inhibitor BAY11-7092 as expected (Fig. 3a). Activity of an NF-κB reporter was stimulated by LPS, which was completely blocked by cerulenin (Fig. 4a), consistent with the role of the NF-κB enhanceosome in BV2 cells. Interestingly, we found that an AP-1 reporter was also stimulated by LPS, which was blocked by cerulenin (Fig. 4b). Since AP-1 is activated by LPS and contributes to proinflammatory gene expression like NF-κB does [24], we wondered if TonEBP also functioned as a transcriptional cofactor for AP-1. In order to directly test this possibility, we performed co-immunoprecipitation analyses to detect interaction between AP-1 and TonEBP as described previously [11]. When c-jun, a subunit of AP-1, was immunoprecipitated, TonEBP was also brought

down (Fig. 4c) demonstrating the interaction between TonEBP and AP-1. Since TonEBP also interacts with p300 in this setting [11], these data provide evidence that TonEBP is a transcriptional cofactor for AP-1. Of note, the interaction was reduced in the presence of cerulenin suggesting that cerulenin disrupted the interaction between TonEBP and AP-1 (Fig. 4c) as it disrupts the interaction between TonEBP and NF-κB [11]. Cerulenin does not change phosphorylation and translocation of NF-κB [11]. Likewise, we found no changes in phosphorylation and nuclear translocation of c-jun (a subunit of AP-1) by treatment of cerulenin (Supplementary Fig. S2) consistent with disruption of the interaction of TonEBP with AP-1 as well as NF-κB. Since there are AP-1 binding sites as well as NF-κB binding sites in the promoter regions of the pro-inflammatory genes [25–27], the TonEBP's transcriptional cofactor function for both AP-1 and NF-κB is consistent with the cerulenin's strong inhibition shown in Figs. 2 and 3.

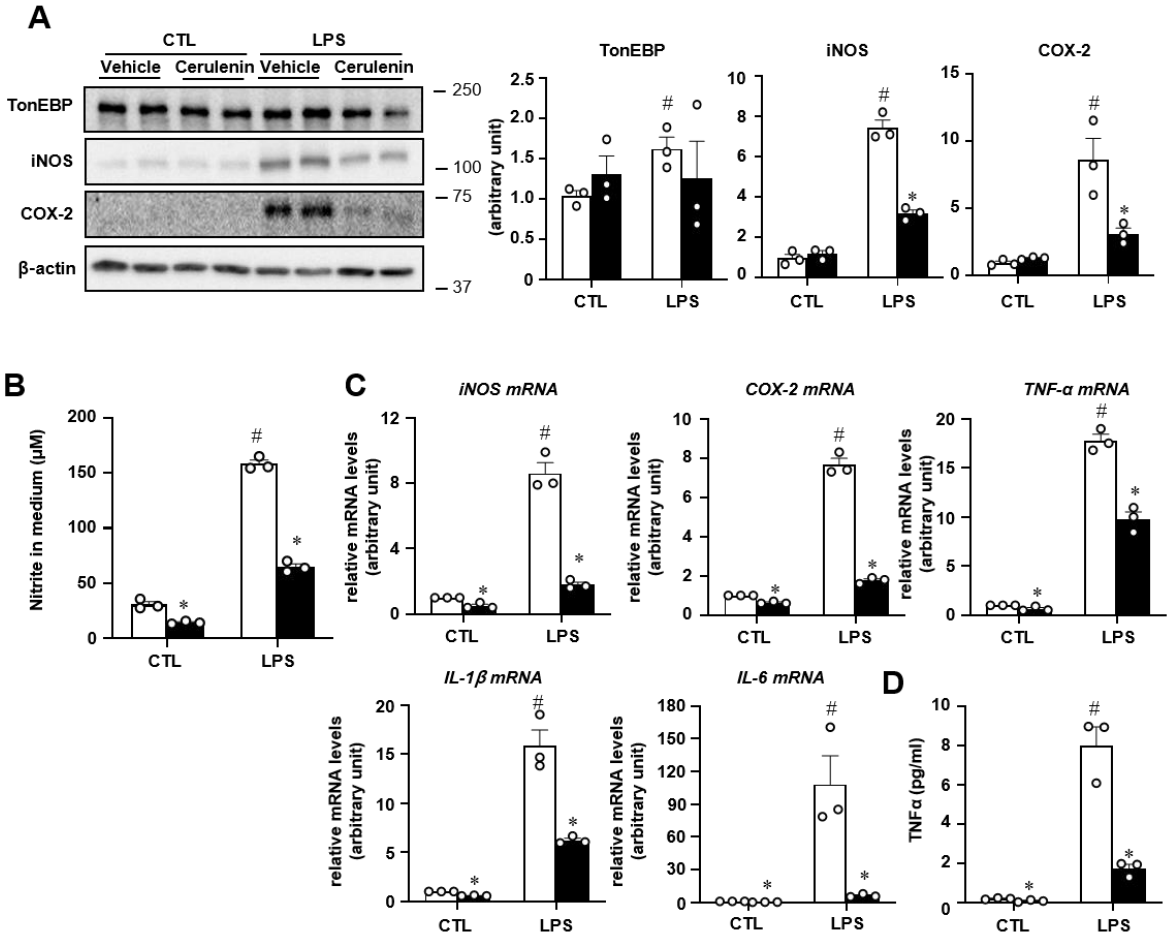

Figure 2.2. Cerulenin inhibits LPS-induced inflammation in BV2 cells. BV2 cells were stably transfected using lentivirus containing empty Cerulenin inhibits LPS-induced inflammation in BV2 cells. **a** The cells were pretreated for 1 h with 10 μM cerulenin (solid bars in b–d) or vehicle (water)

(open bars in **b–d**), followed by a 24 h treatment with 0 (CTL:1x PBS) or 10 ng/ml of LPS. Immunoblotting and quantitation were performed as in Fig. 1. **b** Nitrite was measured from the media of cells treated as above except that LPS treatment was for 24 h. **c** RT-qPCR was performed on cells treated as in **b** except that LPS was treated for 1 h (for TNF-α and IL-1β) or 6 h (for iNOS, COX-2, and IL-6). **d** TNF-α was measured in the medium after the cells were treated as in **b** for 6 h with LPS. Mean + SD, n = 3. *P < 0.05 compared to vehicle. #P < 0.05 compared to CTL

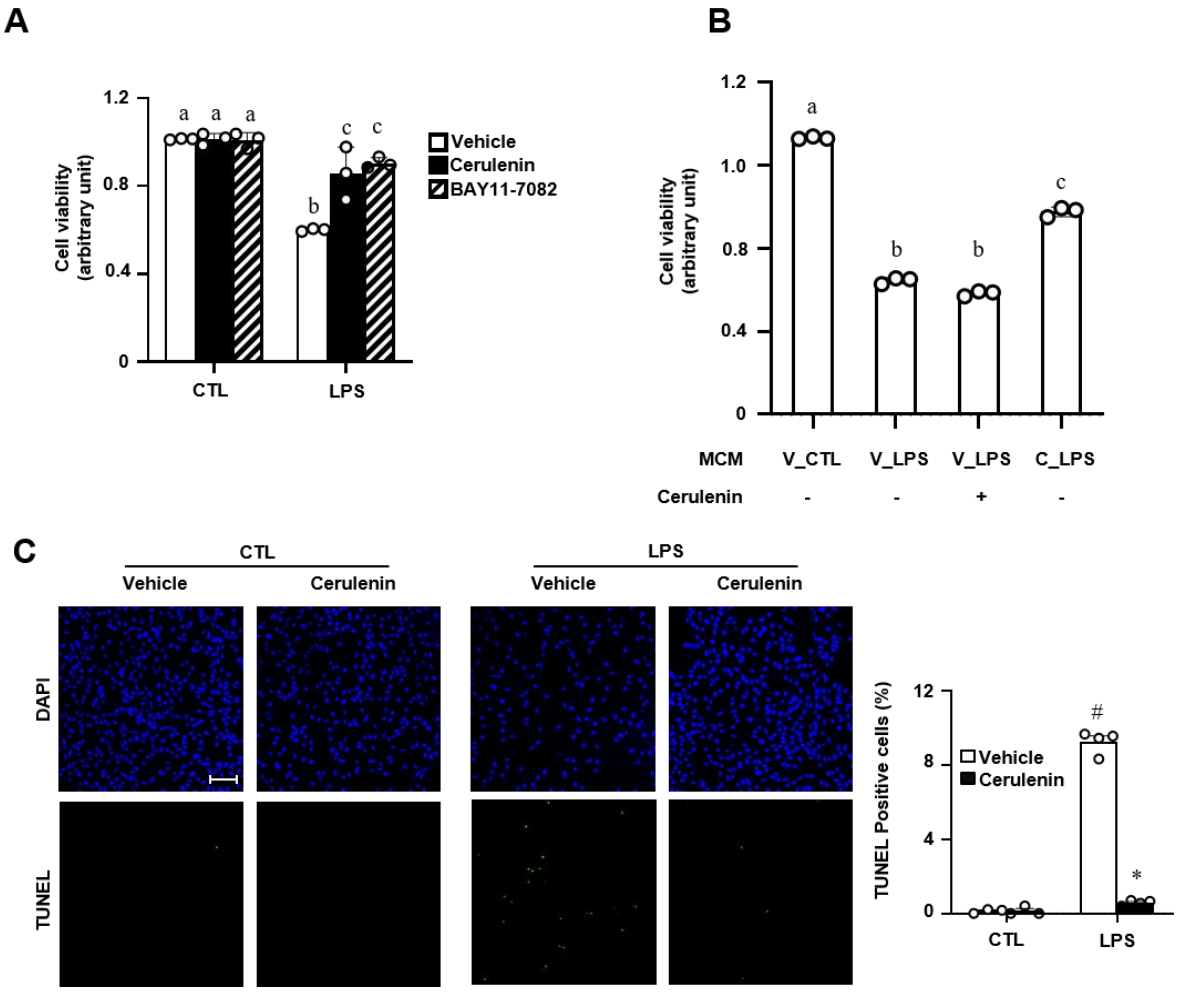

Figure 2.3. Cerulenin blocks LPS-induced secretion of neurotoxins by BV2 cells. a BV2 cells were pretreated for 1 h with vehicle (0.01% DMSO), 10 μM cerulenin, or 5 μM BAY11-7082, followed by treatment for 24 h with 0 (CTL:1x PBS) or 100 ng/ml LPS to obtain conditioned media. HT22 cells grown in regular medium were switched to the conditioned media. After 24 h, cell viability was measured using MTT assay. **b** HT22 cells were cultured in various microglia-conditioned media (MCM) shown with or without addition of 10 μM cerulenin as indicated. Cell viability was measured as above. V, vehicle, C, cerulenin. **c** HT22 cells grown on chamber slides were treated as in **a**: pretreatment with

vehicle or cerulenin followed by treatment with CTL or LPS. Fixed cells were analyzed by TUNEL assay. Nuclei were visualized with DAPI. Percent of TUNEL positive cells are shown on the right. Two-way ANOVA with Tukey's post hoc test was used for multiple comparisons. Bar = 200 μm. Different letters indicate statistical differences at $P < 0.05$. Mean + SD, n = 3-4. *$P < 0.05$, compared to vehicle in **c**. #$P < 0.05$ compared to CTL in **c**

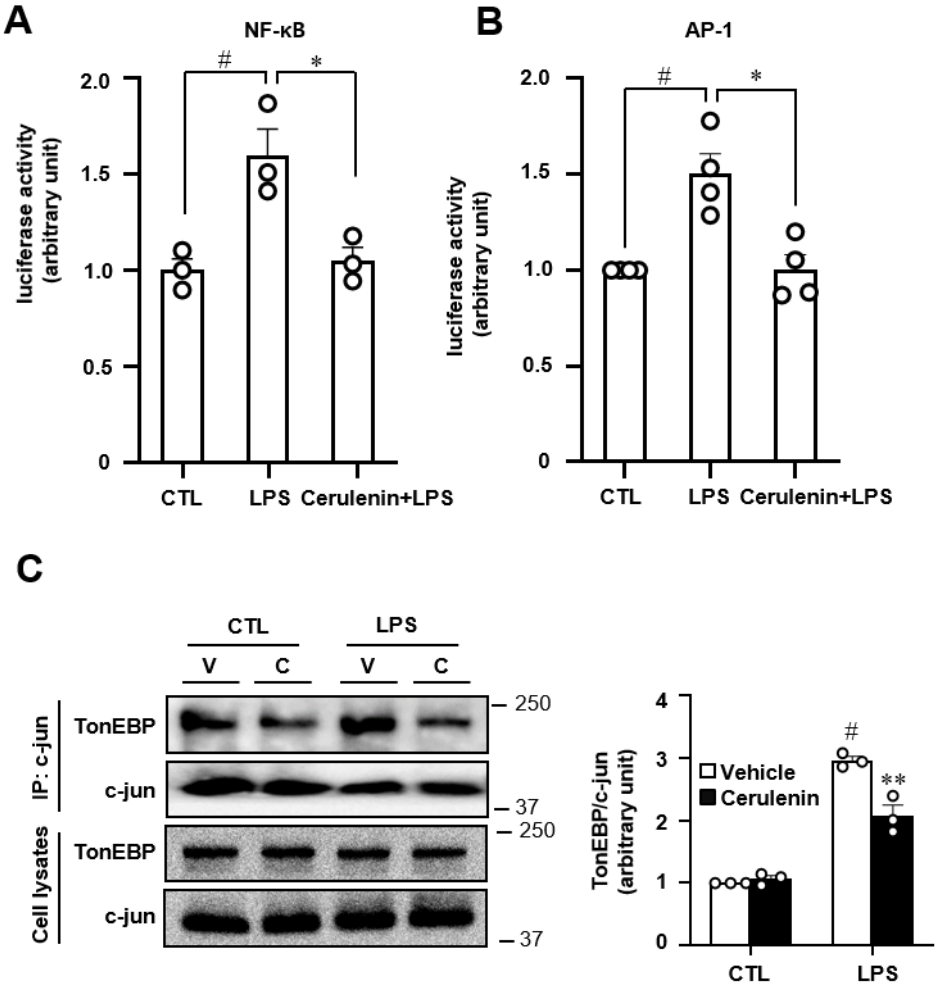

Figure 2.4. Cerulenin inhibits AP-1 transcriptional activity by disrupting its interaction with TonEBP. a BV2 cells were transfected with an NF-κB luciferase reporter. Luciferase activity was measured 3 h after treatment with 100 ng/ml LPS or vehicle (CTL:1x PBS). Where indicated, some cells were pretreated for 1 h with 10 μM cerulenin before treatment with LPS. Mean + SD, n = 3. #$P < 0.05$, compared to LPS. *$P < 0.05$ compared to CTL. **b** BV2 cells were transfected with an AP-1 luciferase reporter. Luciferase activity was measured 3 h after treatment with 100 ng/ml LPS or vehicle (CTL:1x PBS). Where indicated, some cells were pretreated for 1 h with 10 μM cerulenin before treatment with LPS. Mean + SD, n = 4. #$P < 0.05$, compared to LPS. *$P < 0.05$ compared to CTL. **c**

MEF cells were pretreated with cerulenin (C) or vehicle (V) followed by treatment with LPS as above. Cell lysates were immunoprecipitated using c-jun antibodies and then immunoblotted for TonEBP and c-jun as shown in left. Right panel shows band intensity for TonEBP corrected by intensity of corresponding c-jun band. **P < 0.05 compared to vehicle. #P < 0.05 compared to CTL

2.4.3. TonEBP mediates LPS-induced microglial activation

In order to directly assess the role of TonEBP in microglial activation in response to LPS, myeloid-specific TonEBP gene deletion was used. We crossed a floxed TonEBP line ($TonEBP^{fl/fl}$) with a transgenic line with cre recombinase expression under the control of lysozyme promoter (LysM-Cre) to produce $TonEBP^{fl/fl}$ LysM-Cre mice [11]. Efficiency of microglial gene deletion in the LysM-Cre line is reported to be 90% [28]. Eight-week-old male $TonEBP^{fl/fl}$ LysM-Cre mice and their $TonEBP^{fl/fl}$ littermates were used for experiments. To induce inflammation of the brain, we performed intracerebroventricular injection of LPS as described [13]. Cortex (CTX) and hippocampus (HIP) were processed for immunostaining and RNA analysis 3 h after LPS injection. Microglial activation was detected by immunohistochemical visualization of Iba-1, a marker for activated microglia [29]. Based on increased area of Iba-1-positive area and number of Iba-1-positive cells, LPS injection resulted in a clear activation of microglia in the $TonEBP^{fl/fl}$ animals (Fig. 5a). The activation was associated with elevated levels of mRNA for TNF-α and IL-1β (Fig. 5b). Both the microglial activation and elevation of mRNA levels were blocked in the animals with myeloidspecific TonEBP deletion, i.e., in the $TonEBP^{fl/fl}$ LysM-Cre animals. These data demonstrate that myeloid TonEBP is required for inflammatory microglial activation. Next, we asked whether TonEBP-dependent actions of NF-κB and AP-1 were involved in the microglial activation. Cerulenin was injected into the brain 1 h prior to LPS injection described above. Cerulenin blocked the activation of microglia (Fig. 6a) and the increased expression of mRNA for TNF-α and IL-1β (Fig. 6b). These data show that TonEBP mediates microglial activation by stimulating the transcriptional activity of NF-κB and AP-1.

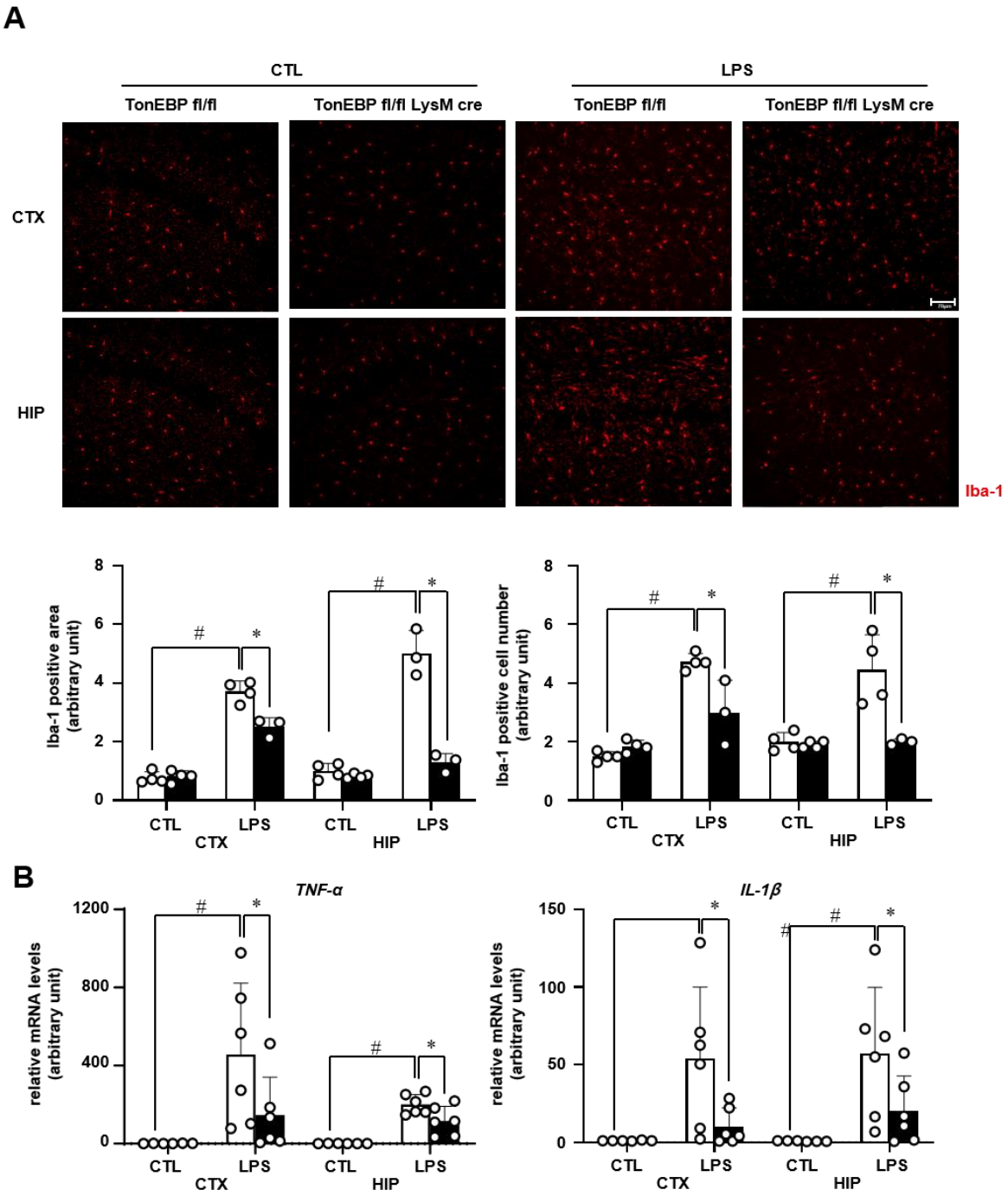

Figure 2.5. Myeloid TonEBP is required for LPS-induced microglia activation. LPS (3 μg per animal) or vehicle (CTL:1x PBS) was injected into the left ventricle of male TonEBPfl/fl,LysM-cre mice (solid bars) and their TonEBPfl/fl littermates (open bars). Brains were analyzed 3 h later. **a** Brains were perfusion-fixed and immunostained for iba-1. Images from cortex (CTX) and hippocampus (HIP) (top) were analyzed for iba-1 positive areas and iba-1 positive cell numbers (bottom). Bar = 70 μm. **b** RNA was isolated from CTX and HIP, and analyzed by RT-qPCR for TNF-α and IL-1β. Mean + SE, n

= 3–6. #P < 0.05, compared to CTL. *P < 0.05 compared to TonEBP fl/fl

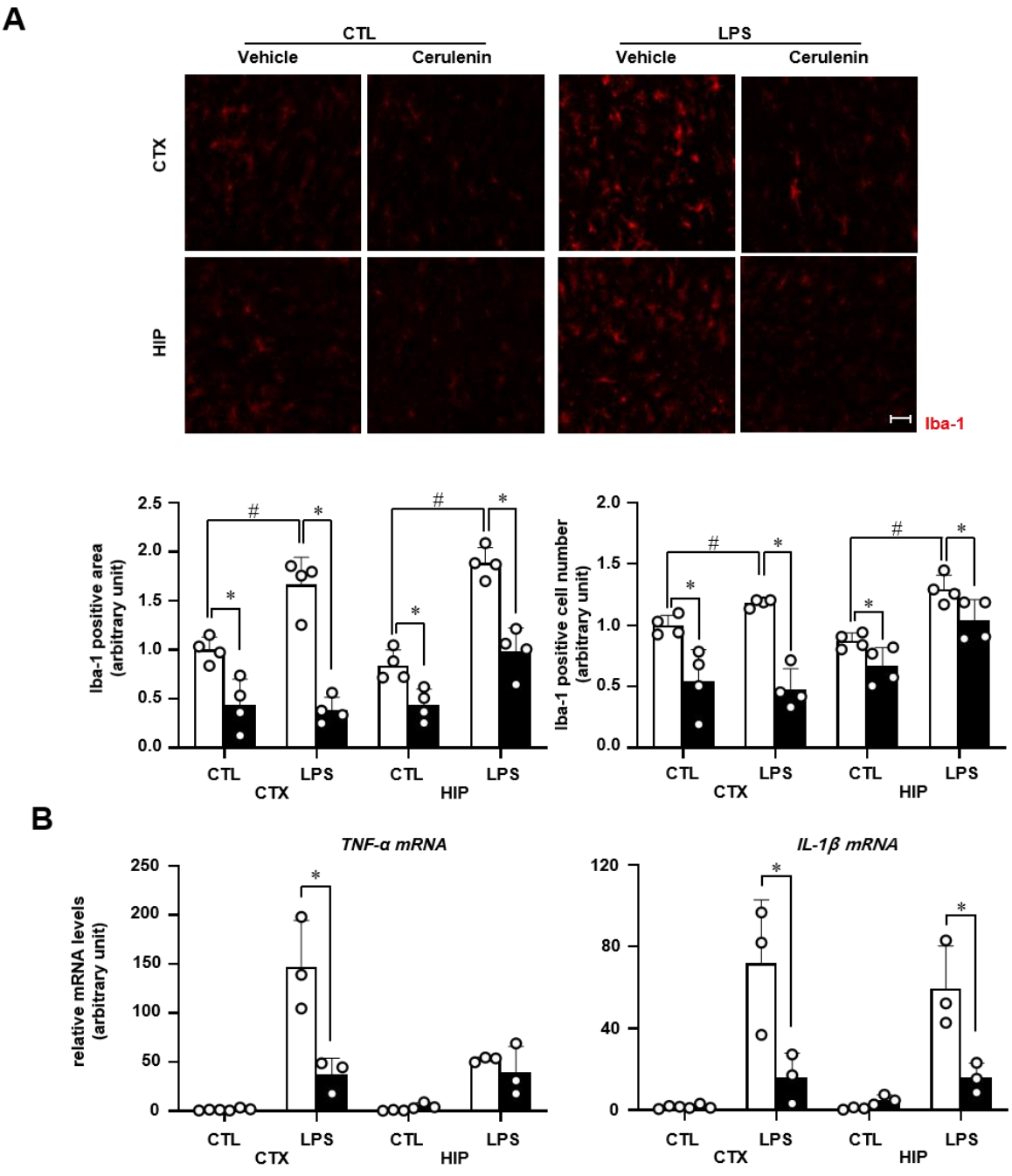

Figure 2.6. Cerulenin inhibits LPS-induced microglia activation. Cerulenin (6 nmol per animal, solid bars) or vehicle (water) (open bars) was injected into the left ventricle. One hour later, LPS (3 μg per animal) or vehicle (CTL:1x PBS) was injected again. Brains were analyzed 3 h later. **a** Brains were perfusion-fixed and immunostained for iba-1. Images from cortex (CTX) and hippocampus (HIP) (top) were analyzed for iba-1 positive area and iba-1 positive cell number (bottom). Bar = 70 μm. **b** RNA

was isolated from CTX and HIP and analyzed by RT-qPCR for TNF-α and IL-1β. Mean + SE, n = 3–4. #P < 0.05, compared to CTL. #P < 0.05, compared to CTL. *P < 0.05 compared to vehicle

2.4.4. TonEBP mediates LPS-induced memory loss in association with reduced number of neuronal cells

Since TonEBP mediates LPS-induced neuroinflammation (see above) and neuroinflammation induces memory loss [30, 31], we asked whether TonEBP is required from LPS-induced memory loss. The male TonEBP$^{fl/fl}$ LysM-Cre mice and their TonEBP$^{fl/fl}$ littermates were injected with LPS or vehicle as described above. Two weeks later, passive avoidance test was performed to assess short-term memory followed by histological analysis of the brains. Short term memory measured by latency in passive avoidance test was halved in the TonEBP$^{fl/fl}$ mice (Fig. 7a) in association with reduced number of neurons in the CA3 region of the hippocampus (Fig. 7b). The reduced neuronal cell number was likely due to cell death as observed in BV2 cells whose TonEBP was knockdown (Fig. 1e). These changes were not observed in the TonEBPfl/fl LysM-Cre mice suggesting that TonEBP is required for the LPS-induced neuronal cell death and memory loss. In order to examine the role of TonEBP-mediated actions of NF-κB and AP-1, we examined the effects of cerulenin. LPS or vehicle was injected into the brain of 8-week male mice as described above. Y-maze test was performed after 1 week to assess spatial memory, and passive avoidance test after 2 weeks as described above (Fig. 8a). In animals injected with LPS, both spatial memory and short-term memory were significantly reduced (Fig. 8b, c) in association with reduced number of neurons in the CA3 region of the hippocampus (Fig. 8d). These changes were blocked when cerulenin was pretreated 1 h before the LPS administration suggesting that TonEBP-mediated neuroinflammation causes neuronal cell death and memory loss. (Supplementary Fig. 1)

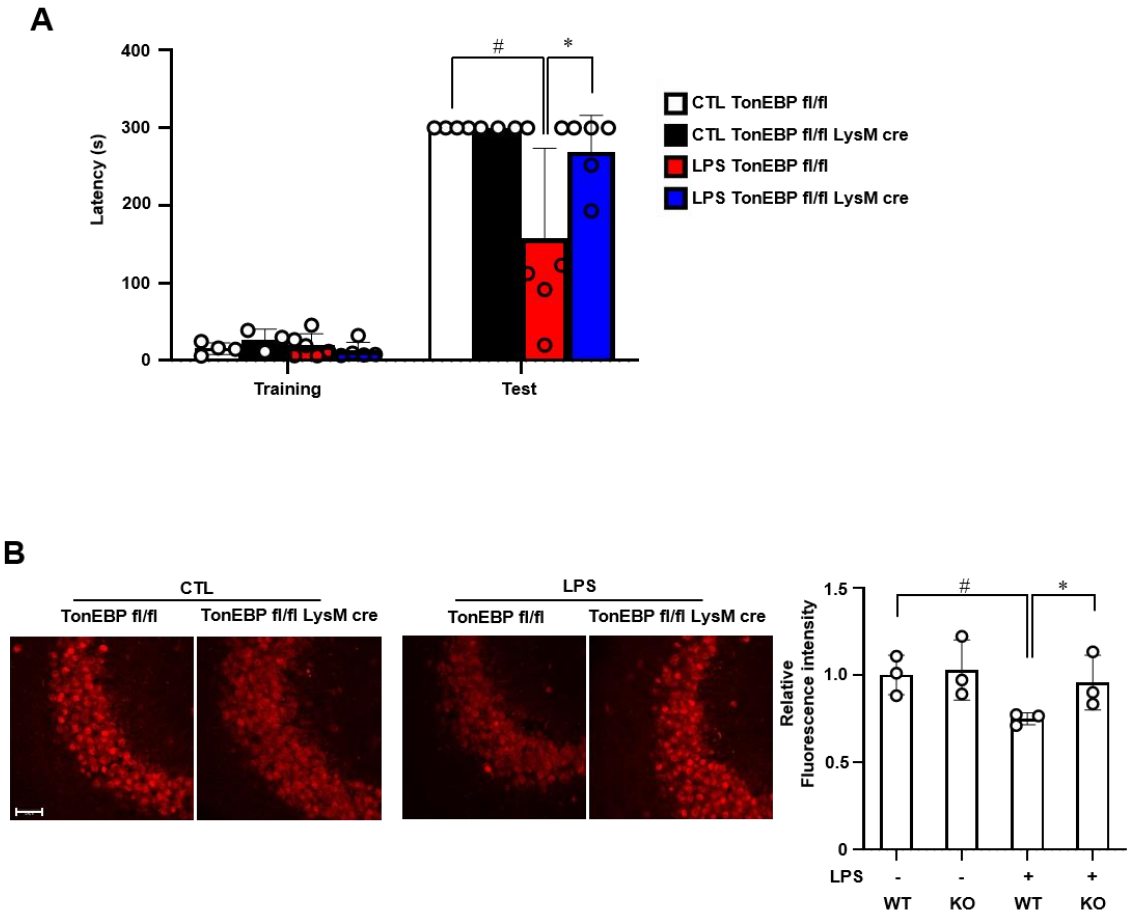

Figure 2.7. Myeloid TonEBP is required for blocking LPS-induced loss of short-term memory. a LPS (3 μg per animal) or vehicle (CTL:1x PBS) was injected into the left ventricle of male TonEBPfl/fl,LysM-cre mice (KO in **b**) and their TonEBPfl/fl littermates (WT in **b**). Two weeks later, passive avoidance test was performed followed by perfusion fixation of the brains. Latency in seconds in passive avoidance test. Mean + SE, n = 3–6. *P < 0.05 B NeuN immunostaining in CA3 region of hippocampus. Florescence intensity of the immunostaining was shown on the right. Bar =50 μm. Mean + SE, n = 3. #P < 0.05, compared to CTL. *P < 0.05 compared to TonEBP fl/fl

2.5. Discussion

The activation of microglia contributes to aging [32, 33] and the pathogenesis of neurodegenerative diseases such as Alzheimer's disease [34–36]. NF-κB and AP-1 are essential transcriptional regulators for the activation of microglia [37–39] as well as for pro-inflammatory activation of macrophages [40, 41]. In macrophages, TonEBP is a key mediator of LPS-induced activation of proinflammatory gene expression [11, 42, 43]. This is achieved in two ways: elevation of TonEBP expression and TonEBP functioning as transcriptional cofactor for NF-κB. Here, we find that TonEBP has the same role in microglia. In addition, we discover that TonEBP is also the transcriptional cofactor for AP-1. In settings of LPS-induced microglial activation and neuronal damage, the TonEBP-mediated actions of AP-1 and NF-κB are required for the inflammatory activation of microglia based on observations from TonEBP deleted animals and effects of cerulenin, which inhibits AP-1 and NF-κB by blocking their interactions with TonEBP and p300. Thus, TonEBP mediates the LPS-induced microglial activation and neuronal damage as transcriptional cofactor for AP-1 and NF-κB, which are the major transcription factors in the pro-inflammatory gene expression.

Neuroinflammation is associated with aging [44, 45], metabolic diseases [46], and a variety of neurodegenerative diseases such as Alzheimer's disease [47, 48], Parkinson's disease [49], multiple sclerosis [50], and amyotrophic lateral sclerosis [51]. Various causes including obesity, diabetes, hypertension, and even lifestyles increase systemic inflammatory response [52, 53]. Systemic increase in proinflammatory mediators (cytokines, chemokines, ROS, and secondary messengers) enhances microglial cell activation [53], which makes neuroinflammation as a disease promoting factor in neurodegenerative diseases. The activated microglia cause neuronal death via inflammatory factors, A1 astrocyte activation, and microglia-mediated synapse loss [5, 6]. Our data presented here uncovers the role of microglial TonEBP in neuronal death. Targeting the TonEBP/AP-1/NF-κB pathway should be an attractive strategy to prevent the neuronal death. In this regard, the actions of cerulenin in inhibiting the prototypical proinflammatory transcription factors AP-1 and NF-κB by disrupting their interactions with TonEBP rather than direct inhibition (such as nuclear translocation or phosphorylation) provide a new mode of intervention and potential therapeutics.

2.6. Conclusions

In sum, this study has shown that TonEBP is required for the LPS-induced microglial activation and proinflammatory gene expression. TonEBP mediates the transcriptional activity of the classical pro-inflammatory transcription factors NF-κB and AP-1. Deletion of TonEBP in myeloid cells or treatment with cerulenin blocks the TonEBP-mediated activation of NF-κB and AP-1, microglial activation, and subsequent neuronal damages. Thus, we have delineated intracellular pathways involved in the microglial activation relevant to neuronal damage.

2.7. Supplementary Figures

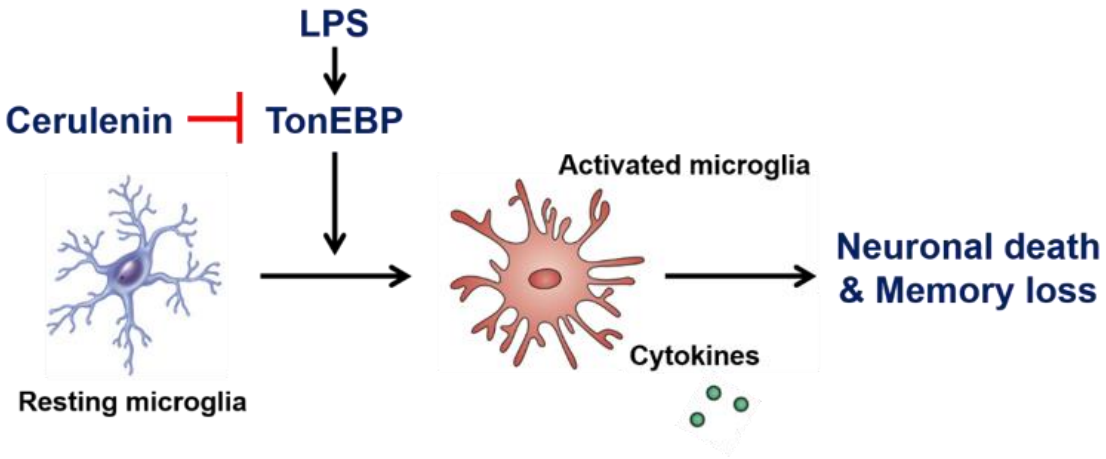

Figure 2.S1. Model of TonEBP in microglia-mediated memory loss induced by LPS.

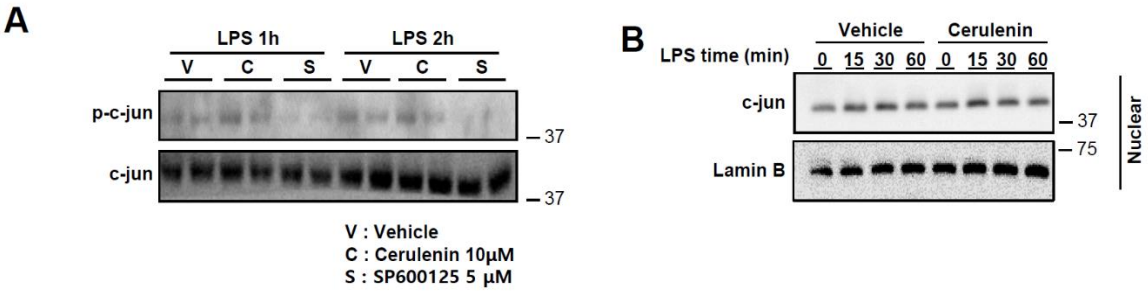

Figure 2.S2. Effects of cerulenin in phosphorylation and nuclear translocation of c-jun. A BV2 cells were pretreated for 1 h with vehicle (V), 10 μM cerulenin (C), or 5 μM SP600125 (S, a JNK inhibitor), followed by treatment with 10 ng/ml of LPS for 1 or 2 h as indicated. Cell lysates were immunoblotted for phosphorylated c-jun (p-c-jun) and c-jun. **B** Cells were pretreated for 1 h with vehicle or cerulenin, followed by a treatment with LPS for up to 60 min as indicated. Nuclear fractions were obtained as described in Methods and immunoblotted for c-jun and Lamin B.

2.8. References

1. DiSabato DJ, Quan N, Godbout JP. Neuroinflammation: the devil is in the details. J Neurochemistry. 2016;139(Suppl 2):136–53.

2. Ginhoux F, Prinz M. Origin of microglia: current concepts and past controversies. Cold Spring Harbor perspectives in biology. 2015;7(8):a020537.

3. Yang I, Han SJ, Kaur G, Crane C, Parsa AT. The role of microglia in central nervous system immunity and glioma immunology. J Clin Neuroscience. 2010;17(1):6–10.

4. Heppner FL, Ransohoff RM, Becher B. Immune attack: the role of inflammation in Alzheimer disease. Nature Reviews Neuroscience. 2015;16(6):358–72.

5. Frakes AE, Ferraiuolo L, Haidet-Phillips AM, Schmelzer L, Braun L, Miranda CJ, et al. Microglia induce motor neuron death via the classical NF-κB pathway in amyotrophic lateral sclerosis. Neuron. 2014;81(5):1009–23.

6. Li Q, Barres BA. Microglia and macrophages in brain homeostasis and disease. Nature reviews Immunology. 2018;18(4):225–42.

7. Miyakawa H, Woo SK, Dahl SC, Handler JS, Kwon HM. Tonicity-responsive enhancer binding protein, a rel-like protein that stimulates transcription in response to hypertonicity. Proc Nat Acad Sci United States of America. 1999;96(5):2538–42.

8. López-Rodríguez C, Aramburu J, Rakeman AS, Rao A. NFAT5, a constitutively nuclear NFAT protein that does not cooperate with Fos and Jun. Proc Natl Acad Sci U S A. 1999;96(13):7214–9.

9. Choi SY, Lee-KwonW, Kwon HM. The evolving role of TonEBP as an immunometabolic stress protein. Nature Reviews Nephrology. 2020;16(6):352–64.

10. López-Rodríguez C, Antos CL, Shelton JM, Richardson JA, Lin F, Novobrantseva TI, et al. Loss of NFAT5 results in renal atrophy and lack of tonicity-responsive gene expression. Proceedings of the National Academy of Sciences of the United States of America. 2004;101(8):2392–7.

11. Lee HH, Sanada S, An SM, Ye BJ, Lee JH, Seo YK, et al. LPS-induced NFκB enhanceosome requires TonEBP/NFAT5 without DNA binding. Scientific reports. 2016;6:24921.

12. Loyher ML, Mutin M, Woo SK, Kwon HM, Tappaz ML. Transcription factor tonicity-responsive

enhancer-binding protein (TonEBP) which transactivates osmoprotective genes is expressed and upregulated following acute systemic hypertonicity in neurons in brain. Neuroscience. 2004;124(1):89–104.

13. Jeong GR, Im S-K, Bae Y-H, Park ES, Jin BK, Kwon HM, et al. Inflammatory signals induce the expression of tonicity-responsive enhancer binding protein (TonEBP) in microglia. J Neuroimmunology. 2016;295-296:21–9.

14. Wenker SD, Chamorro ME, Vittori DC, Nesse AB. Protective action of erythropoietin on neuronal damage induced by activated microglia. FEBS J.2013;280(7):1630–42.

15. Shukla SM, Sharma SK. Sinomenine inhibits microglial activation by Aβ and confers neuroprotection. J Neuroinflammation. 2011;8:117.

16. Franklin KB, Paxinos G. The mouse brain in stereotaxic coordinates; 2008.

17. Ortiz O, Delgado-García JM, Espadas I, Bahí A, Trullas R, Dreyer JL, et al. Associative learning and CA3-CA1 synaptic plasticity are impaired in D1R null, Drd1a-/- mice and in hippocampal siRNA silenced Drd1a mice. J Neuroscience. 2010;30(37):12288–300.

18. Bryan KJ, Lee HG, Perry G, Smith MA, Casadesus G. Frontiers in Neuroscience Transgenic mouse models of Alzheimer's disease: behavioral testing and considerations. In: Buccafusco JJ, editor. Methods of behavior analysis in neuroscience. Boca Raton (FL): CRC Press/Taylor & Francis Copyright © 2009, Taylor & Francis Group, LLC; 2009.

19. Meunier J, Ieni J, Maurice T. The anti-amnesic and neuroprotective effects of donepezil against amyloid beta25-35 peptide-induced toxicity in mice involve an interaction with the sigma1 receptor. Brit J Pharmacol. 2006;149(8):998–1012.

20. Tsunekawa H, Noda Y, Mouri A, Yoneda F, Nabeshima T. Synergistic effects of selegiline and donepezil on cognitive impairment induced by amyloid beta (25-35). Behavioural brain research. 2008;190(2):224–32.

21. Lee JH, Suh JH, Choi SY, Kang HJ, Lee HH, Ye BJ, et al. Tonicity-responsive enhancer-binding protein promotes hepatocellular carcinogenesis, recurrence and metastasis. Gut. 2019;68(2):347–58.

22. Lull ME, Block ML. Microglial activation and chronic neurodegeneration. Neurotherapeutics : the journal of the American Society for Experimental NeuroTherapeutics. 2010;7(4):354–65.

23. Guadagno J, Xu X, Karajgikar M, Brown A, Cregan SP. Microglia-derived TNFα induces apoptosis in neural precursor cells via transcriptional activation of the Bcl-2 family member Puma. Cell death &

disease. 2013;4(3):e538.

24. Chanput W, Mes J, Vreeburg RA, Savelkoul HF, Wichers HJ. Transcription profiles of LPS-stimulated THP-1 monocytes and macrophages: a tool to study inflammation modulating effects of food-derived compounds. Food Function. 2010;1(3):254–61.

25. Hannemann N, Jordan J, Paul S, Reid S, Baenkler HW, Sonnewald S, et al. The AP-1 transcription factor c-Jun promotes arthritis by regulating cyclooxygenase-2 and arginase-1 expression in macrophages. J Immunology (Baltimore, Md : 1950). 2017;198(9):3605–14.

26. Foletta VC, Segal DH, Cohen DR. Transcriptional regulation in the immune system: all roads lead to AP-1. Journal of leukocyte biology. 1998;63(2):139–52.

27. Redhu NS, Saleh A, Halayko AJ, Ali AS, Gounni AS. Essential role of NF-κB and AP-1 transcription factors in TNF-α-induced TSLP expression in human airway smooth muscle cells. American journal of physiology Lung cellular and molecular physiology. 2011;300(3):L479–85.

28. Pulido-Salgado M, Vidal-Taboada JM, Garcia Diaz-Barriga G, Serratosa J, Valente T, Castillo P, et al. Myeloid C/EBPβ deficiency reshapes microglial gene expression and is protective in experimental autoimmune encephalomyelitis. Journal of neuroinflammation. 2017;14(1):54.

29. Kanazawa H, Ohsawa K, Sasaki Y, Kohsaka S, Imai Y. Macrophage/microgliaspecific protein Iba1 enhances membrane ruffling and Rac activation via phospholipase C-gamma -dependent pathway. The Journal of biological chemistry. 2002;277(22):20026–32.

30. Choi DY, Lee JW, Lin G, Lee YK, Lee YH, Choi IS, et al. Obovatol attenuates LPS-induced memory impairments in mice via inhibition of NF-κB signaling pathway. Neurochemistry international. 2012;60(1):68–77.

31. Zhao J, Bi W, Xiao S, Lan X, Cheng X, Zhang J, et al. Neuroinflammation induced by lipopolysaccharide causes cognitive impairment in mice. Scientific reports. 2019;9(1):5790.

32. Von Bernhardi R, Eugenin-von Bernhardi L, Eugenin J. Microglial cell dysregulation in Brain Aging and Neurodegeneration. Front Aging Neurosci. 2015;7:124.

33. Norden DM, Godbout JP. Review: microglia of the aged brain: primed to be activated and resistant to regulation. Neuropathology and applied neurobiology. 2013;39(1):19–34.

34. Hemonnot A-L, Hua J, Ulmann L, Hirbec H. Microglia in Alzheimer disease:

well-known targets and new opportunities. Front Aging Neurosci. 2019;11:233.

35. Mandrekar-Colucci S, Landreth GE. Microglia and inflammation in Alzheimer's disease. CNS & neurological disorders drug targets. 2010;9(2):156–67.

36. Navarro V, Sanchez-Mejias E, Jimenez S, Muñoz-Castro C, Sanchez-Varo R, Davila JC, et al. Microglia in Alzheimer's disease: activated, dysfunctional or degenerative. Front Aging Neurosci. 2018;10:140.

Chapter 3. TonEBP in myeloid cells promotes obesity-induced insulin resistance and inflammation through adipose tissue remodeling

3.1. Abstract

The phenotypic and functional plasticity of adipose tissue macrophages during obesity play a crucial role in orchestration of adipose and systemic inflammation. Tonicity-responsive enhancer-binding protein (TonEBP, also called NFAT5) is a stress protein that mediates cellular responses to a range of metabolic insults. Here, we show that myeloid cell-specific TonEBP depletion reduced inflammation and insulin resistance in mice with high-fat diet-induced obesity, but did not affect adiposity. This phenotype was associated with a reduced accumulation and a reduced pro-inflammatory phenotype of metabolically activated macrophages; decreased expression of inflammatory factors related to insulin resistance; and enhanced insulin sensitivity. TonEBP expression was elevated in the adipose tissue macrophages of obese mice, and Sp1 was identified as a central regulator of TonEBP induction. TonEBP depletion in macrophages decreased induction of insulin resistance-related genes and promoted induction of insulin sensitivity-related genes under obesity-mimicking conditions, and thereby improved insulin signaling and glucose uptake in adipocytes. mRNA expression of TonEBP in peripheral blood mononuclear cells was positively correlated with blood glucose levels in mice and humans. These findings suggest that TonEBP in macrophages promotes obesity-associated systemic insulin resistance and inflammation, and downregulation of TonEBP may induce a healthy metabolic state during obesity.

3.2. Introduction

Obesity is associated with chronic low-grade inflammation characterized by progressive accumulation of immune cells in metabolic tissues, especially visceral adipose tissue [1]. Adipose tissue inflammation is considered to be a main driving force for the development of insulin resistance and type 2 diabetes (T2D) in obese individuals [2]. As a major cell type that contributes to inflammatory responses, macrophages accumulate in the adipose tissue of humans and rodents with increasing body weight [3] and adipose tissue macrophages (ATMs) are major effector cells that orchestrate adipose and systemic inflammation in obesity [4].

Macrophages are highly heterogeneous and possess broad plasticity, which means that they can change their phenotypes and distinct functional activation states according to local environmental factors, and thereby play distinct roles in regulation of tissue homeostasis and inflammation [5]. They are generally classified as pro-inflammatory M1 macrophages or anti-inflammatory M2 macrophages [6]. Traditionally, ATMs are considered to accumulate during obesity due to recruitment of circulating monocytes and subsequent differentiation into macrophages [7, 8]. In addition to the increased number of ATMs, the phenotype of these cells dramatically changes during obesity. ATMs in the lean state typically have an anti-inflammatory-like phenotype, which helps to maintain tissue homeostasis. By contrast, ATMs during obesity respond to metabolic cues such as excess free fatty acids (FFAs), glucose, and gut-derived endotoxin, and adopt a metabolically activated (MMe) phenotype that is distinct from M1 or M2 activation [9, 10]. MMe ATMs exert both detrimental and beneficial functions via independent pro-inflammatory and anti-inflammatory pathways during obesity [9, 10]. Thus, the balance between these two pathways in MMe ATMs could result in distinct metabolic states and influence the progression of obesity and its common comorbidities, including glucose intolerance and T2D.

Tonicity-responsive enhancer-binding protein (TonEBP), also known as nuclear factor of activated T-cells 5 (NFAT5), is a pleiotropic stress protein involved in distinct stress responses in various cell types [11]. It can mediate physiological or pathological responses depending on the context. For example, TonEBP-mediated responses to osmotic stress, bacterial infection, and genotoxin-induced DNA damage are protective. By contrast, TonEBP-mediated responses to autoimmune and metabolic stresses are pathogenic in human diseases such as autoimmune diseases, acute kidney injury, hepatocellular carcinoma, atherosclerosis, and obesity [11]. Many pathological conditions and agents stimulate TonEBP expression in T-cells, macrophages, and dendritic cells, and elevated levels of

TonEBP promote pathogenic activation of these cells in a cell type-specific manner [11]. Numerous studies show that TonEBP promotes inflammatory and autoimmune diseases in humans and rodents. Conversely, downregulation of TonEBP reduces inflammation and thereby helps to prevent these diseases [11]. Although the role of TonEBP in macrophages is well-studied, relatively little is known about its intrinsic role in the identity and function of ATMs during obesity. Therefore, this study examined the impact of macrophage TonEBP in the context of obesity-associated inflammation and insulin resistance. We found that TonEBP expression was elevated in the ATMs of HFD-induced obese mice, and this promoted the development of obesity-associated inflammation and insulin resistance. Consequently, myeloid TonEBP-deficient mice showed reduced inflammation and insulin resistance, and were protected against obesity-induced metabolic dysfunction. Thus, we identified TonEBP as a crucial factor in the activation states of ATMs and in the control of metabolic dysfunction during obesity.

3.3. RESEARCH DESIGN AND METHODS

Mice

All animal procedures were approved by and performed according to guidelines of the Institutional Animal Care and Use Committee of the Ulsan National Institute of Science and Technology (UNISTACUC-20-27). Lysozyme 2-cre knock-in (LysM-cre) mice were obtained from the Jackson Laboratory (Bar Harbor, ME, USA). TonEBPfl/fl mice [12] were crossed with LysM-cre heterozygous mice to generate mice lacking TonEBP in myeloid cells. For the obese mice model, male mice aged 8 weeks were fed a CD (10% fat as kcal; Research Diets, New Brunswick, NJ, USA) or HFD (60% fat as kcal; Research Diets) for 12 weeks. Age-matched littermates without the Cre transgene were used as controls. Mouse bone marrow (BM)-derived macrophages (BMDMs) were obtained by culturing BM cells with macrophage colony-stimulating factor (M-CSF) for 7 days [13]. Mouse mononuclear cells isolated from BM or blood using Histopaque-1077 (Sigma-Aldrich, St. Louis, MO, USA). Monocytes were further purified by positive selection on CD11b microbeads followed by separation on MACS columns (Miltenyi Biotec, Bergisch, Germany).

Human samples

The study was approved by the Institutional Review Board of the Ulsan National Institute of Science and Technology (UNISTIRB-15-25-A). Human monocyte-derived macrophages were prepared by macrophage colony-stimulating factor (M-CSF) [14]. Human peripheral blood mononuclear cells (PBMCs) from diabetic and healthy subjects were provided by the Seoul National University Hospital Human Biobank, a member of the National Biobank of Korea, which is supported by the Ministry of Health and Welfare. All samples derived from the National Biobank of Korea were obtained with informed consent under institutional review board-approved protocols.

Cell culture, transfection, and adenovirus infection

Human monocyte-like THP-1 cells (ATCC TIB-202) were cultured in RPMI-1640 containing 10% FBS, and then differentiated into macrophages by exposure to 5 ng/ml phorbol 12-myristate 13-acetate (PMA; Sigma-Aldrich) for 2 days. The murine macrophage cell line RAW264.7 (ATCC TIB-71) was cultured in DMEM containing 10% FBS. All siRNA duplexes were purchased from Integrated DNA

Technologies (Coralville, IA, USA). PMA-differentiated THP-1 macrophages and RAW264.7 cells were transfected with scrambled (Scr) siRNA or siRNAs specific for target genes for 48 h using Lipofectamine RNAiMAX (Invitrogen, Carlsbad, CA, USA). For overexpression, RAW264.7 cells were infected with an empty vector control virus (Ad-EV) or an adenovirus carrying the human TonEBP gene (Ad-TonEBP) at a multiplicity of infection of 50 for 24 h.

Immunohistochemistry

Tissue sections of Epi-WAT and liver were stained with hematoxylin–eosin (H&E) to examine morphological changes. Immunohistochemistry was performed by incubating samples with primary antibodies as indicated. Images were recorded using an Olympus FV1000 confocal fluorescence microscope. Signal intensity was determined using ImageJ software (http://imagej.nih.gov/ij/).

Flow cytometry

Cells were immunophenotyped by flow cytometry using multicolor fluorochrome-conjugated antibodies. Cell surface markers were identified using primary antibodies purchased from BD Biosciences (Franklin Lakes, NJ, USA; Supplementary Table 1). Flow cytometry data were acquired on a BD LSR Fortessa instrument (BD Biosciences) and analyzed using FlowJo software (Tree Star, Ashland, OR, USA).

Real-time PCR

Total RNA was extracted from tissues and cells using TRIzol reagent (Invitrogen). After reverse transcription, real-time PCR was performed using CFX384 Real-Time PCR Detection System (Bio-Rad, Hercules, CA, USA). Measured cycle threshold values were normalized using the cyclophilin A or GAPDH reference gene and expressed as fold changes relative to control samples. The primers are described in Supplementary Table 2.

Immunoblotting, cytokine analysis, and glucose uptake assay

Western blotting was performed using standard methods [15]. The primary antibodies used are described in Supplementary Table 1. Reactive bands were detected by chemiluminescence using the

ImageQuant LAS 4000 imaging system (GE Healthcare Life Sciences). Levels of cytokines in serum from mice and culture medium were measured using enzyme-linked immunosorbent assay kits (R&D Systems, Minneapolis, MN, USA). The glucose uptake rate was measured as described previously [16].

Luciferase reporter assay

Cells were transfected for 24 h with human TonEBP promoter-driven luciferase reporter vectors. The Renilla luciferase reporter plasmid was used as a control for transfection efficiency. Transfected cells were treated as indicated in the figure legends and lysed in passive lysis buffer. The luciferase assay was performed using the dual-luciferase reporter system (Promega, Madison, WI, USA).

Chromatin Immunoprecipitation Quantitative PCR

Chromatin immunoprecipitation (ChIP) was performed using a commercial kit (Millipore, Bedford, MA, USA). In brief, cells were crosslinked with 1% formaldehyde followed by addition of 125 mM glycine. After washing, cells were sonicated and immunoprecipitated with anti-IgG, anti-Sp1 IgG (ab231778, Abcam) and anti-C/EBPβ IgG (3082S, Cell signaling) antibodies at 4 °C overnight. After elution and reverse crosslinking the antibody/DNA complexes, DNA was purified by DNA purification kit (Qiagen, Redwood, CA) and subjected to real-time PCR using suitable primers. The primers are described in Supplementary Table 2. Immunoprecipitated DNA from each sample was normalized to its respective chromatin input and IgG controls.

Statistical analysis

Data are expressed as the mean + standard error of the mean (s.e.m.) or standard deviation (s.d.). The statistical significance of differences between two conditions was estimated using an unpaired t-test. A one-way analysis of variance followed by Tukey's post-hoc test was used to compare multiple conditions. All statistical analyses were performed using GraphPad Prism 8.2 software (GraphPad, San Jose, CA, USA).

Data and resource availability

The datasets generated during and/or analyzed during the current study are available from the corresponding author upon reasonable request

3.4. Results

3.4.1. Myeloid TonEBP deficiency prevents HFD-induced glucose intolerance and insulin resistance

To investigate the intrinsic role of TonEBP in myeloid cells (i.e., macrophages) during the development of obesity and insulin resistance, we generated a mouse model with myeloid cell-specific genetic deletion of TonEBP (MKO) by crossing floxed TonEBP (TonEBP$^{fl/fl}$) mice with TonEBP$^{fl/fl}$; LysM-Cre$^{+/-}$ mice. TonEBP$^{fl/fl}$ co-housed littermates that did not express Cre recombinase (WT) were used as controls. TonEBP levels were much lower in peritoneal macrophages and BMDMs from MKO mice than in those from their WT littermates, confirming the deletion of TonEBP in LysM-expressing macrophages (Supplementary Fig. 1A and B). MKO and WT mice showed similar weight gain (Fig. 1A) and food intake (Supplementary Fig. 1C) during feeding of a CD or HFD for 12 weeks. The weights of the liver, epididymal white adipose tissue (epi-WAT), and subcutaneous WAT after feeding of a HFD for 12 weeks did not differ between MKO and WT mice (Fig. 1B). In addition, MKO mice showed similar HFD-induced hypertriglyceridemia but reduced hypercholesterolemia in comparison with their WT counterparts (Supplementary Fig. 1D). A HFD induced hyperglycemia and hyperinsulinemia and increased the homeostasis model assessment of insulin resistance (HOMA-IR) index in mice (Fig. 1C–E). Notably, these effects were less severe in MKO mice than in WT mice (Fig. 1C–E). MKO mice showed improved glucose tolerance and insulin sensitivity at week 8 of HFD feeding (Fig. 1F). In addition, Epi-WAT and livers isolated from MKO mice showed more potent insulin signaling than those isolated from WT mice (Fig. 1G). CD-fed MKO and WT mice had similar serum glucose and insulin levels (Fig. 1C and D). Collectively, these data demonstrate that TonEBP in myeloid cells is related to the development of obesity-associated metabolic deterioration.

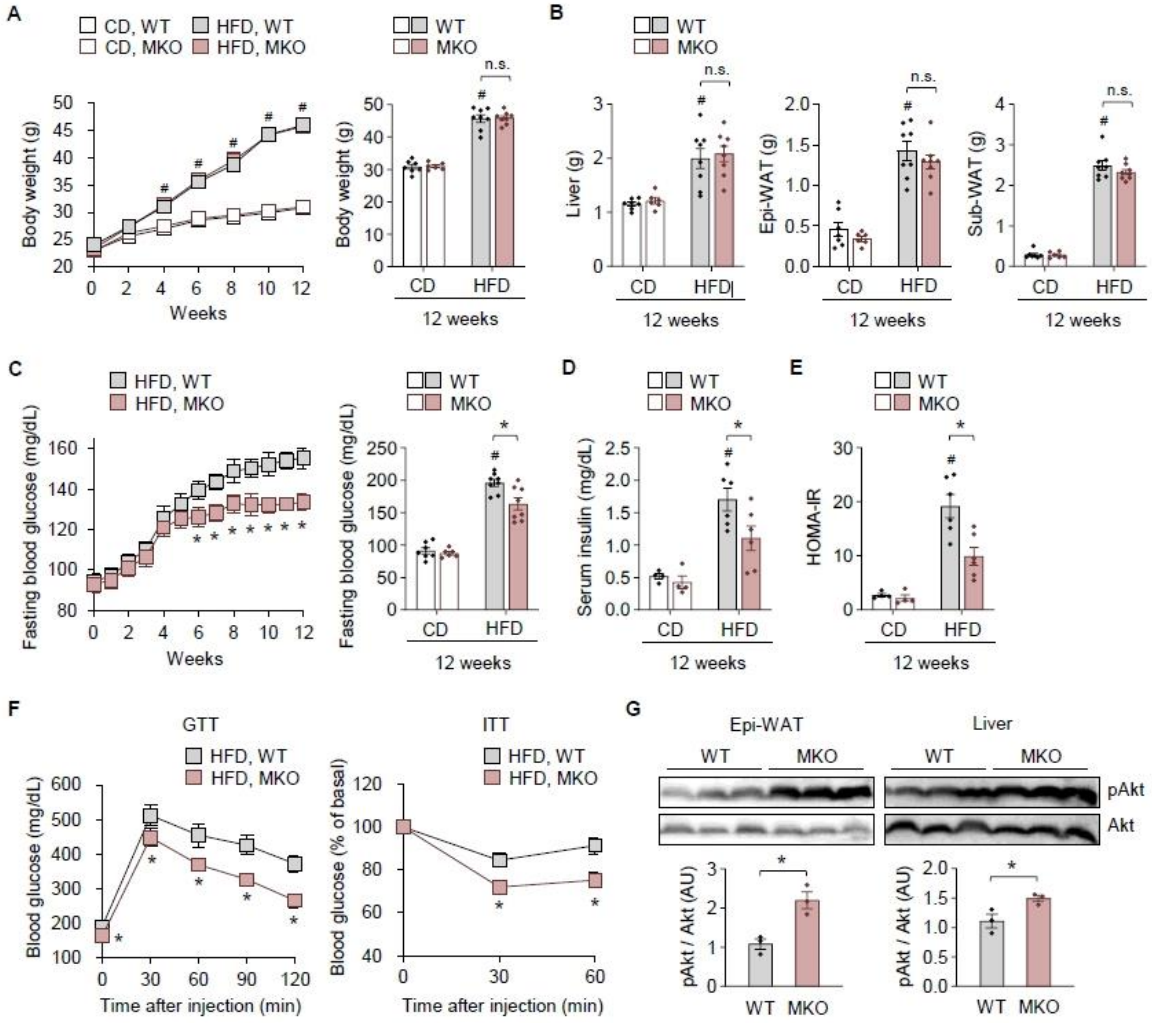

Figure 3.1. Myeloid TonEBP deficiency prevents HFD-induced glucose intolerance and insulin resistance. Male *TonEBP*$^{fl/fl}$ *LysM*-cre mice (MKO) and their *TonEBP*$^{fl/fl}$ littermates (WT) aged 8 weeks were fed a normal CD (n = 14) or HFD (n = 15) for 12 weeks. (**A**) Changes in body weight after switching to a HFD. (**B**) Liver, epi-WAT, and subcutaneous WAT (Sub-WAT) weights. (**C**) Changes in fasting (18 h) blood glucose levels after switching to a HFD. (**D**) Circulating insulin concentrations after fasting 18 h. (**E**) HOMA-IR. (**F**) Glucose tolerance test (GTT, **left**, n = 10) and insulin tolerance test (ITT, **right**, n = 11) after 8 weeks on a HFD. For GTT, mice were fasted for 18 h and orally administrated with glucose (2 g/kg). ITT was performed by an intraperitoneal injection of human insulin (0.75 U/kg) to mice fasted for 6 h. Blood glucose concentrations were measured in blood taken from the tail vein at the indicated time points after glucose or insulin injection. The results of the ITT are expressed as a percentage of basal blood glucose. (**G**) Phosphorylation of AKT in epi-WAT (**left**) and the liver (**right**) in response to insulin administration after 8 weeks on a HFD (n = 3). Mice fasted overnight were injected intraperitoneally with human insulin (0.75 U/kg) and scarified 30 min later.

Tissues were rapidly removed and snap-frozen in liquid nitrogen for immunoblotting. *n* represents the number of biologically independent animals (or samples). All data are presented as mean + s.e.m. AU, arbitrary unit. The *p*-values were determined by an ANOVA with Tukey's *post-hoc* test. $^{\#}$ $p < 0.05$ vs. CD. * $p < 0.05$.

3.4.2. Myeloid TonEBP deficiency reduces HFD-induced macrophage accumulation and inflammation in adipose tissue and the liver

Given that increased macrophage infiltration and chronic inflammation in peripheral tissues, such as the liver and adipose tissue, are hallmarks of obesity-induced insulin resistance [17], we examined the epi-WAT and liver phenotypes. In comparison with their WT counterparts, HFD-fed MKO mice showed decreases of crown-like structures (CLS), which are hallmarks of adipose tissue inflammation (Fig. 2A). mRNA expression of *F4/80* and *TonEBP* was increased in epi-WAT of mice fed a HFD, and lower in HFD-fed MKO mice (Fig. 2B and 2C). HFD-fed MKO mice showed decreases of F4/80^{+} ATMs (Fig. 2D), consistent with their reduced *F4/80* mRNA expression (Fig. 2B). Furthermore, expression of genes encoding CCL2, which is the important chemokine regulating infiltration of monocytes/macrophages, and pro-inflammatory cytokines related to insulin resistance, namely, TNFα and IL-1β, were lower in MKO mice than in their WT counterparts (Fig. 2E). Consistently, HFD-fed MKO mice had lower serum levels of CCL2, TNFα, and IL-1β (Fig. 2F). Notably, neither epi-WAT phenotype nor expression of these genes differed between WT and MKO mice fed a CD for 12 weeks. MKO mice were also protected against HFD-induced downregulation of adiponectin, which is an adipokine positively associated with insulin sensitivity, compared with WT mice, but the leptin level had not significant change in both groups (Fig. 2G). Collectively, these data suggest that TonEBP in myeloid cells promotes HFD-induced epi-WAT remodeling toward inflammation and insulin resistance.

Chronic HFD feeding causes hepatic steatosis and inflammation [1, 18]. HFD-fed WT mice had elevated circulating levels of alanine aminotransferase (ALT) and aspartate aminotransferase (AST) (Fig. 2H), but these levels were attenuated in HFD-fed MKO mice (Fig. 2H). mRNA expression of *F4/80*, *TNFα*, and *Ccl2* was also lower in livers of HFD-fed MKO mice (Fig. 2I). Consistent with the reduced mRNA level of *F4/80*, livers of HFD-fed MKO mice contained fewer F4/80^{+} macrophages (Fig. 2J).

Taken together, these data demonstrate that TonEBP mediates the detrimental effects of obesity, such as macrophage accumulation, inflammation, and hepatic steatosis in adipose tissue and the liver.

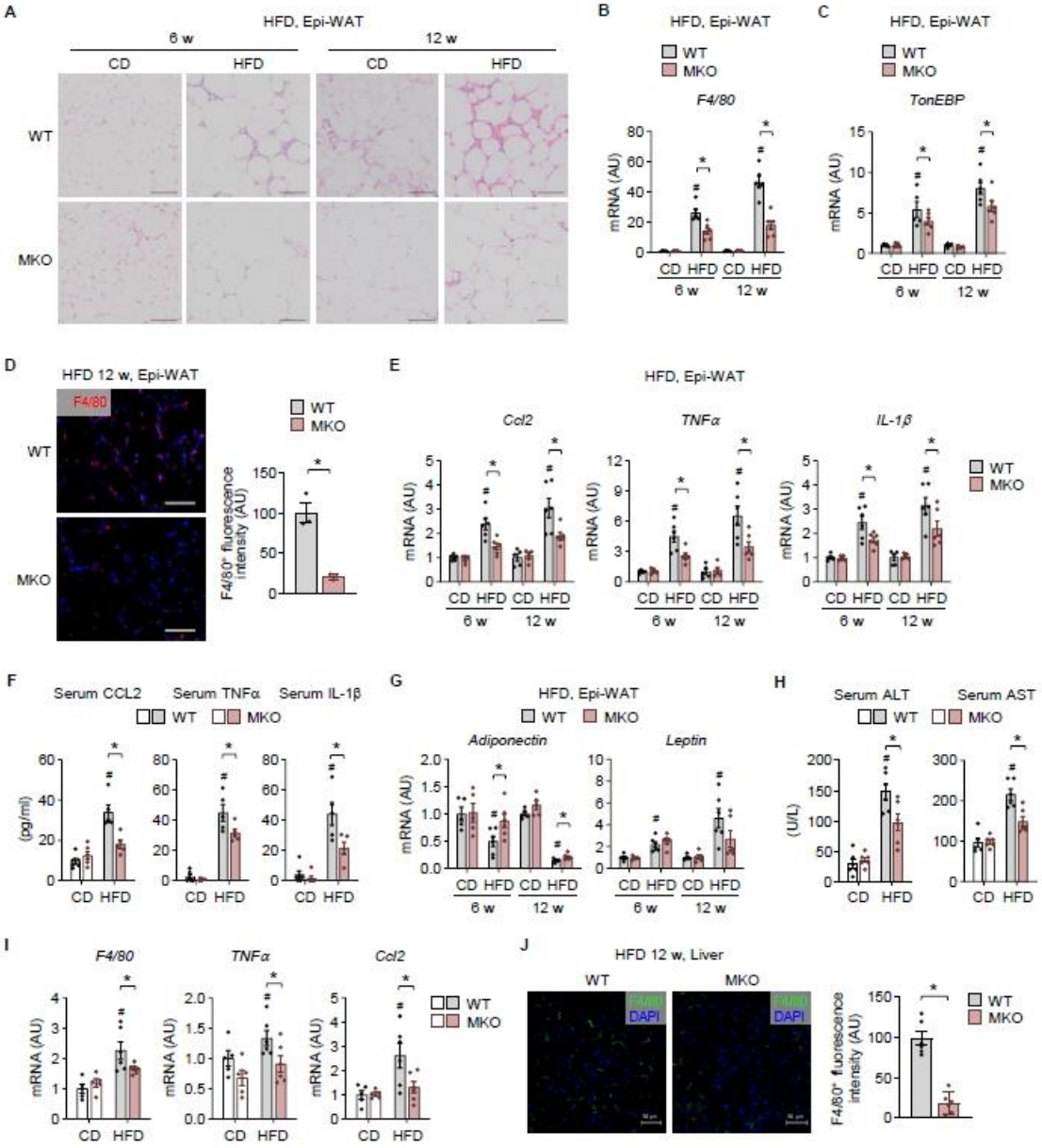

Figure 3.2. Myeloid TonEBP deficiency reduces HFD-induced macrophage accumulation and inflammation in adipose tissue and the liver. (**A-J**) WT and MKO mice were fed a CD or HFD for 6, and 12 weeks. (**A**) Representative images of H&E-stained sections of epi-WAT from mice fed CD (n = 5) or HFD (n = 6) (**B**, **C**) mRNA levels of *F4/80* (**B**) and *TonEBP* (**C**) in epi-WAT from mice fed a CD (n = 5) or HFD (n = 6) (**D**) Representative images (**left**) and quantification (**right**) of F4/80 immunostaining in epi-WAT of mice fed a HFD for 12 weeks (n = 3). (**E**) mRNA levels of *Ccl2*, *TNF-α*, and *IL-1β* in epi-WAT from mice fed a CD (n = 5) or HFD (n = 6). (**F**) Serum levels of CCL2, TNF-α, and IL-1β in mice fed a CD (n = 6) or HFD (n = 5) for 12 weeks. (**G**) mRNA levels of *adiponectin* and *leptin* in epi-WAT from mice fed CD (n = 5) or HFD (n = 6). (**H–J**) WT and MKO mice were

analyzed after 12 weeks on a CD or HFD (n = 6). (**H**) Serum ALT and AST concentrations. (**I**) mRNA levels of *F4/80*, *TNF-α*, and *Ccl2* in the liver. (**J**) Representative images (**left**) and quantification (**right**) of F4/80 immunostaining in livers of HFD-fed mice (n = 6). n represents the number of biologically independent animals (or samples). All data are presented as mean + s.e.m. Scale bars, 100 μm (**A**) and 50 μm (**D, J**). AU, arbitrary unit. The p-values were determined by an ANOVA with Tukey's *post-hoc* test. $^{\#}$ $p < 0.05$ vs. CD. * $p < 0.05$.

3.4.3. TonEBP deficiency promotes macrophage polarization toward improvement of insulin sensitivity

In both mice and human subjects, the activation state of ATMs is causally linked to obesity-induced insulin resistance [17] and steatohepatitis [19]. Therefore, we examined macrophage populations in stromal vascular fractions (SVFs) of epi-WAT. Consistent with a previous study [20], HFD feeding increased the population of ATMs ($CD11b^{+}F4/80^{+}$) in WT mice, and this was suppressed by myeloid TonEBP deficiency (Fig. 3A and Supplementary Fig. 2A). More importantly, TonEBP deficiency in myeloid cells reduced the population of pro-inflammatory M1-like ATMs ($CD11b^{+}F4/80^{+}CD11c^{+}CD206^{-}$) in HFD-fed mice (Fig. 3B and C, and Supplementary Fig. 2B). By contrast, the population of anti-inflammatory M2-like ATMs ($CD11b^{+}F4/80^{+}CD11c^{-}CD206^{+}$) was larger in HFD-fed MKO mice than in HFD-fed WT mice (Fig. 3B and C, and Supplementary Fig. 2B). Hence, the ratio of M1-like-to-M2-like ATMs was lower in MKO mice (Fig. 3C), indicating that inflammatory responses are reduced in epi-WAT of HFD-fed MKO mice. Notably, mRNA expression of *TonEBP* was elevated in SVFs of epi-WAT from HFD-fed mice (Fig. 3D). As expected given the decrease in epi-WAT (Fig. 2B and C), mRNA expression of *F4/80* was lower in SVFs of epi-WAT from HFD-fed MKO mice (Fig. 3D). We further confirmed that TonEBP expression was markedly higher in ATMs from epi-WAT from HFD-fed mice than in those from epi-WAT from NC-fed mice (Fig. 3E). Furthermore, immunofluorescence staining of epi-WAT from HFD-fed WT mice showed colocalization of TonEBP with F4/80, whereas TonEBP was not detected in macrophages of epi-WAT from HFD-fed MKO mice (Fig. 3F), suggesting that TonEBP expression increases in ATMs during obesity.

Consistent with the increased macrophage content, metabolically activated pro-inflammatory and anti-inflammatory gene expression was increased in SVFs of epi-WAT from HFD-fed WT mice (Supplementary Fig. 2C). Importantly, expression of mRNAs encoding pro-inflammatory-related TNFα, IL-1β, and CCL2 was lower in MKO mice when normalized to *F4/80* mRNA levels, while expression of mRNAs encoding anti-inflammatory-related CD206, IL-10, and PPARγ1 was higher (Fig. 3G). These data indicate that TonEBP expression in myeloid cells contributes to the increase of pro-

inflammatory-like ATMs and to the decrease in anti-inflammatory-like ATMs in HFD-fed mice. Based on these findings, we investigated whether TonEBP intrinsically affects the polarization state of macrophages. To this end, BM cells were differentiated into BMDMs by culture in the presence of M-CSF, which drives differentiation of monocytes into unactivated M0 macrophages [21]. Interestingly, TonEBP deficiency increased basal expression of anti-inflammatory-related genes (*CD206*, and *PPARγ1*) without affecting the expression of the pro-inflammatory-related genes *TNFα*, *IL-1β*, and *Ccl2* (Supplementary Fig. 2D) in BMDMs (M0). Additionally, the percentage of BMDMs (Supplementary Fig. 2E), and mRNA expression of *F4/80* (Supplementary Fig. 2F), did not differ between these two groups of mice, demonstrating that TonEBP does not modulate the capacity of monocytes to macrophages differentiation. Taken together, these data demonstrate that TonEBP suppresses polarization toward anti-inflammatory macrophages during differentiation of macrophages. Similar effects were observed in macrophages differentiated from the human monocyte cell line THP-1. Two siRNAs (#1 and #2) targeting different regions of *TonEBP* mRNA reduced expression of pro-inflammatory-associated genes and increased expression of anti-inflammatory-associated genes in THP-1-derived macrophages (Supplementary Fig. 3A and B), suggesting that TonEBP suppresses polarization of differentiated human macrophages toward an anti-inflammatory phenotype.

Given the importance of PPARγ in priming monocytes toward anti-inflammatory polarization and in suppression of the inflammatory response in macrophages [22], we further explored the role of TonEBP in PPARγ expression in macrophages. mRNA expression of *TonEBP* decreased upon M-CSF-induced differentiation of BM-derived monocytes (BM-Mo) into macrophages (Fig. 3H). Notably, mRNA expression of both *PPARγ1* and *PPARγ2* was higher in BM-Mo and BMDM from MKO mice than in the corresponding cells from WT mice (Fig. 3H). mRNA levels of *PPARγ1* were also higher in SVFs from 8-week-old MKO mice than in those from WT mice (Supplementary Fig. 3C). Similarly, siRNA-mediated TonEBP knockdown increased PPARγ1 expression in murine RAW264.7 macrophages (Fig. 3I). Conversely, overexpression of TonEBP using an adenoviral vector reduced mRNA expression of *PPARγ1* (Fig. 3J). Importantly, TonEBP depletion increased *PPARγ1* expression in primary human monocyte-derived macrophages obtained from three donors, as described previously [23] (Fig. 3K), and in THP-1-derived macrophages (Fig. 3L). Furthermore, TonEBP knockdown stimulated induction of PPARγ1 by the M2 inducer IL-4 (20 ng/ml) [24] (Supplementary Fig. 3D). However, TonEBP knockdown did not affect STAT6 activation or C/EBPβ expression, which are involved in M2 polarization [25] (Supplementary Fig. 3D). These data suggest that TonEBP modulates the pro-inflammatory/anti-inflammatory phenotype at least partly by suppressing the PPARγ1 expression in monocytes/macrophages.

We next asked how TonEBP suppressed the PPARγ1 expression. Since TonEBP suppresses the

PPARγ2 promoter via blocking the recruitment of C/EBPβ [26] and there is C/EBPβ binding site in the PPARγ1 promoter [27], we examined C/EBPβ binding to the PPARγ1 promoter. ChIP analysis using specific primers for the binding site (Supplementary Table 2) showed that C/EBPβ binding to the PPARγ1 promoter was elevated in response to TonEBP knockdown (Supplementary Fig 3E). These data demonstrate that TonEBP suppresses the PPARγ1 promoter via blocking the recruitment of C/EBPβ.

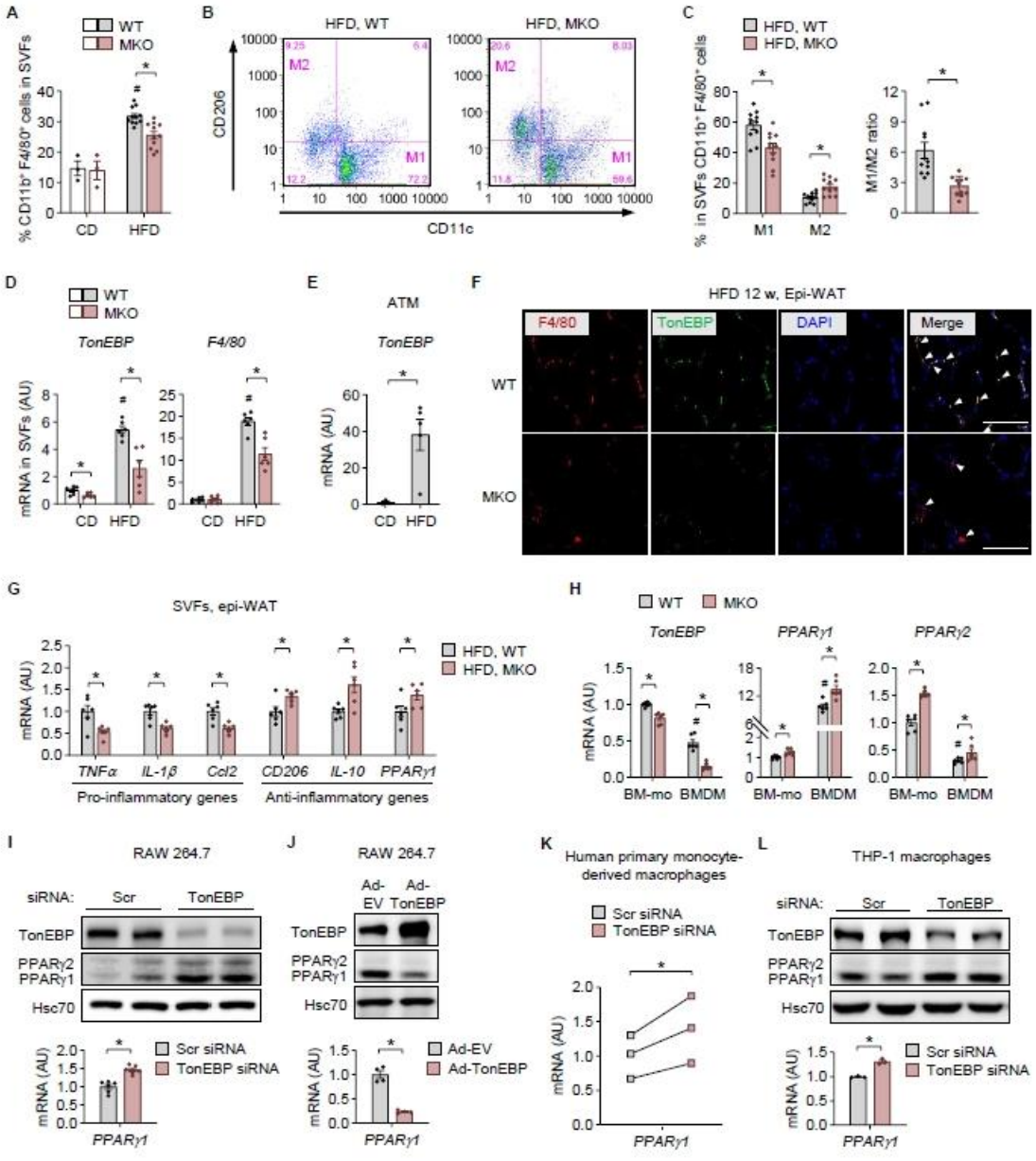

Figure 3.3. TonEBP deficiency promotes macrophage polarization toward improvement of insulin sensitivity. (**A–C**) Flow cytometry analysis of cells isolated from SVFs of epi-WAT from MKO and WT mice fed a CD (n = 3) or HFD (n = 11) for 12 weeks. (**A**) Percentage of total macrophages

($CD11b^+F4/80^+$) in SVFs. (**B**) Representative flow cytometry plots showing the frequencies of M1 ($CD11c^+CD206^-$) and M2 ($CD11c^-CD206^+$) macrophages within the macrophage population in mice fed a HFD. (**C**) Quantification of M1 and M2 macrophages (**left**) and the M1/M2 ratio (**right**). (**D**) mRNA levels of *TonEBP* and *F4/80* in SVFs of epi-WAT from mice fed a HFD ($n = 6$). (**E**) ATMs were isolated from SVFs of epi-WAT from WT mice fed a CD ($n = 3$) or HFD ($n = 5$) for 12 weeks using anti-CD11b antibody coupled to magnetic beads. mRNA levels of TonEBP. (**F**) Representative images of immunofluorescence staining of F4/80 (red), TonEBP (green) and DAPI (blue) in epi-WAT from WT and MKO mice fed a HFD for 12 weeks ($n = 3$). Colocalization of F4/80 and TonEBP is shown in yellow in the merged image (arrows). Scale bar, 50 μm. (**G**) mRNA levels of metabolically activated pro- and anti-inflammatory genes in SVFs of epi-WAT from mice fed a HFD ($n = 6$). (**H**) mRNA levels of *TonEBP*, *PPARγ1*, and *PPARγ2* in BM-Mo and BMDMs from WT and MKO mice ($n = 6$). (**I**) Representative protein levels of TonEBP and PPARγ (**top**) and mRNA levels of *PPARγ1* (**bottom**) in RAW264.7 cells transfected with Scr or *TonEBP*-targeted siRNA ($n = 3$). (**J**) Representative protein levels of TonEBP and PPARγ (**top**) and mRNA levels of *PPARγ1* (**bottom**) in RAW264.7 cells infected with an adenovirus expressing TonEBP (Ad-TonEBP) or an empty vector (Ad-EV) ($n = 4$). (**K**) mRNA levels of *PPARγ1* in primary human monocyte-derived macrophages transfected with Scr or *TonEBP*-targeted siRNA. Primary human mononuclear cells were isolated from blood, and monocytes were further purified using CD14 microbead positive selection. The macrophages were obtained from a 7-day culture with human M-CSF (20 ng/ml), and transfected with the indicated siRNA ($n = 3$). (**L**) Representative protein levels of TonEBP and PPARγ (**top**), and mRNA levels of *PPARγ1* (**bottom**) in THP-1-derived macrophages transfected with Scr or *TonEBP*-targeted siRNA ($n = 6$). *n* represents the number of biologically independent animals (or samples) (**A–H, K**) or independent experiments with at least two replicates (**I, J, L**). All data are presented as mean + s.e.m. (or s.d.). AU, arbitrary unit. The *p*-values were determined by an ANOVA with Tukey's *post-hoc* test. $^{\#}\ p < 0.05$ vs. CD or BM-Mo (**H**). $^{*}\ p < 0.05$. mRNA levels were normalized to those of cyclophilin A (internal control). mRNA levels in SVFs were further normalized to those of F4/80 to correct for the amount of macrophages (**G**).

3.4.4. TonEBP deficiency in macrophages improves insulin sensitivity of adipocytes under obesity-mimicking conditions *in vitro*

To address how TonEBP regulates pro-inflammatory responses in MMe ATMs, we examined the effects of TonEBP on macrophage responses to saturated FFA palmitate (PA), the main driver of the MMe phenotype [9, 10]. PA increased TonEBP expression in THP-1 macrophages (Fig. 4A). Consistent with previous findings [9, 10], it also increased mRNA expression of the pro-inflammatory-genes *TNFα*,

IL-1β, and *Ccl2*, which are responsible for the development of obesity-induced insulin resistance [28], and of *IL-10* [8] and *PPARγ1* [22], which encode anti-inflammatory proteins that play important roles as modulators of insulin sensitivity (Fig. 4B). Notably, TonEBP knockdown markedly reduced PA-mediated induction of *TNFα*, *IL-1β*, and *Ccl2* expression, but enhanced expression of *IL-10* and *PPARγ1* (Fig. 4B). Similar effects were observed in mouse BMDM and RAW264.7 cells (Supplementary Fig. 4A-C). TonEBP depletion also promoted PA-mediated induction of genes involved in lipid metabolism (*Cd36*, *Plin2*, and *Abca1*) that are regulated by PPARγ [9, 10] in THP-1 macrophages (Fig. 4C). Furthermore, mRNA levels of these genes were higher in SVFs of epi-WAT from HFD-fed MKO mice (Fig. 4D). Given the importance of the opposing actions of NF-κB and PPARγ on MMe phenotype in ATMs [9, 10], we examined whether TonEBP affects PA-stimulated transcriptional activity of NF-κB and PPARγ in macrophages. PA-stimulated NF-κB activation was decreased by TonEBP depletion consistent with the transcriptional activator function of TonEBP [29, 30]. Consistent with the suppressor function of TonEBP for the PPARγ1 promoter (see above), PA-stimulated PPARγ activation was increased by TonEBP knockdown (Fig. 4E). Collectively, these data demonstrate that TonEBP promotes the pro-inflammatory phenotype of MMe macrophages via at least two independent mechanism; the activation of the pro-inflammatory NF-κB pathway and the suppression of anti-inflammatory PPARγ pathway.

Circulating levels of LPS and PA are increased in obese subjects [31, 32] and animal models of obesity [33, 34]. The synergistic interaction between them is known to promote pro-inflammatory responses via TLR4/NF-kB signaling and stimulate the development of obesity-related diseases including T2DM [35]. Thus, to mimic the conditions of obesity *in vitro*, we activated macrophages with 0.1 or 1 ng/ml LPS and/or 0.2 mM PA, which are similar to the concentrations found in the serum of obese subjects [31, 32]. mRNA expression of *TNFα*, *IL-1β*, *Ccl2*, and *IL-10* was higher in cells treated with PA plus LPS than in cells treated with PA or LPS alone in THP-1 macrophages (Fig. 4F). Notably, mRNA expression of *TNFα*, *IL-1β*, and *Ccl2* was lower in TonEBP-deficient cells, while mRNA expression of *IL-10* was higher (Fig. 4F). Obesity-induced activation of ATMs impairs insulin sensitivity of nearby adipocytes [36]. To investigate whether TonEBP depletion in macrophages changes the insulin response of adipocytes, an indirect coculture experiment was performed using mature 3T3-L1 adipocytes and conditioned medium (CM) from RAW264.7 cells. Similar to THP-1 macrophages, the expression of insulin response-associated genes was higher in RAW264.7 cells treated with PA plus LPS than in those treated with LPS alone, whereas the levels of TNFα and iNOS in TonEBP-deficient RAW264.7 cells were lower than in control cells after treatment with both LPS alone and the combination of PA and LPS, and the level of IL-10 was higher (Fig. 4G and Supplementary Fig. 4D). Exposure to CM from PA plus LPS-stimulated cells reduced insulin-stimulated glucose uptake and Akt

phosphorylation compared with exposure to CM from vehicle-treated cells (Fig. 4H and I). Notably, exposure to CM from TonEBP-deficient RAW264.7 cells improved insulin-stimulated glucose uptake and Akt phosphorylation compared with exposure to CM from control cells stimulated with PA plus LPS (Fig. 4H and I). Collectively, these data demonstrate that TonEBP in macrophages impairs insulin sensitivity of adipocytes, and that macrophage TonEBP plays an important role in obesity-induced inflammation and subsequent insulin resistance.

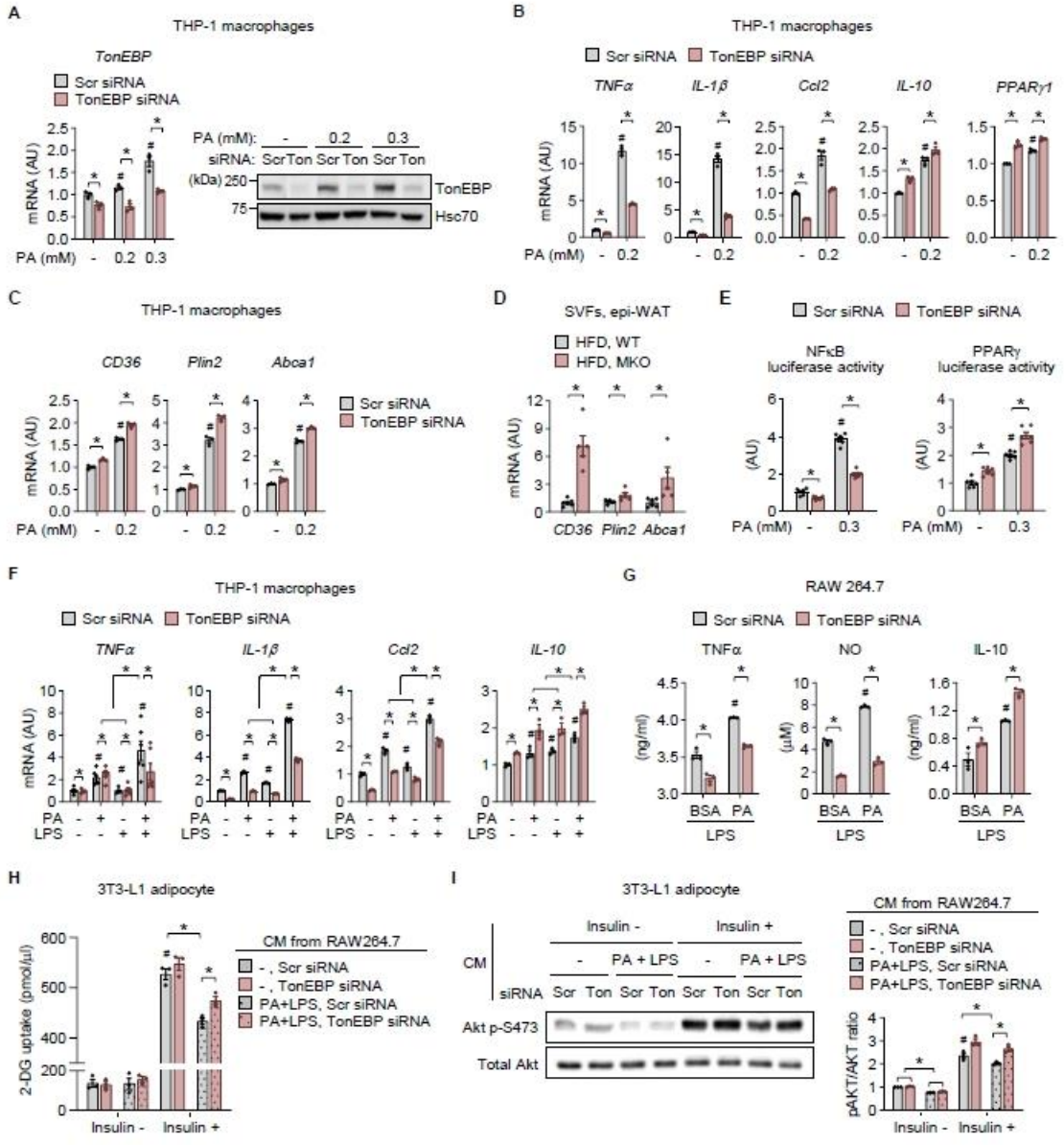

Figure 3.4. TonEBP deficiency in macrophages improves insulin sensitivity of adipocytes under obesity-mimicking conditions in vitro. (**A-C**) THP-1-derived macrophages were transfected with Scr

or *TonEBP*-targeted siRNA. siRNA-transfected cells were exposed to BSA (-) or PA (0.2 or 0.3 mM) for 6 or 18 h. (**A**) TonEBP *mRNA* levels at 6 h (**left**) and representative immunoblots of TonEBP and Hsc70 at 18 h (**right**) ($n = 3$). (**B, C**) mRNA expression of the indicated genes at 18 h. (**D, E**) RAW264.7 cells transfected with the indicated siRNA transfected a second time with κB- (**D**) or PPRE (**E**)-luciferase reporter vector. Cells were exposed to BSA (-) or PA (0.3 mM) for 12 h. Luciferase activity was measured ($n = 4$). (**F**) THP-1-derived macrophages transfected with Scr or *TonEBP*-targeted siRNA were exposed to BSA or PA (0.2 mM) in the absence or presence of LPS (0.01 ng/ml) for 18 h. mRNA levels of *TNFα*, *IL-1β*, *Ccl2*, and *IL-10*, which are related to the insulin response ($n = 3$). (**G**) RAW264.7 cells transfected with Scr or *TonEBP*-targeted siRNA were exposed to BSA or PA (0.2 mM) in the presence of LPS (1 ng/ml) for 18 h. Concentrations of TNFα, NO, and IL-10 in CM from cells ($n = 3$). (**H**, **I**) RAW264.7 cells transfected with the indicated siRNA were incubated in the absence or presence of PA (0.2 mM) plus LPS (1 ng/ml) for 24 h, and CM was collected. Differentiated 3T3-L1 adipocytes were exposed to CM for 24 h. Cells were serum-starved for 2 h and then incubated for 30 min in low glucose media containing 20 μM 6-NBDG without or with 100 nM insulin. (**H**) Stimulation of glucose uptake in response to insulin in 3T3-L1 adipocytes exposed to CM from RAW264.7 cells treated as indicated ($n = 3$). (**I)** Representative immunoblots of phosphorylated Akt in response to insulin (**left**), and the ratio of phosphorylated to total Akt (**right**) in 3T3-L1 adipocytes exposed to CM from RAW264.7 cells treated as indicated ($n = 3$). *n* represents the number of independent experiments with more than three replicates (**A-C, E–I**) or biologically independent samples (**D**). All data are presented as mean + s.d. (or s.e.m.). AU, arbitrary unit. The *p*-values were determined by an ANOVA with Tukey's *post-hoc* test. $^{\#}p < 0.05$ vs. Scr siRNA; BSA (-) (**A-C, E),** Scr siRNA; BSA (-); LPS (-) (**F**), Scr siRNA; BSA (-); LPS (**G**) or insulin (-) (**H, I**). $^{*}p < 0.05$.

3.4.5. Sp1 is a central mediator of TonEBP induction in response to TLR4 stimulation in macrophages

TonEBP expression in macrophages is upregulated through TLR4 stimulation by LPS and various pathologic stimuli [11], and here, we showed that TonEBP expression was increased by PA treatment (Fig. 4A and Supplementary Fig. 4B). Therefore, we investigated transcriptional regulation of *TonEBP* in response to LPS and PA, a potent agonist of TLR4. We constructed a pGL3 luciferase reporter vector by inserting a 5 kb promoter sequence (-4591/+409) of the human *TonEBP* gene. Murine RAW264.7 and human THP-1 macrophages transfected with this reporter construct exhibited luciferase activity, which was stimulated by LPS and PA (Fig. 5A and Supplementary Fig. 5A). To define DNA regions responsible for stimulation of TonEBP, we generated serial deletion constructs (Fig. 5B). RAW264.7

cells transfected with a construct in which the sequence between −1931 and −1873 (D4) was deleted did not exhibit LPS-stimulated luciferase activity (Fig. 5C). Database analysis of the sequences in this region revealed similarity to a non-consensus recognition sequence (−1896 to −1887) of the transcription factor Sp1 that is remarkably conserved in human and mouse (Fig. 5D). Therefore, we investigated whether Sp1 is required for induction of TonEBP in response to LPS and PA. The mRNA expression of Sp1 was increased by treatment with LPS (1 ng/ml) for 18 h, but not by PA (0.2 and 0.3 mM) (Supplementary Fig. 5B). Notably, Sp1 knockdown reduced LPS-induced *TonEBP* promoter-driven luciferase expression without influencing luciferase activity under unstimulated conditions (Fig. 5E). Consistently, Sp1 knockdown decreased TonEBP expression induced by LPS (Fig. 5F). Similarly, LPS-induced TonEBP expression was reduced by the selective Sp1-DNA-binding inhibitor mithramycin A in THP-1-derived macrophages (Fig. 5G). Mithramycin A also reduced PA-induced mRNA expression of TonEBP in RAW264.7 cells (Supplementary Fig. 5C).

To investigate whether reduction of *TonEBP* expression upon Sp1 knockdown was dependent on the Sp1-binding sequence in the promoter, we constructed Sp1-deleted (mt1) and -substituted (mt2) mutants (Fig. 5H). Neither mutant exhibited LPS-induced transcriptional activity (Fig. 5I), confirming that the Sp1-binding site functions in LPS-induced TonEBP expression. Next, to investigate whether Sp1 binds to the Sp1-binding site in the *TonEBP* promoter, we performed ChIP-qPCR in THP-1 macrophages (Fig. 5J). When DNA was precipitated from THP-1 macrophages using an anti-Sp1 antibody, fragments of the *TonEBP* promoter containing the Sp1-binding sequence detected using two primer sets (A and B) were enriched in LPS-treated cells, and this enrichment was reduced by mithramycin A (Fig. 5J). Taken together, these data demonstrate that Sp1 binds to the Sp1-binding site in the *TonEBP* promoter and thereby induces TLR4-mediated TonEBP expression.

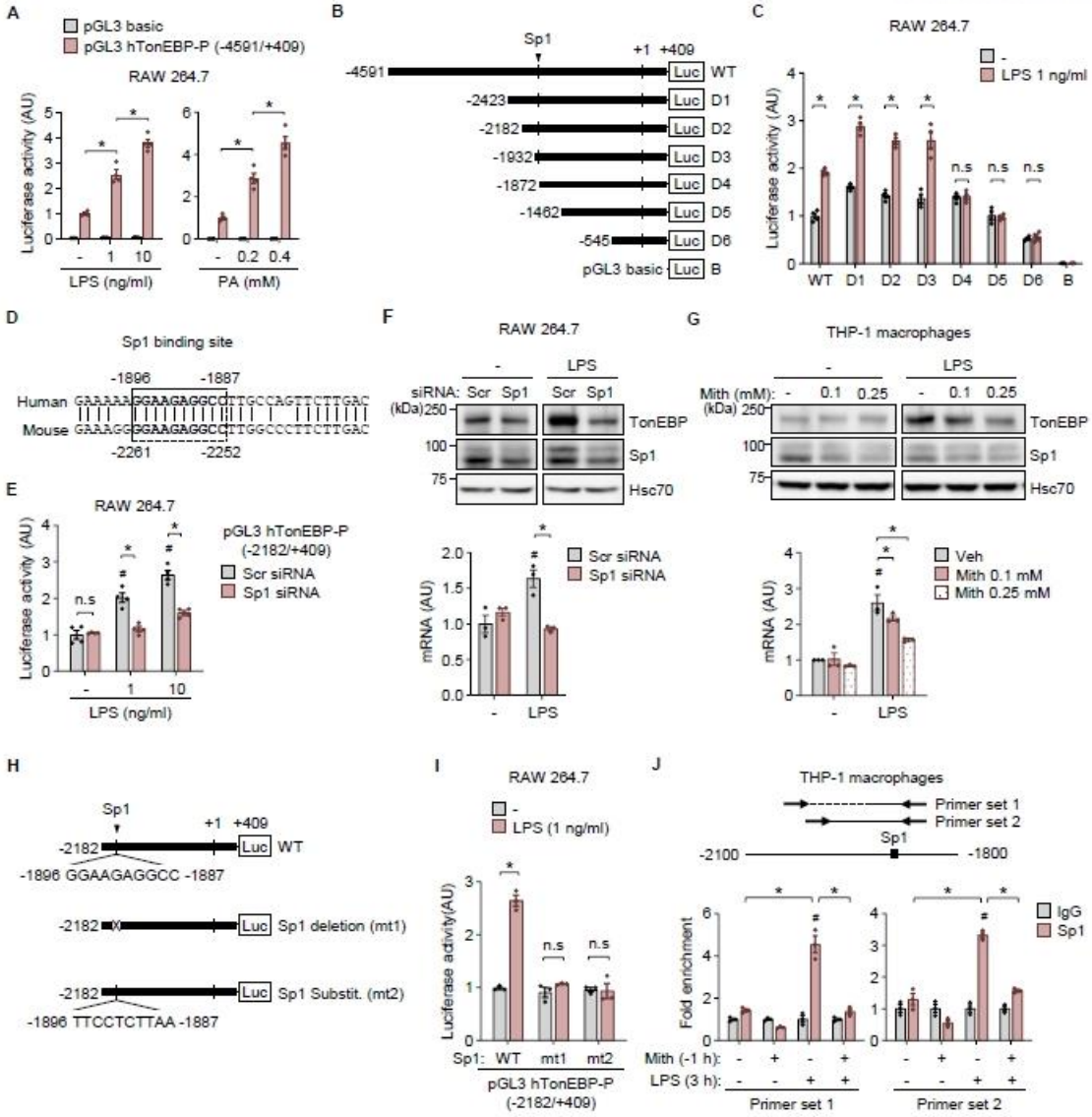

Figure 3.5. Sp1 is a central mediator of TonEBP induction in response to TLR4 stimulation in macrophages. (**A**) RAW264.7 cells were transfected with the human *TonEBP* promoter-luciferase construct containing the −4591 to +409 region or the pGL3 basic vector. Luciferase activity was measured after LPS (8 h) or PA (10 h) treatment as indicated (n = 4). (**B**) The *TonEBP* promoter-luciferase construct containing the −4591 to +409 region of the human *TonEBP* gene and a series of 5′ promoter deletion mutants. 'Sp1' denotes the predicted Sp1-binding sequence. (**C**) RAW264.7 cells were transfected with each of the 5′-deletion mutants of the *TonEBP* promoter construct. Luciferase activity was measured 8 h after treatment with vehicle (-) or 1 ng/ml LPS (n = 3). (**D**) Nucleotide sequence alignment of the promoters of the human and mouse *TonEBP* genes (NCBI, BLAST, and alignment tools). The conserved predicted Sp1-binding sites are shown in bold letters. (**E**, **F)** RAW264.7 cells were transfected with Scr or *Sp1*-targeted siRNA. (**E**) siRNA-transfected cells were transfected

with the −2182/+409 promoter construct including the Sp1-binding site. Luciferase activity was measured 8 h after treatment with 0, 1, or 10 ng/ml LPS (n = 3). (**F**) siRNA-transfected RAW264.7 cells were treated with vehicle (-) or LPS (1 ng/ml) for 18 h (for protein) or 6 h (for RNA). Representative immunoblots of TonEBP, Sp1, and Hsc70 (**top**), and TonEBP *mRNA* levels (**bottom**) (n = 3). (**G**) THP-1-derived macrophages were treated with vehicle (-) or mithramycin A (mith, 0.1 and 0.25 mM) for 1 h followed by vehicle (-) or LPS (0.1 ng/ml) for 18 h (for protein) or 6 h (for RNA). Representative immunoblots of TonEBP, Sp1, and Hsc70 (**top**), and TonEBP *mRNA* levels (**bottom**) (n = 3). (**H**) The TonEBP promoter-luciferase construct containing the −2182 to +409 region of the human *TonEBP* gene (Sp1 WT) and the mutant −2182/+409 construct in which the Sp1 site was deleted (mt1) or mutated (mt2). (**I**) RAW264.7 cells were transfected with the −2182/+409 promoter construct and Sp1-WT, -mt1, or -mt2. Luciferase activity was measured after treatment with vehicle (-) or LPS (1 ng/ml) for 8 h (n = 3). (**J**) THP-1-derived macrophages were pre-treated for 1 h (-1 h) with vehicle (-) or mithramycin A (200 μM), and then treated with vehicle (-) or LPS (1 ng/ml) for 3 h. ChIP analysis of Sp1 and normal rabbit IgG on the *TonEBP* promoter was performed as described in the Materials and Methods. Two primer sets were designed for ChIP-qPCR at the predicted Sp1-binding site region of the *TonEBP* promoter. Relative occupancy was calculated by performing qPCR analysis and normalizing the C_T values with input controls. All data are presented as mean + s.d. (n = 3). n represents the number of independent experiments with more than three replicates. AU, arbitrary unit. The p-values were determined by an ANOVA with Tukey's *post-hoc* test. $^{\#}$ $p < 0.05$ vs. Scr siRNA; (-) (**E–G**) or IgG (**J**). * $p < 0.05$. n.s.: not significant.

3.4.6. The *TonEBP* mRNA expression level in PBMCs is positively correlated with blood glucose levels in mice and humans

PBMCs from subjects with chronic inflammatory diseases are proinflammatory, and release inflammatory cytokines and chemoattractant mediators into the systemic circulation [37, 38]. Therefore, we investigated mRNA expression of *TonEBP* in PBMCs. Feeding a HFD increased mRNA expression of *TonEBP*, *TNFα* and *IL-1β* in PBMCs from WT mice, but this effect was significantly attenuated in PBMCs from MKO mice (Fig. 6A). Notably, fasting blood glucose levels were positively correlated with the mRNA levels of *TonEBP*, *TNFα* and *IL-1β* in PMBCs (Fig. 6B and Supplemental Fig. 6A). In addition, there was a significant association between the mRNA levels of *TonEBP* and *TNFα* (Supplemental Fig. 6B). More importantly, mRNA expression of *TonEBP* was higher in PBMCs from diabetic patients than from non-diabetic subjects, and was positively correlated with fasting blood glucose levels (Fig. 6C and Supplemental Table 3). These data suggest that TonEBP plays a critical role

in the proinflammatory state of PBMCs, and that variability of TonEBP expression in PBMCs can affect this state in diabetic patients and mice.

Obesity-induced inflammation and metabolic dysfunction in humans and mice are associated with increased numbers of circulating inflammatory monocytes [39, 40]. Therefore, we examined blood inflammatory $CD11b^{+}Ly6C^{+}$ monocytes in mice, which are considered the counterpart of human inflammatory monocytes [5]. Whereas MKO mice had a similar percentage of total myeloid cells ($CD11b^{+}$) to WT mice (Fig. 6E), TonEBP deficiency in myeloid cells attenuated the increase of circulating inflammatory monocytes induced by a HFD (Fig. 6D). More importantly, TonEBP deficiency reduced surface expression of CCR2, a chemokine receptor that mediates migration of monocytes and is highly expressed by inflammatory monocytes (Fig. 6F and Supplementary Fig. 6C and 6D). Additionally, deficiency of TonEBP in myeloid cells did not affect the populations of monocyte subsets (Supplementary Fig. 7A-C) among cells isolated from BM. Collectively, these data raise the possibility that TonEBP contribute to the differentiation of circulating inflammatory monocytes and their migration capacity via CCR2-CCL2 signaling during obesity.

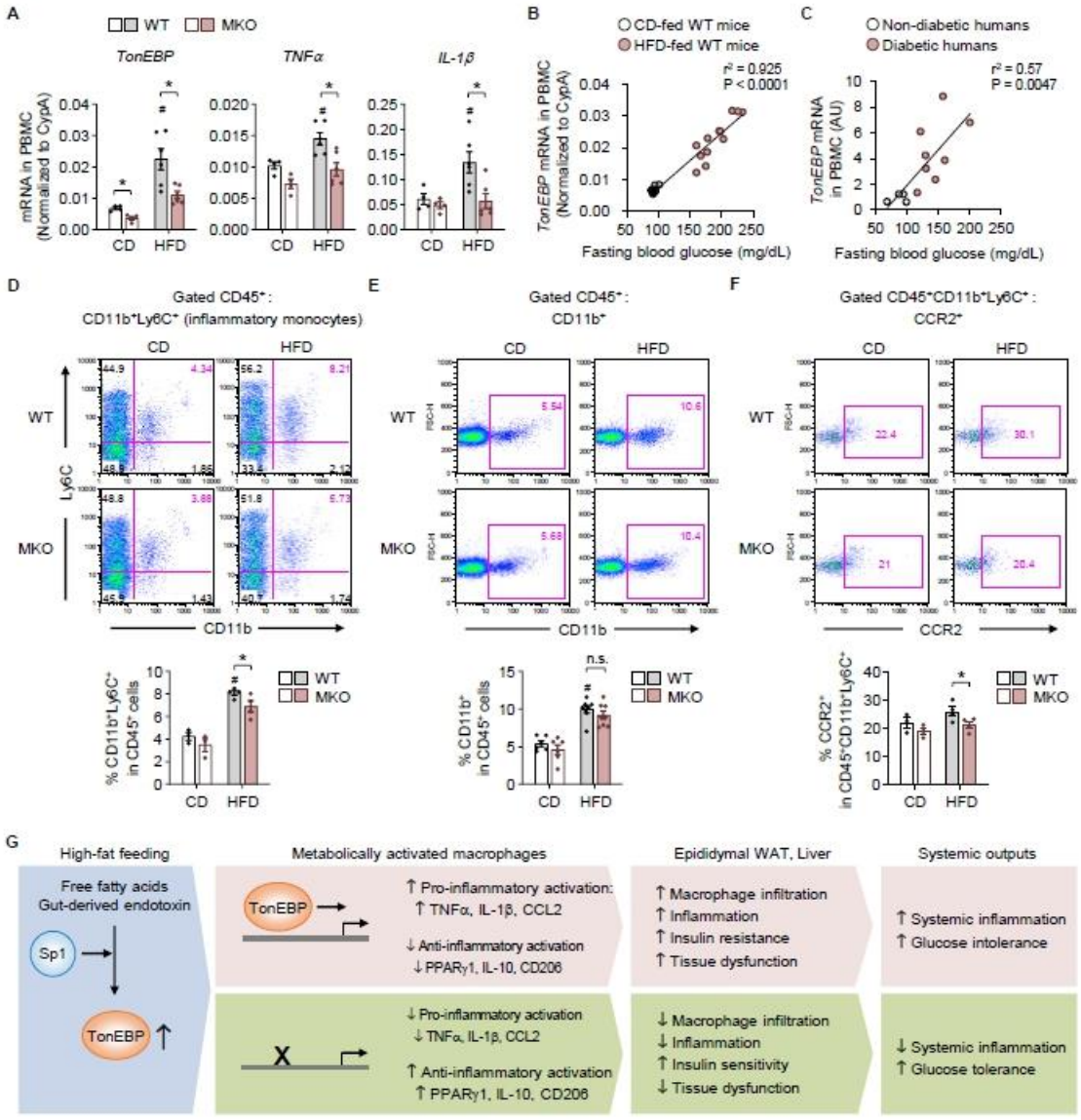

Figure 3.6. The TonEBP mRNA expression level in PBMCs is positively correlated with blood glucose levels in mice and humans. (**A**) mRNA levels of *TonEBP*, *TNFα*, and *IL-1β* in PBMCs from WT and MKO mice fed a CD (n = 4) or HFD (n = 5) for 12 weeks. (**B**) Correlation between fasting blood glucose levels and mRNA expression of *TonEBP* in PBMCs from WT mice fed a CD (n = 8) and HFD (n = 12) for 12 weeks. (**C**) Correlation between fasting blood glucose levels and mRNA expression of *TonEBP* in PBMCs from non-diabetic (n = 4) and diabetic (n = 8) individuals. (**D–F**) Representative flow cytometry plots (**top**) and quantification (**bottom**) of myeloid cells ($CD45^+CD11b^+$) (CD, n = 6; HFD, n = 8) (**D**), inflammatory monocytes ($CD45^+CD11b^+Ly6C^+$) (CD, n = 3; HFD, n = 4) (**E**), and CCR2 expression on inflammatory monocytes (CD, n = 3; HFD, n = 4) (**F**) in PBMCs from WT and MKO mice fed a CD or HFD for 12 weeks. (**G**) Proposed model for the role of macrophage TonEBP in the development of systemic insulin resistance and inflammation during obesity. n represents the

number of biologically independent samples. Correlations were assessed by the non-parametric Spearman's test. All data are presented as mean + s.e.m. AU, arbitrary unit. The *p*-values were determined by an ANOVA with Tukey's *post-hoc* test. $^{\#}$ $p < 0.05$ vs. CD. * $p < 0.05$.

3.5. Discussion

In adipocytes, TonEBP suppresses white adipocyte beiging by repressing thermogenesis. Accordingly, mice lacking TonEBP specifically in adipocytes exhibit reduced weight gain and insulin resistance [41]. The current study demonstrated that mice lacking TonEBP in myeloid cells show reduced inflammation and insulin resistance, even in the absence of changes in weight gain and adiposity (Fig. 6G). These findings suggest that TonEBP affects metabolic physiology in at least two cell types, namely, adipocytes and macrophages. Adipose tissue is a *bona fide* endocrine organ that regulates systemic metabolic homeostasis and plays a crucial role in metabolic homeostasis and dysfunction through crosstalk between cell types and organs. TonEBP depletion in myeloid cells also has beneficial effects on obesity-induced hepatic dysfunction. Given the important role of islet-associated macrophages in T2DM [42], it is possible that TonEBP influences the obesity-associated islet inflammation and β-cell dysfunction. Thus, we suggest that TonEBP represents a key node in this crosstalk by regulating multiple aspects of the physiological response to metabolic stimuli and obesity in metabolic tissues.

Increasing evidences highlight the importance of cross-talk between ATMs and other immune cells in shaping the immunometabolic profile of the adipose tissue contributing to inflammation and insulin resistance during obesity. While ATMs of obese mice trigger the reduction of Tregs [43, 44], which is responsible for improvement of insulin sensitivity and reduced inflammation in obese human and mice [45], they promote the accumulation of mast cells and CD8+ effector T cells, which leads to macrophage recruitment into adipose tissue [46, 47], inflammation and insulin resistance in obesity [48, 49]. Thus, the complex interplay between ATMs and other immune cells might also have been contributed to the beneficial effect in HFD-feeding MKO mice.

PBMCs are implicated in the mechanisms linking immune-inflammation to the modulation of chronic disease development [50]. Hence, these cells may be a new source of non-invasive diagnostic and prognostic biomarkers. Hyperglycemia functions as a crucial driving force of these processes by modulating the response of PBMCs [51]. Increased TonEBP activity in monocytes is associated with early diabetic nephropathy (DN) in humans [52]. Data from various human cohorts also indicate that single-nucleotide polymorphisms of TonEBP are associated with inflammation, DN, and the risk of T2D [11]. Importantly, our finding that mRNA levels of *TonEBP* are elevated in PMBCs of diabetic patients and HFD-induced diabetic mice support these previous findings. *TonEBP* mRNA expression in PMBCs was positively correlated with blood glucose levels in human and mice. In addition, there was a strong association between *TonEBP* and *TNFα* mRNA levels in PMBCs of obese mice, suggesting that TonEBP plays a critical role in the proinflammatory state of PBMCs, and that variability of TonEBP

expression can affect this state. Therefore, targeting TonEBP levels in PBMCs is potentially a new therapeutic strategy to counteract metabolic diseases such as T2D, and these levels are also potentially an additional biomarker to predict outcomes.

Obese patients have increased FFA levels in blood [32, 53]. Elevated saturated fatty acids, particularly PA, lead to inflammatory responses, which are an important risk factor for the onset of obesity-associated metabolic disorders [35, 54]. In adipose tissue, macrophages are surrounded by adipocytes, which constantly release FFAs. PA and its metabolites promote potent metabolic inflammation in macrophages via various signaling pathways [54]. Here, we show that TonEBP depletion in human and mouse macrophages decreases induction of pro-inflammatory gene expression and cytokine secretion, but promotes expression of genes related to anti-inflammatory macrophages in response to PA, and thereby improves insulin signaling and glucose uptake in adipocytes. In addition, PA can induce and enhance inflammatory reactions via distinct mechanisms, including endoplasmic reticulum stress. Future studies should investigate the impact of TonEBP on various PA-mediated cellular events, including endoplasmic reticulum stress. Furthermore, the molecular mechanism by which TonEBP regulates PA-mediated cellular events involved in MMe macrophages remains to be determined.

Many pathological conditions and agents induce *TonEBP* gene expression via TLR4 stimulation, and increased expression of TonEBP promotes its homeostatic and pathologic functions [11]. In the present study, we provide evidence that the transcription factor Sp1 is a crucial mediator of transcriptional regulation of the *TonEBP* gene induced by TLR4 activation (Fig. 5). This is interesting in view of the previous finding that Sp1 and TonEBP play distinct roles in expression of pro- and anti-inflammatory genes. First, TonEBP and Sp1 have opposite roles in transcriptional regulation of IL-10, a potent anti-inflammatory and immunosuppressive molecule in macrophages. Sp1 is a major transcription factor involved in LPS-mediated induction of *IL-10* gene expression, and is recruited to a putative binding site in the promoter region in mouse and human macrophages [55]. By contrast, TonEBP suppresses LPS-mediated transactivation of the *IL-10* gene. Interestingly, TonEBP suppresses transcription of the *IL-10* gene by reducing chromatin accessibility and thus recruitment of Sp1 to its promoter [23]. The present study and these previous findings suggest there is a previously unrecognized bidirectional regulatory loop between Sp1 and TonEBP in the context of LPS-mediated IL-10 expression. Specifically, Sp1 activates *TonEBP* transcription in response to LPS. TonEBP, in turn, negatively regulates recruitment of Sp1 to the *IL-10* promoter and thereby abrogates the capacity of Sp1 to stimulate *IL-10* transcription. Thus, the reciprocal actions of Sp1 and TonEBP are an important aspect of regulation of IL-10 expression. Second, TonEBP and Sp1 are important positive regulators of NF-kB p65, which is a central signaling hub in inflammatory responses. Sp1 facilitates p65 binding to promoters and promotes expression of its proinflammatory target genes, such as *Ccl2* [56]. Similarly, TonEBP promotes

transcriptional activity of NF-κB via interaction with p65 and expression of its proinflammatory target genes [29]. This regulatory relationship between Sp1 and TonEBP has functional implications for counteracting the anti-inflammatory role of Sp1 and stimulating the proinflammatory role of TonEBP and Sp1, thereby promoting pro-inflammamtory activation of macrophages. These results demonstrate a mechanism that may help to explain the differential regulation of pro- and anti-inflammatory genes. Further investigations of crosstalk between TonEBP, Sp1, and NF-κB in macrophages will likely provide important insights into the mechanisms underlying pro- and anti-inflammatory polarization, providing leads for therapeutic targeting of this crosstalk in inflammation biology.

In summary, our findings reveal that macrophage TonEBP is a crucial driver of obesity-associated inflammation and insulin resistance. Depletion of TonEBP profoundly alters the ratio of pro-inflammatory-to-anti-inflammatory MMe macrophages and reduces macrophage accumulation in adipose tissue and the liver. Considering the key role of macrophages in adipose tissue function, targeted modulation of TonEBP activity in ATMs might open up new avenues for inducing healthy adipose tissue remodeling to prevent progression of obesity-associated morbidities.

3.6. Supplementary Tables & Figures

	Antigen (Clone)	Fluoropore	Cat. No. Company
Flow cytometry analysis			
SVFs	F4/80 (T45-2342)	PE	565610, BD Biosciences
	CD11b (M1/70)	PerCP	550993, BD Biosciences
	CD11c (HL3)	FITC	557400, BD Biosciences
	CD206 (MR5D3)	APC	565250, BD Biosciences
PBMC	CD45 (RA3-6B2)	FITC	553087, BD Biosciences
	CD11b (M1/70)	PerCP	550993, BD Biosciences
	Ly6C (AL-21)	PE-Cy7	560593, BD Biosciences
	CCR2 (SA203G11)	APC	150603, Biolegend
BMDM	F4/80 (T45-2342)	PE	565610, BD Biosciences
	CD11b (M1/70)	PerCP	550993, BD Biosciences
	CD11c (HL3)	FITC	557400, BD Biosciences
	CD206 (MR5D3)	APC	565250, BD Biosciences
BM	CD45 (RA3-6B2)	FITC	553087, BD Biosciences
	CD11b (M1/70)	PerCP	550993, BD Biosciences
	Ly6C (HK1.4)	APC	128015, Biolegend
	Ly6G (1A8)	PE	551461, BD Biosciences
	CCR2 (SA203G11)	PE-Cy7	150612, Biolegend
Immunoblotting			
	AKT		#9272, Cell signaling (1:1000)
	phospho AKT(s273)		#9271, Cell signaling (1:1000)
	TonEBP		PA1-023, ThermoFisher Scientific (1:1000)
	F4/80		ab6640, Abcam (1:1000)
	PPARγ (81B8)		#2443, Cell signaling (1:1000)
	Sp1 (EPR22648-50)		ab231778, Abcam (1:1000)
	Stat6 (D3H4)		#5397, Cell signaling (1:1000)
	Phospho-Stat6 (Tyr641)		#9361, Cell signaling (1:1000)
	C/EBP beta (C-19)		sc-150, Santa Cruz (1:1000)
	iNOS		610432, BD Biosciences (1:1000)
	Hsc70		#200-301-A28, Rockland (1:2000)
	β-actin		5441, Sigma-Aldrich (1:2000)
	Goat anti-mouse (Horseradish-peroxidase conjugated)		62-6520, ThermoFisher Scientific (1:5000)
	Goat anti-rabbit (Horseradish-peroxidase conjugated)		62-6120, ThermoFisher Scientific (1:5000)

Table 3.S1. Primary antibodies used for flow cytometry analysis and immunoblotting

Primers for gene expression analysis

Species	Gene	Forward primer (5'-3')	Reverse primer (5'-3')	Accession No.*
Mouse	*Adiponectin*	TGGAATGACAGGAGCTGAAGG	ACACTGAACGCTGAGCGATACACA	NM_009605
	Arg-1	CTCCAAGCCAAAGTCCTTAGAG	AGGAGCTGTCATTAGGGACATC	NM_007482
	Ccl2	AACTGCATCTGCCCTAAGGT	AGTGCTTGAGGTGGTTGTGGAA	NM_011333
	CD206	TCTTTTACGAGAAGTTGGGGTCAG	ATCATTCCGTTCACCAGAGGG	NM_008625
	CypA	CAGCCATGGTCAACCCCACCG	CTGCTGTCTTTGGAACTTTGTCTG	NM_008907
	F4/80	CTTTGGCTATGGGCTTCCAGTC	GCAAGGAGGACAGAGTTTATCGTG	NM_010130
	IL-10	ACCTGGTAGAAGTGATGCCCCAGGCA	CTATGCAGTTGATGAAGATGTCAAA	NM_010548
	IL-1β	CAAAGGCGGCCAGGATATAA	CTAGGGATTGAGTCCACATTCAG	NM_000576
	iNOS	TCTCCCTTTCCTCCCTTCTT	CTTCAGTCAGGAGGTTGAGTTT	NM_010927
	Leptin	GGGCTTCACCCCATTCTGA	TGGCTATCTGCAGCACATTTTG	NM_008493
	Mgl1	GACAACACCACCTCCAAGATAA	TCCACATCCACTTTCAGAGAAC	NM_00120425
	PPARγ1	AGGAGAAGTCACACTCTGACAGGA	TCAGTGGTTCACCGCTTCTT	NM_001127330
	PPARγ2	TTCGCTGATGCACTGCCTATGA	AAGGAATGCGAGTGGTCTTCCA	NM_011146
	TNFα	TGGGACAGTGACCTGGACTGT	TTCGGAAAGCCCATTTGAGT	NM_013693
	TonEBP	AAGCAGCCACCACCAAACATGA	AAATTGCATGGGCTGCTGCT	NM_133957
	Ym1	GGCTACACTGGAGAAAATAGTCCCC	CCAACCCACTCATTACCCTGATAG	NM_009892
Human	*Ccl2*	GGCTGAGACTAACCCAGAAAC	GAATGAAGGTGGCTGCTATGA	NM_002982
	CD163	GGGATGTCCAACTGCTATCAA	GACTCATTCCCACGACAAGAA	NM_203416
	CD206	GGACGTGGCTGTGGATAAAT	ACCCAGAAGACGCATGTAAAG	NM_002438
	CD80	TCTGGTGCTCTTTCCCTTTATC	AGTCTCTGAAGTTGACCTGTTATT	NM_005191
	GAPDH	GGTGTGAACCATGAGAAGTATGA	GAGTCCTTCCACGATACCAAAG	NM_002046
	IL-10	TTTCCCTGACCTCCCTCTAA	CGAGACACTGGAAGGTGAATTA	NM_000572
	IL-1β	CAAAGGCGGCCAGGATATAA	CTAGGGATTGAGTCCACATTCAG	NM_000576
	PPARγ1	CTCAAACGAGAGTCAGCCTTTA	GTGGGAGTGGTCTTCCATTAC	NM_138712
	PPARγ2	AGCGATTCCTTCACTGATACAC	GTGGGAGTGGTCTTCCATTAC	NM_015869
	TNFα	AGAGGGAGAGAAGCAACTACA	GGGTCAGTATGTGAGAGGAAGA	NM_000594
	TonEBP	AGCTGTTGTTGCTGCTGATGCT	TCCACTTGCATAGCCTTGCTGT	NM_006599

* Accession No. refer to Genebank (NCBI)

Primers for ChIP assay

Species	Gene	Forward primer (5'-3')	Reverse primer (5'-3')
Mouse	PPARγ1	TGCTAAAGAATTTTAAAAAGCCAGT	CCCCTGGAGCTGGAGTTAC
Human	TonEBP Region A	CAACGGGGAATAAAAAGGTCA	CCCAGACCGATGTAATCACT
	Region B	TCAACGGGGAATAAAAAGGT	CCCAGACCGATGTAATCACT

Table 3.S2. Primers used in qPCR for gene expression analysis and ChIP assay

No.	Age	Gender	BMI	Blood glucose level (mg/dL)	DM type
1	78	F	28.04	201	T2DM
2	51	F	20.93	131	T2DM
3	72	M	24.61	117	T2DM
4	53	M	30.43	146	T2DM
5	57	M	25.18	161	T2DM
6	71	F	24.19	122	T2DM
7	63	M	26.36	158	T2DM
8	78	M	25.02	130	T2DM
9	65	F	23.73	69	Non-DM
10	52	M	22.8	100	Non-DM
11	72	M	24.32	95	Non-DM
12	61	M	25.64	88	Non-DM

DM, Diabetes Mellitus: T2DM, Type 2 DM: BMI, Body mass index

Table 3.S3. Clinical characteristics of diabetic and non-diabetic subjects studied

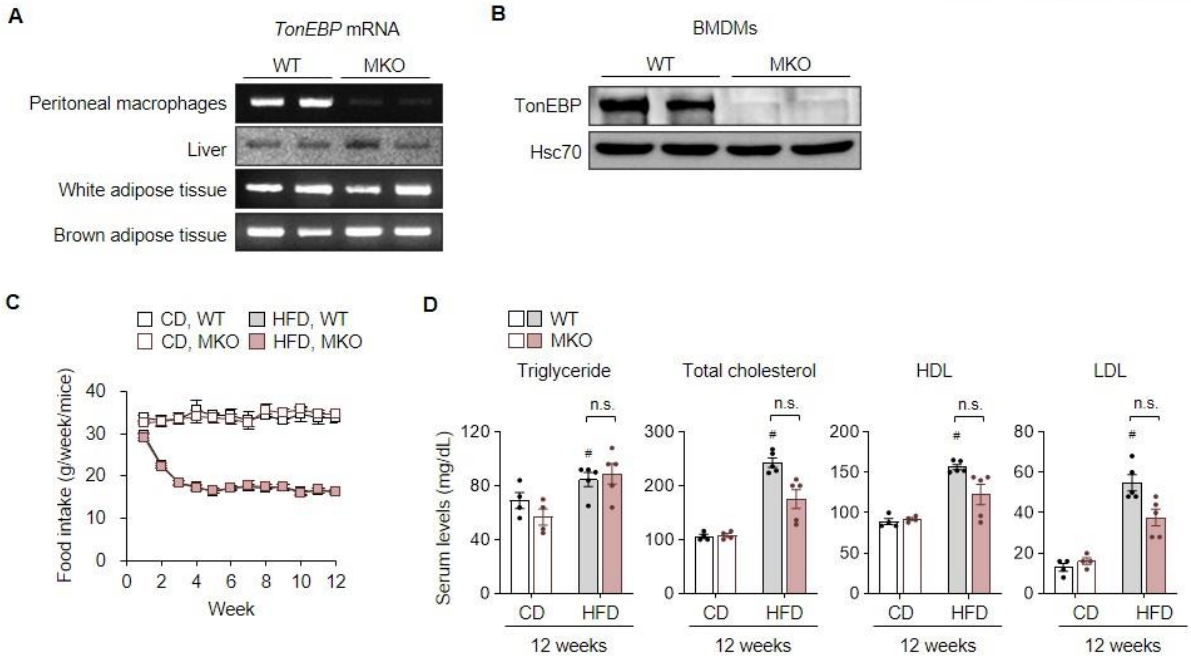

Figure 3.S1. (related to Fig. 1) (**A**) mRNA levels of *TonEBP* in peritoneal macrophages, liver, white adipose tissue, and brown adipose tissue isolated from male MKO and WT littermates aged 8 weeks measured by RT-PCR. (**B**) Protein levels of TonEBP in M-CSF-differentiated bone marrow-derived macrophages (BMDMs) from male *TonEBP*$^{fl/fl}$*LysM*-cremice (MKO) and their *TonEBP*$^{fl/fl}$littermates (WT) aged 8 weeks. (**C, D**) Male MKO and their WT littermates aged 8 weeks were fed a normal CD or HFD for 12 weeks. (**C**) Food intake (CD, *n*= 14; HFD, *n*= 15). (**D**) Serum levels of triglycerides and cholesterol (total, HDL, and LDL) (CD, *n*= 4; HFD, *n*= 5). *n*represents the number of biologically independent animals (or samples). All data are presented as mean + s.e.m. The *p*-values were determined by an ANOVA with Tukey's *post-hoc*test. #*p*< 0.05 vs. CD. n.s.: not significant.

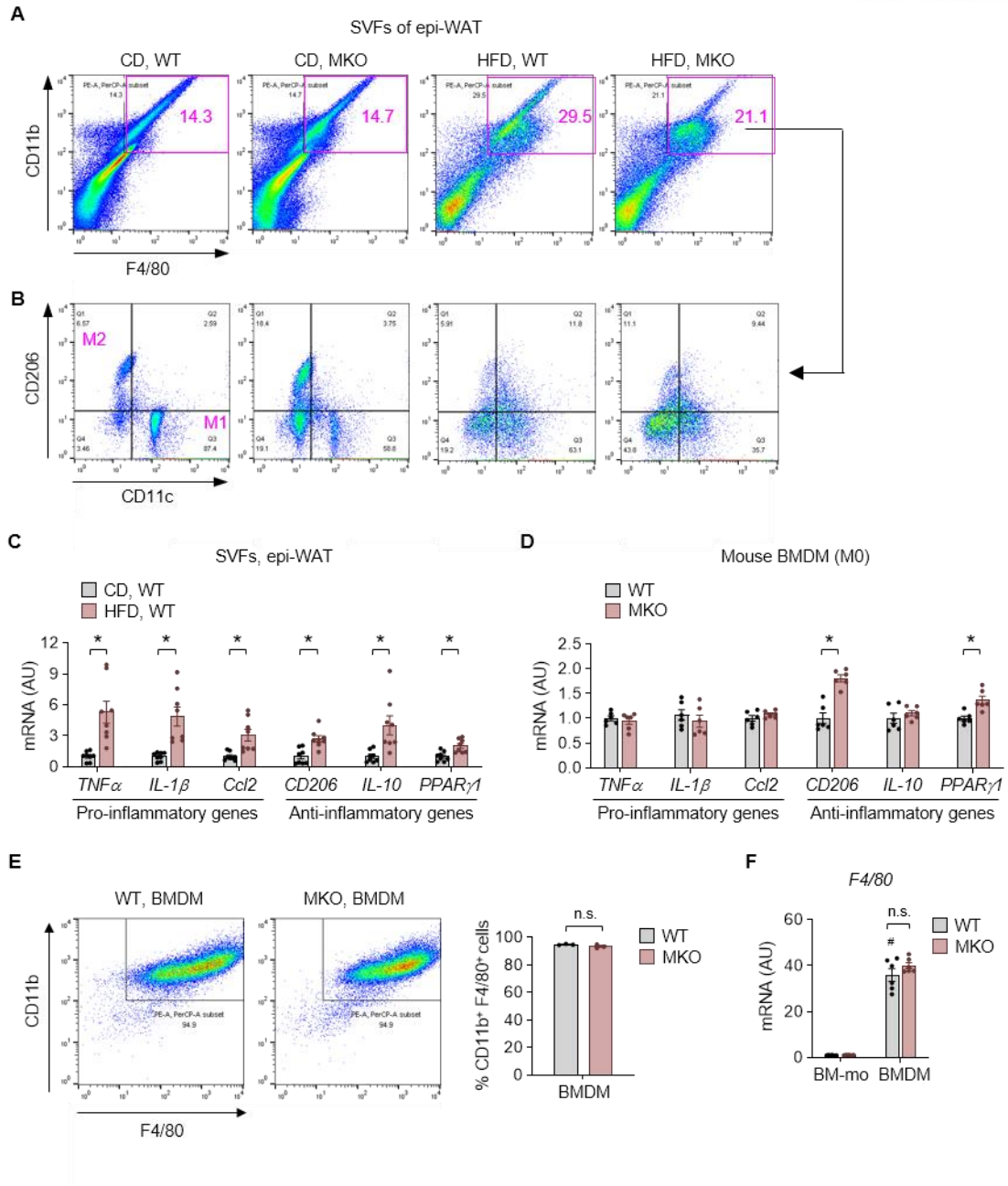

Figure 3.S2. (related to Fig. 3) (**A, B**) Flow cytometry analysis of cells isolated from SVFs of epi-WAT from MKO and WT mice fed a CD (n = 3) or HFD (n = 11) for 12 weeks. (**A**) Representative flow cytometry plots showing the percentage of total macrophages ($CD11b^+F4/80^+$) among cells isolated from SVFs. (**B**) Representative flow cytometry plots showing the frequencies of M1 ($CD11c^+CD206^-$)-like and M2 ($CD11c^-CD206^+$)-like phenotypes among $CD11b^+F4/80^+$ cells. (**C**) mRNA levels of metabolically activated pro- and anti-inflammatory genes in SVFs of epi-WAT from WT mice fed a CD or HFD (n = 6). (**D**) mRNA levels of pro- and anti-inflammatory genes in BMDMs from WT and MKO mice (n = 6). (**E**) Representative flow cytometry plots showing the frequencies of $CD11b^+F4/80^+$ cells

(**left**) and quantification of $CD11b^{+}F4/80^{+}$ cells (**right**) among BMDMs from WT and MKO mice (n = 4). (**F**) mRNA levels of *F4/80* in BM-Mo and BMDMs from WT and MKO mice (n = 6). n represents the number of biologically independent animals (or samples). All data are presented as mean + s.e.m. (or s.d.). The p-values were determined by a one-way ANOVA. $^{\#}$ $p < 0.05$ vs. BM-mo (**F**). ***** $p < 0.05$. n.s.: not significant

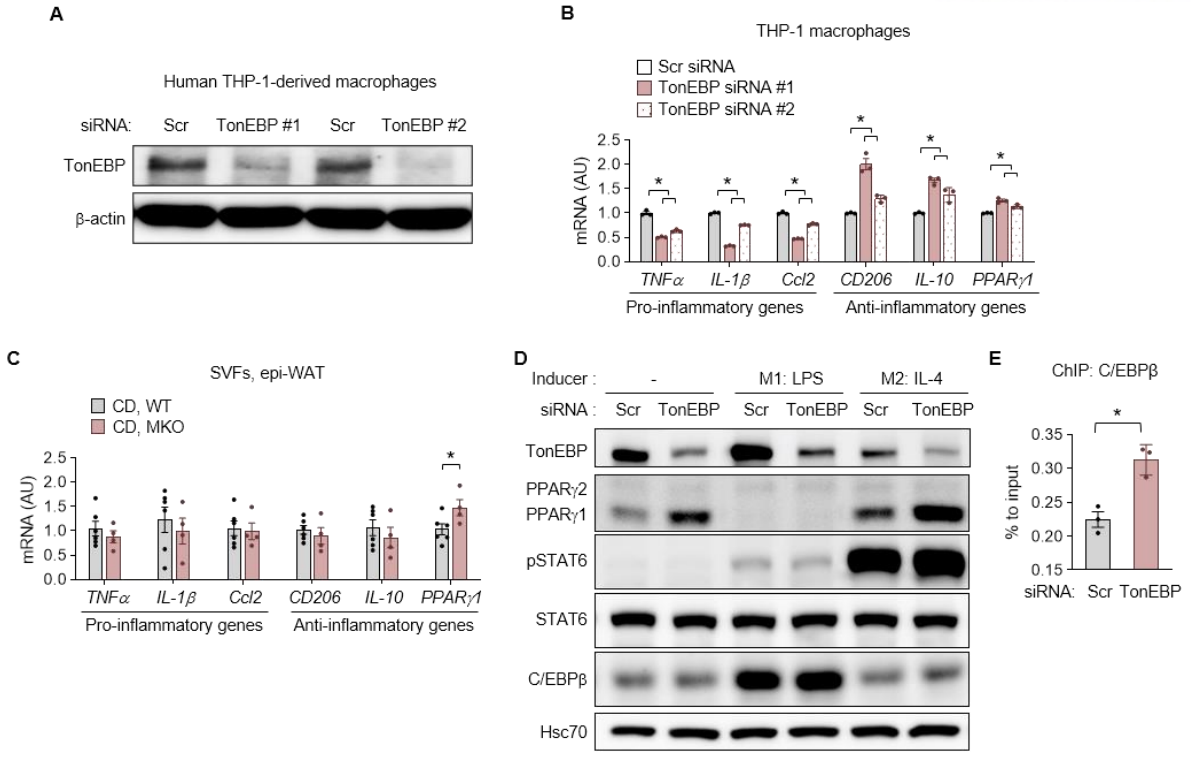

Figure 3.S3. (related to Fig. 3) (**A**) THP-1-derived macrophages were transfected with Scr siRNA or two siRNAs (#1 or #2) targeting different regions of human *TonEBP* mRNA for 48 h. Representative immunoblots of TonEBP and β-actin (n = 3). (**B**) mRNA levels of pro- and anti-inflammatory genes in THP-1-derived macrophages transfected with Scr siRNA or siRNAs (#1 or #2) targeting different regions of human TonEBP mRNA (n = 3). (**C**) mRNA levels of metabolically activated pro- and anti-inflammatory genes in SVFs of epi-WAT from 8-week-old WT (n = 6) and MKO (n = 4) mice fed a CD. (**D**) RAW264.7 cells transfected with Scr or *TonEBP*-targeted siRNA were treated with vehicle (-), the M1 inducer LPS (100 ng/ml), or the M2 inducer IL-4 (20 ng/ml). Representative immunoblots of TonEBP, PPARγ, pSTAT6, STAT6, C/EBPβ, and HSC70 (n = 3). (**E**) ChIP was performed using anti-C/EBPβ antibodies on RAW264.7 cells transfected with Scr or *TonEBP*-targeted siRNA. Precipitated DNA samples were analyzed by q-PCR for the PPARγ1 promoter (Suppl Table 2). n represents the number of independent experiments with triplicates (**A, B, D**), or biologically independent samples (**C**). All data are presented as mean + s.e.m. (or s.d.). The p-values were determined by a one-way ANOVA. * $p < 0.05$.

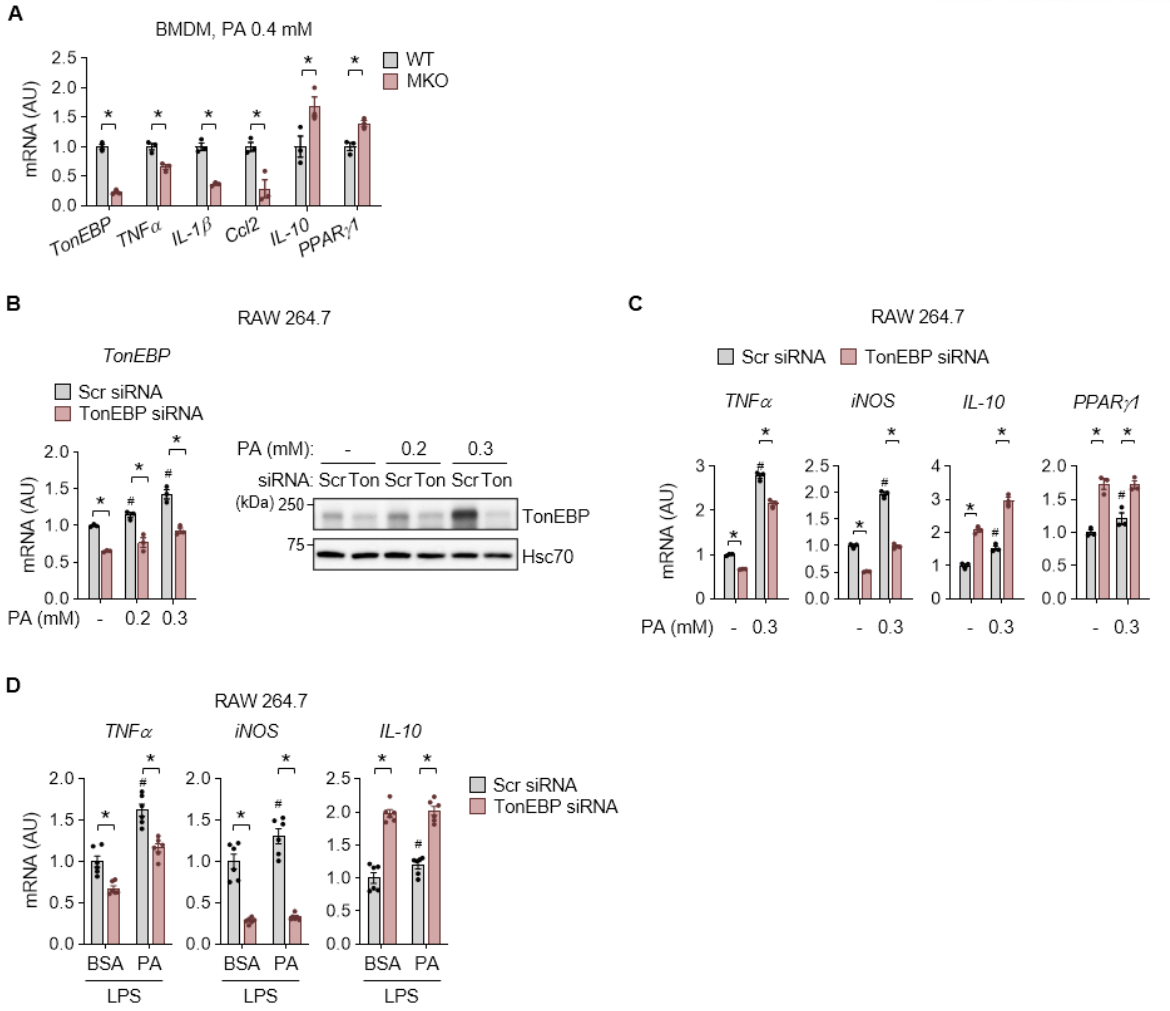

Figure 3.S4. (related to Fig. 4) (**A**) BMDMs from WT and MKO mice were exposed to BSA (-) or PA (0.4 mM) for 18 h. mRNA expression of the indicated genes ($n = 3$). (**B, C**) RAW264.7 cells transfected with Scr or *TonEBP*-targeted siRNA. siRNA-transfected cells were exposed to BSA (-) or PA (0.2 or 0.3 mM) for 6 or 18 h. (**B**) *TonEBP* mRNA levels at 6 h (**left**) and representative immunoblots of TonEBP and Hsc70 at 18 h (**right**) ($n = 3$). (**C**) mRNA expression of the indicated genes at 18 h. (**D**) RAW264.7 cells transfected with indicated siRNA were exposed to BSA or PA (0.2 mM) in the presence of LPS (1 ng/ml) for 18 h. mRNA levels of *TNFα*, *iNOS*, and *IL-10*, which are related to the insulin response, at 18 h. All data are presented as mean + s.d. AU, arbitrary unit. The *p*-values were determined by an ANOVA with Tukey's *post-hoc* test. $^{\#}$ $p < 0.05$ vs. Scr siRNA; BSA (-) (**C**), BSA (**D**). * $p < 0.05$.

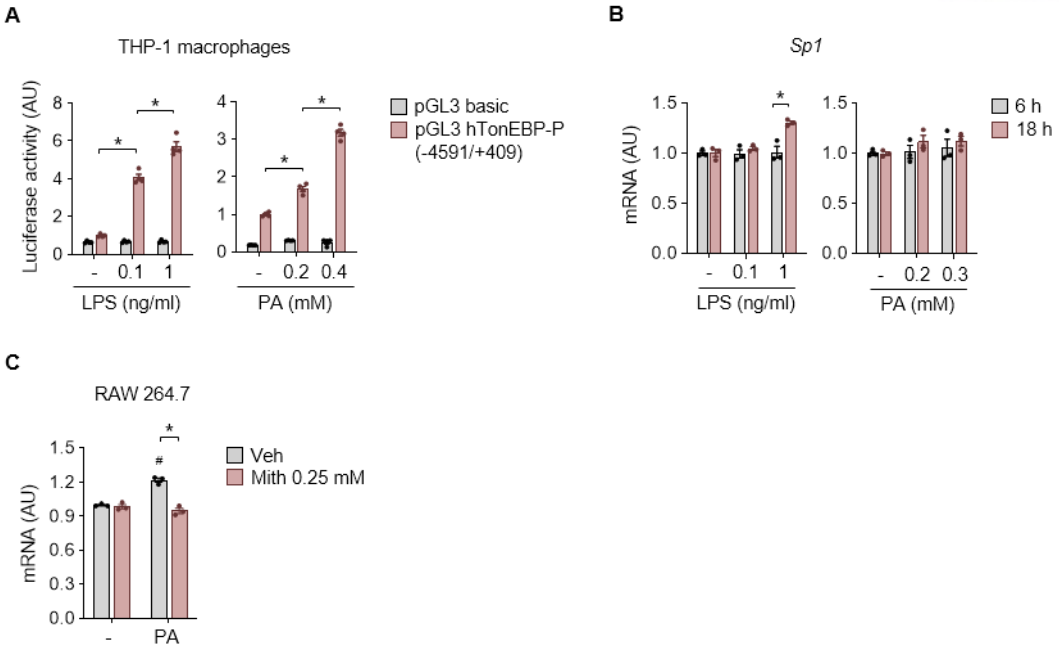

Figure 3.S5. (related to Fig. 5) (**A**) THP-1-derived macrophages were transfected with the human *TonEBP* promoter-luciferase construct containing the −4591 to +409 region or the pGL3 basic vector. Luciferase activity was measured after LPS (8 h) or PA (10 h) treatment as indicated (n = 4). (**B**) RAW264.7 cells were exposed to LPS or PA as indicated for 6 or 18 h. mRNA levels of *Sp1* (n = 3). (**C**) RAW264.7 cells were treated with vehicle (-) or mithramycin A (mith, 0.25 mM) for 1 h followed by vehicle (-) or PA (0.4 mM) for 6 h. TonEBP *mRNA* levels (n = 3). n represents the number of independent experiments with triplicates. All data are presented as mean + s.d. AU, arbitrary unit. The p-values were determined by an ANOVA with Tukey's *post-hoc* test. $^{\#}$ $p < 0.05$ vs. (-) (**C**). * $p < 0.05$.

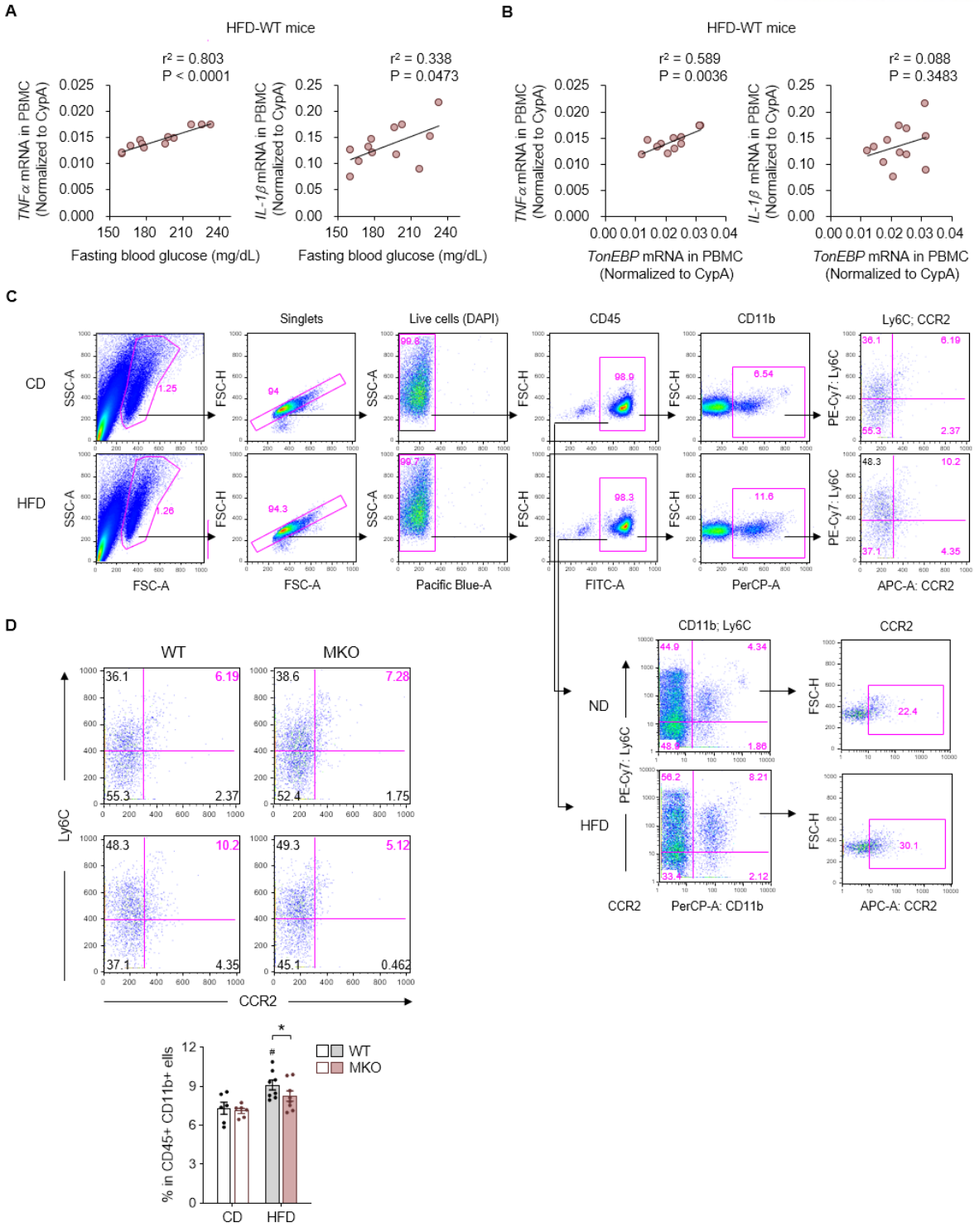

Figure 3.S6. (related to Fig. 6) (**A**) Correlation between fasting blood glucose levels and mRNA expression of *TNFα* (**left**) and *IL-1β* (**right**) in PBMCs from WT mice fed a HFD for 12 weeks (*n* = 12). (**B**) Correlation between mRNA expression of *TonEBP* and *TNFα* (**left**) and *TonEBP* and *IL-1β* (**right**) in PBMCs from WT mice fed a HFD for 12 weeks (*n* = 12). (**C, D**) Flow cytometry analysis of

PBMCs from WT and MKO mice fed a CD or HFD for 12 weeks (CD, n = 6; HFD, n = 8). (**C**) Representative flow cytometry gating strategies. (**D**) Representative flow cytometry plots (**top**) and quantification (**bottom**) of $Ly6C^+CCR2^+$ cells among myeloid cells ($CD45^+CD11b^+$) (CD, n = 3; HFD, n = 4). n represents the number of biologically independent samples. Correlations were assessed by the non-parametric Spearman's test. All data are presented as mean + s.e.m. The p-values were determined by a one-way ANOVA. $^{\#}$ $p < 0.05$ vs. WT; CD (**D**). * $p < 0.05$.

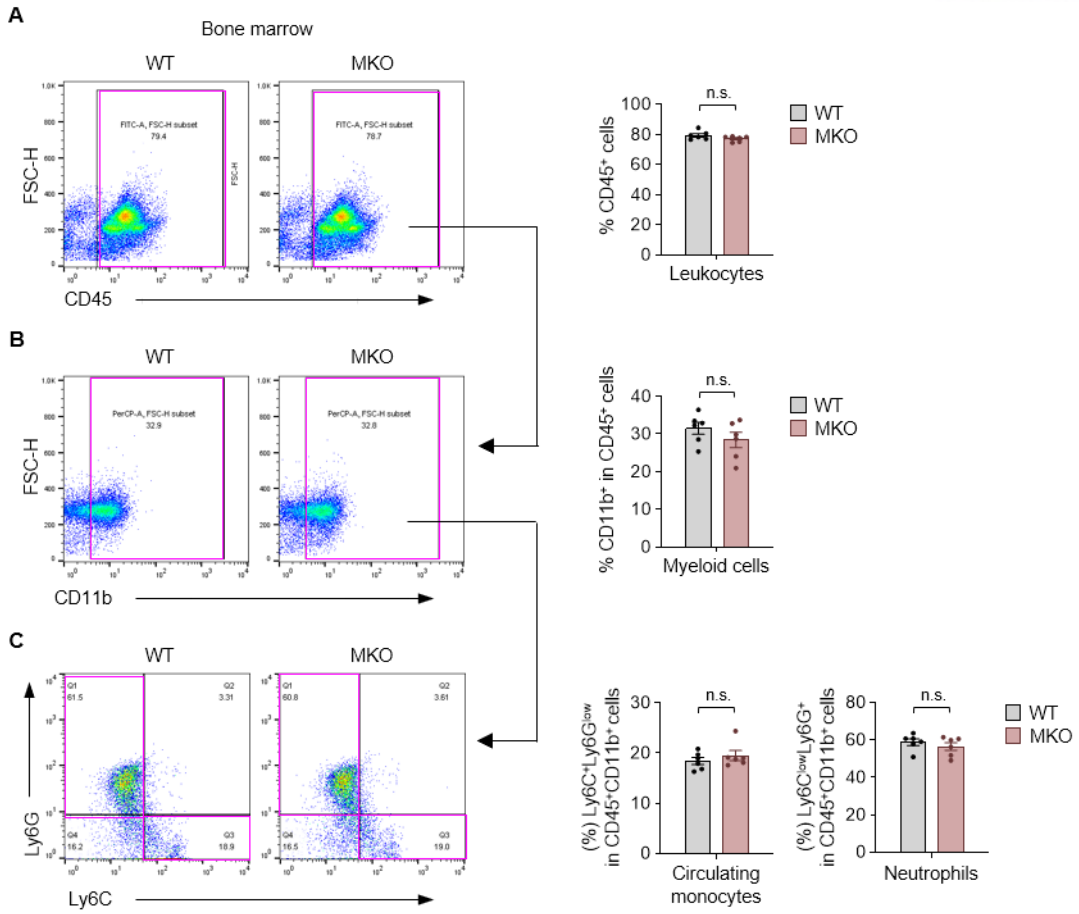

Figure 3.S7. (related to Fig. 6) Flow cytometry analysis of BM from male WT and MKO mice aged 8 weeks (n = 6). Representative flow cytometry plots (**left**) and quantification (**right**) of leukocytes ($CD45^+$) (**A**), myeloid cells ($CD11b^+$ in $CD45^+$) (**B**), circulating monocytes ($Ly6C^+Ly6G^{low}$ among $CD45^+CD11b^+$ cells), and neutrophils ($Ly6C^{low}Ly6G^+$ among $CD45^+CD11b^+$ cells) (**C**). n represents the number of biologically independent samples. All data are presented as mean + s.e.m. The p-values were determined by a one-way ANOVA. n.s.: not significant.

3.7. References

1. Hotamisligil GS. Inflammation and metabolic disorders. Nature 2006;444:860-867
2. Lumeng CN, Saltiel AR. Inflammatory links between obesity and metabolic disease. J Clin Invest 2011;121:2111-21117
3. Weisberg SP, McCann D, Desai M, Rosenbaum M, Leibel RL, Ferrante AW, Jr. Obesity is associated with macrophage accumulation in adipose tissue. J Clin Invest 2003;112:1796-1808
4. Heilbronn LK, Campbell LV. Adipose tissue macrophages, low grade inflammation and insulin resistance in human obesity. Curr Pharm Des 2008;14:1225-1230
5. Gordon S, Taylor PR. Monocyte and macrophage heterogeneity. Nat Rev Immunol 2005;5:953-964
6. Murray PJ, Allen JE, Biswas SK, et al. Macrophage activation and polarization: nomenclature and experimental guidelines. Immunity 2014;41:14-20.
7. Oh DY, Morinaga H, Talukdar S, Bae EJ, Olefsky JM. Increased macrophage migration into adipose tissue in obese mice. Diabetes 2012;61:346-354
8. Lumeng CN, Bodzin JL, Saltiel AR. Obesity induces a phenotypic switch in adipose tissue macrophage polarization. J Clin Invest 2007;117:175-184
9. Kratz M, Coats BR, Hisert KB, et al. Metabolic dysfunction drives a mechanistically distinct proinflammatory phenotype in adipose tissue macrophages. Cell Metab 2014; 20:614-625
10. Coats BR, Schoenfelt KQ, Barbosa-Lorenzi VC, et al. Metabolically activated adipose tissue macrophages perform detrimental and beneficial functions during diet-induced obesity. Cell Rep 2017;20:3149-3161
11. Choi SY, Lee-Kwon W, Kwon HM. The evolving role of TonEBP as an immunometabolic stress protein. Nat Rev Nephrol 2020;16:352-64
12. Küper C, Beck FX, Neuhofer W. Generation of a conditional knockout allele for the NFAT5 gene in mice. Front Physiol 2014;5:507
13. Weischenfeldt J, Porse B. Bone marrow-derived macrophages (BMM): isolation and applications. CSH Protocols. 2008; 10.1101/pdb.prot5080
14. Troegeler A, Lastrucci C, Duval C, et al. An efficient siRNA-mediated gene silencing in primary human monocytes, dendritic cells and macrophages. Immunol Cell Biol 2014;92:699-708
15. Mahmood T, Yang PC. Western blot: technique, theory, and trouble shooting. N Am J Med Sci 2012;4:429-434
16. Jung DW, Ha HH, Zheng X, Chang YT, Williams DR. Novel use of fluorescent glucose analogues

to identify a new class of triazine-based insulin mimetics possessing useful secondary effects. Mol Biosyst 2011;7:346-358

17. Chawla A, Nguyen KD, Goh YP. Macrophage-mediated inflammation in metabolic disease. Nat Rev Immunol 2011;11:738-749
18. Postic C, Girard J. Contribution of de novo fatty acid synthesis to hepatic steatosis and insulin resistance: lessons from genetically engineered mice. J Clin Invest 2008;118:829-838
19. Alisi A, Carpino G, Oliveira FL, Panera N, Nobili V, Gaudio E. The Role of Tissue Macrophage-Mediated Inflammation on NAFLD Pathogenesis and Its Clinical Implications. Mediators Inflamm 2017;2017:8162421
20. Strissel KJ, Stancheva Z, Miyoshi H, et al. Adipocyte death, adipose tissue remodeling, and obesity complications. Diabetes 2007;56:2910-2918
21. Martinez FO, Gordon S, Locati M, Mantovani A. Transcriptional profiling of the human monocyte-to-macrophage differentiation and polarization: new molecules and patterns of gene expression. J Immunol 2006;15;177: 7303-7311
22. Odegaard JI, Ricardo-Gonzalez RR, Goforth MH, et al. Macrophage-specific PPARgamma controls alternative activation and improves insulin resistance. Nature 2007;447:1116-1120
23. Choi SY, Lee HH, Lee JH, et al. TonEBP suppresses IL-10-mediated immunomodulation. Sci Rep 2016;6:25726
24. Huang JT, Welch JS, Ricote M, et al. Interleukin-4-dependent production of PPAR-gamma ligands in macrophages by 12/15-lipoxygenase. Nature 1999;400:378-382
25. Lawrence, T., Natoli, G. Transcriptional regulation of macrophage polarization: enabling diversity with identity. Nat Rev Immunol 2011;11:750–761
26. Lee JH, Lee HH, Ye BJ, et al. TonEBP suppresses adipogenesis and insulin sensitivity by blocking epigenetic transition of PPARγ2. Sci Rep 2015;5:10937
27. Zhu Y, Qi C, Korenberg, J.R, et al. Structural organization of mouse peroxisome proliferatoractivated receptor y (mPPARy) gene: Alternative promoter use and different splicing yield two mPPARy isoforms. Proc. Natl. Acad. Sci. USA 1995;92:7921–7925
28. Tilg H, Moschen AR. Inflammatory mechanisms in the regulation of insulin resistance. Mol Med 2008;14:222-231
29. Lee HH, Sanada S, An SM, et al. LPS-induced NFκB enhanceosome requires TonEBP/NFAT5 without DNA binding. Sci Rep 2016;6:24921
30. Jeong GW, Lee HH, et al. Microglial TonEBP mediates LPS-induced inflammation and memory loss as transcriptional cofactor for NF-κB and AP-1. J Neuroinflammation 2020;17:372
31. Al-Attas OS, Al-Daghri NM, Al-Rubeaan K, et al. Changes in endotoxin levels in T2DM subjects

on anti-diabetic therapies. Cardiovasc Diabetol 2009;8:20

32. Mook S, Halkes Cj C, Bilecen S, Cabezas MC. In vivo regulation of plasma free fatty acids in insulin resistance. Metabolism 2004;53:1197-1201
33. Cani PD, Amar J, Iglesias MA, et al. Metabolic endotoxemia initiates obesity and insulin resistance. Diabetes 2007;56:1761-1772
34. Lam TK, van de Werve G, Giacca A. Free fatty acids increase basal hepatic glucose production and induce hepatic insulin resistance at different sites. Am J Physiol Endocrinol Metab 2003;284:E281-290
35. Khodabandehloo H, Gorgani-Firuzjaee S, Panahi G, Meshkani R. Molecular and cellular mechanisms linking inflammation to insulin resistance and β-cell dysfunction. Transl Res 2016;167:228-256
36. Lauterbach MA, Wunderlich FT. Macrophage function in obesity-induced inflammation and insulin resistance. Pflugers Arch 2017;469:385-396
37. Sirota P, Hadi E, Djaldetti M, Bessler H. Difference in inflammatory cytokine production by mononuclear cells from obese and non-obese schizophrenic patients. Acta Psychiatr Scand 2015;132:301-315
38. Akhter N, Madhoun A, Arefanian H, et al. Oxidative Stress Induces Expression of the Toll-Like Receptors (TLRs) 2 and 4 in the Human Peripheral Blood Mononuclear Cells: Implications for Metabolic Inflammation. Cell Physiol Biochem 2019;53:1-18
39. Friedrich K, Sommer M, Strobel S, et al. Perturbation of the Monocyte Compartment in Human Obesity. Front Immunol 2019;10:1874
40. Takahashi K, Mizuarai S, Araki H, et al. Adiposity elevates plasma MCP-1 levels leading to the increased CD11b-positive monocytes in mice. J Biol Chem 2003;278:46654-46660
41. Lee HH, An SM, Ye BJ, et al. TonEBP/NFAT5 promotes obesity and insulin resistance by epigenetic suppression of white adipose tissue beiging. Nat Commun 2019;10:3536
42. Ying W, Fu W, Lee YS, Olefsky JM. The role of macrophages in obesity-associated islet inflammation and β-cell abnormalities. Nat Rev Endocrinol 2020;16(2):81-90
43. Cipolletta D, Feuerer M, Li Amy, et al. PPAR-γ is a major driver of the accumulation and phenotype of adipose tissue Treg cells. Nature. 2012;486:549-53
44. Onodera T, Fukuhara A, Jang MH, et al. Adipose tissue macrophages induce PPARγ-high FOXP3(+) regulatory T cells. Sci Rep 2015;5:16801
45. Eller K, Kirsch A, Wolf A, et al. Potential Role of Regulatory T Cells in Reversing Obesity-Linked Insulin Resistance and Diabetic Nephropathy. Diabetes 2011;60:2954-62
46. Liu J, Divoux A, Sun JS, et al. Genetic deficiency and pharmacological stabilization of mast cells

reduce diet-induced obesity and diabetes in mice. Nat Med 2009;15:940-5

47. Nishimura S, Manabe I, Nagasaki M, et al. CD8+ effector T cells contribute to macrophage recruitment and adipose tissue inflammation in obesity. Nat Med 2009;15:914-20
48. Divoux A, Moutel S, Poitou C, et al. Mast cells in human adipose tissue: link with morbid obesity, inflammatory status, and diabetes. J Clin Endocrinol Metab 2012;97:E1677-85
49. Gurung P, Moussa K, Adams-huet B, et al. Increased mast cell abundance in adipose tissue of metabolic syndrome: relevance to the proinflammatory state and increased adipose tissue fibrosis. American Journal of Physiology-Endocrinology and Metabolism 2019;316:E504-9.
50. van Dijk SJ, Feskens EJ, Bos MB, et al. Consumption of a high monounsaturated fat diet reduces oxidative phosphorylation gene expression in peripheral blood mononuclear cells of abdominally overweight men and women. J Nutr 2012;142:1219-1225
51. Schiekofer S, Andrassy M, Chen J, et al. Acute hyperglycemia causes intracellular formation of CML and activation of ras, p42/44 MAPK, and nuclear factor kappaB in PBMCs. Diabetes 2003;52:621-633
52. Yang B, Hodgkinson AD, Oates PJ, Kwon HM, Millward BA, Demaine AG. Elevated activity of transcription factor nuclear factor of activated T-cells 5 (NFAT5) and diabetic nephropathy. Diabetes 2006;55:1450-1455
53. Pankow JS, Duncan BB, Schmidt MI, et al. Fasting plasma free fatty acids and risk of type 2 diabetes: the atherosclerosis risk in communities study. Diabetes Care 2004;27:77-82
54. Korbecki J, Bajdak-Rusinek K. The effect of palmitic acid on inflammatory response in macrophages: an overview of molecular mechanisms. Inflamm Res 2019;68:915-932
55. Ma W, Lim W, Gee K, et al. The p38 mitogen-activated kinase pathway regulates the human interleukin-10 promoter via the activation of Sp1 transcription factor in lipopolysaccharide-stimulated human macrophages. J Biol Chem 2001;276:13664-13674
56. Boekhoudt GH, Guo Z, Beresford GW, Boss JM. Communication between NF-kappa B and Sp1 controls histone acetylation within the proximal promoter of the monocyte chemoattractant protein 1 gene. J Immunol 2003;170:4139-4147

Conclusion

Inflammation occurs when our body encounters external viruses, bacteria or toxic chemicals or gets injury. Healing response to external stimuli is accompanied by symptoms such as pain, heat, swelling and redness. This response to sudden stimuli is acute inflammation. However, there are inflammatory response that our body continues without external stimuli. It is chronic inflammation. This chronic inflammation is associated in disease process. There are many cells involved in the inflammatory response, but we conducted a study on the most important macrophage among them.

TonEBP is a transcription factor involved in the adaptation to osmotic stress and innate immunity. A reduced expression of TonEBP is associated with dramatically lowering the severity of various inflammatory diseases. TonEBP haplo-deficient mice exhibit decreased inflammation, and are less susceptible to inflammatory and autoimmune diseases.

In this study, I discovered novel impact of TonEBP in microglia and macrophage polarization in inflammatory response.

1. I specifically focused on this suppressing activation of microglia in LPS-induced inflammation by disrupting the function of TonEBP. I demonstrated that TonEBP deficiency attenuated microglial activation and inflammatory cytokine production in response to LPS stimulation, thus preventing neuronal cell death. Cerulenin, which targets the function of TonEBP, also inhibited activation of microglia in this study. Cerulenin blocked binding between TonEBP and the pro-inflammatory transcriptional complex. I identified that the transcription factor AP-1 is involved in the TonEBP-mediated complex, binding TonEBP. Treatment with cerulenin, which disrupted TonEPB function, inhibited TonEBP-AP-1 binding. Thus, cerulenin treatment decreased microglial activation, alleviating neuroinflammation and preventing neuronal cell death, which was supported by significant improvement of memory loss.

In the study, we demonstrated that TonEBP, a central regulator of chronic inflammatory disease, played an important role in microglia activation. Disrupting TonEBP function prevented neuroinflammation-induced memory impairment. Future studies will further evaluate the role of TonEBP in AD. We also demonstrated that drugs targeting TonEBP could be developed as AD therapeutics. This approach could potentially alleviate AD by suppressing inflammation, contributing to the development of therapeutic agents.

2. I investigated that TonEBP in macrophages contributes to obesity-associated insulin resistance and disruption of glucose homeostasis. Indeed, when fed a HFD, mice lacking TonEBP in myeloid cells, including monocytes and macrophages, show no difference in weight gain or adiposity, but exhibit a broad range of metabolically beneficial effects such as systemically improved insulin sensitivity, glucose homeostasis, and reduced inflammation, demonstrating that TonEBP in myeloid cells plays an important role in obesity-associated morbidity. PA induces TonEBP expression in monocytes and macrophages, which inhibits M2 polarization and promotes M1 polarization. Such an M1–M2 imbalance of ATMs in turn promotes both adipose tissue and systemic inflammation, as well as insulin resistance. Here, I found an additional molecular basis for TonEBP-mediated suppression of M2 macrophage polarization. Specifically, TonEBP represses expression of PPARγ (particularly PPARγ1), a key transcription factor involved in M2 polarization and insulin sensitivity, in macrophages.

In sum, TonEBP is a stress protein responding to inflammatory stimuli by regulating microglia and ATM. The elevated expression of TonEBP drives disease progression. Thus, TonEBP in microglia and macrophage which play a major role in the inflammatory response is an attractive target for therapeutic strategy.

Acknowledgement

석·박사 통합 학위과정을 모두 마무리하고 2023년 2월 졸업을 하게 되었습니다. 2013년 인턴으로 처음 실험실에 들어와서 2015년 대학원 입학 후 8년의 과정을 거쳐 드디어 제가 박사학위 수여를 앞두고 지금 학위 논문을 마무리하고 있다는 것이 아직은 얼떨떨하기만 합니다. 제가 학위를 무사히 마칠 수 있도록 학위과정 동안 도움을 주신 많은 분들에게 감사의 말씀을 전합니다.

우선 아무것도 몰랐던 저에게 연구자로서 길을 열어 주신 지도교수님이신 권혁무 교수님께 감사드립니다. 학위기간동안 지쳐서 포기하지 않도록 늘 북돋아 주시고, 바쁘신 중에도 올바른 연구 방향을 제시해 주시고 연구자에게 필요한 것들에 대해 늘 지도해 주셨습니다. 앞으로 학생이 아닌 연구자로서 혼자 설 수 있도록 성장시켜 주신 교수님께 감사의 말씀 올립니다. 또한 바쁜 시간에도 불구하고 학위 논문을 잘 마무리할 수 있도록 지도해주신 박찬영 교수님, 고명곤 교수님, 박성호 교수님, 백승훈 교수님께도 감사드립니다. 이외에도 학위과정 동안에 많은 도움을 주신 이화선 교수님 외 생명과학부 모든 교수님들께도 감사의 말씀 올리고자 합니다.

또한, 박사 학위 기간 동안 교수님만큼 저에게 많음 가르침과 도움을 주신 최수연 교수님께도 깊은 감사의 말씀을 드립니다. 실험실에 들어왔을 때부터 선배로서 많이 챙겨주고 이끌어준 환희형, 은진이누나, 현제형, 준호형, 병진이형, 같이 실험실에 들어온 승민이, 실험실 생활을 지금까지 같이 하고 있는 현이형, 창준이, 고운이, 그리고 연구에만 집중할 수 있도록 행정적으로 많이 도와준 규리선생님에게 감사드립니다.

가장 큰 힘이 되어준 가족들에게도 감사의 말씀을 전합니다. 긴 학위과정동안 항상 같은 자리에서 흔들림없이 큰 버팀목이 되어 주신 부모님, 언제나 저를 믿어 주셨기에 긴 시간 버틸 수 있었습니다. 그리고 소중한 나의 동생 욱진이, 현진이에게 고맙다는 말

전하고자 합니다. 그리고 항상 응원해주는 사랑하는 아내 정민이에게도 믿고 따라와줘서 고맙고 사랑한다고 전합니다. 그리고 살아계셨다면 저를 너무나도 자랑스러워해주실 할아버지, 할머니, 외할아버지, 외할머니께 이 박사 논문을 보여드립니다. 그리고 정민이 가족분들께도 감사드립니다.

미처 언급하지 못하였으나 모든 학위과정 동안 도움을 주신 다른 많은 분들께도 감사의 마음을 표하며, 앞으로도 계속 포기하지 않고 열심히 연구에 정진하여 더 발전하고 제 일을 책임지는 사람이 되도록 노력하겠습니다. 감사합니다.